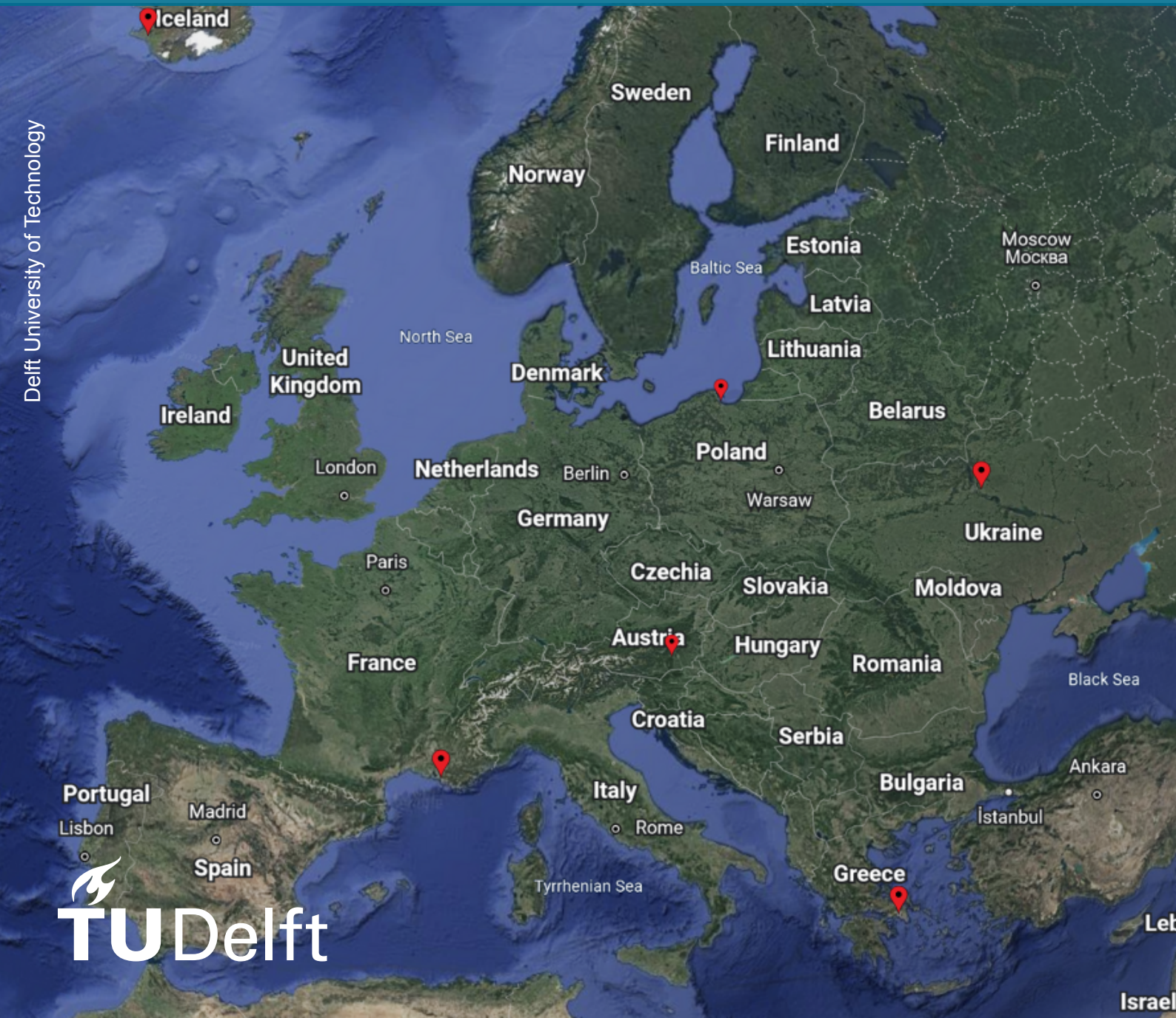


Analysing Sites for Solar and Airborne Wind Energy Hybrid Power Plants

A feasibility analysis of the resource characterization and energy generation for identifying hybrid system locations

Alizé Hall



Cover: Created by Alizé Hall based off Google (2022) Europe

Copyright © 2023 by Alizé Hall
All rights reserved



Analysing Sites for Solar and Airborne Wind Energy Hybrid Power Plants

A feasibility analysis of the resource characterization and energy generation for identifying hybrid system locations

by

Alizé Hall

in partial fulfilment of the requirements to obtain the degree of

Master of Science
in Sustainable Energy Technology (SET)

at the Delft University of Technology

Wind Energy Group, Faculty of Aerospace Engineering,
& Faculty of Electrical Engineering, Mathematics and Computer Science

to be defended publicly on March 29, 2023, at 11:00.

Student Number:	5380928	
Project Duration:	November 2021 - March 2023	
Thesis Committee:	Dr.-Ing. Roland Schmehl	TU Delft, Main Supervisor
	Dr. Stefan Pfenninger	TU Delft
	Ir. Rishikesh Joshi	TU Delft, Daily Supervisor

Contact Information

Author: Alizé Hall

An electronic version of this thesis is available at <http://repository.tudelft.nl/>

Acknowledgments

I would like to express my gratitude to several people. To start off my defence committee, which includes my thesis chair, Professor Roland Schmehl, my daily supervisor PhD candidate Rishikesh Joshi, and my final committee member Professor Stefan Pfenninger. I appreciate all of their time, valuation, and insights along the way. Especially to Roland and Rishi who further sparked my interest in this cutting-edge new renewable technology.

Next, I would like to show my appreciation to Lavinia Thimm for taking the time to meet with me on several occasions to discuss airborne wind energy topics. She helped me understand the different considerations needed when evaluating such an incredible resource. As well as the TU Delft Airborne Wind Energy research group for helping me gain knowledge along the course of my thesis.

Finally, I would not have made it without my friends and family constantly cheering me on despite most of them being on the other side of the world. A special thanks to my partner Nancy and our cat Celsius for being my support system in Delft.

Preface

“Society grows great when old men plant trees whose shade they know they shall never sit in.”- Ancient Greek Proverb

This thesis project fulfils the final requirements for acquiring an MSc in Sustainable Energy Technology from the Technical University of Delft. I started my graduate journey during the difficulty of the Covid pandemic. TU Delft had the best program, where I studied the autonomous track with wind, solar, and storage technologies. This thesis combines those subjects and focuses heavily on airborne wind and the correlation with solar for hybrid plants. I was drawn to the multi-faceted and innovative research topics. The conclusions come from the model that can be found in Chapter 3. For those interested in the relationship between both resources, Chapter 4 consists of Pearson’s correlation coefficients and how they affect each other. The final chapter concludes with observations on the feasibility of hybrid power plants based on the effects of geographic location.

*Alizé Hall
Delft, March 2023*

Abstract

A method to help renewables flourish is mitigating the variability that is inherent in natural resources. To do so, we explore the intricacies of the relationship between airborne wind (AWE) and solar energy to uncover the possibilities of future energy-generating hybrid power plants (HPP). Which leads to steering away from fossil fuel reliance, while increasing the dependability of renewable technologies.

The resources were investigated at one primary test site, where anomalies and trends were uncovered. By tracking the solar radiation and wind speed over time, the complementarity of the two is studied. When the Pearson correlation coefficients are negative, a non-variable energy generation capacity can be found leading to less intermittency in energy stock. These results are expanded to evaluate other locations in Europe, identifying the main contributing factors of a successful hybrid set-up. The case study location was Marseille based on pre-analysis of solar and wind availability.

Using resource correlation, energy output, and location data, the model developed to assess the location feasibility of HPPs found that most areas are not suited for annual generation situations, but are more successful on a quarterly basis. The HPP setup would allow the dependency on fossil fuels and storage options to decrease while having a flexible implementation option meaning it is a viable option for off-grid / remote locations and urban areas to help lighten the grid load.

The model created can be further developed into an HPP site map, to help further identify areas that would benefit from more renewable options without as many drawbacks. Overall, this research leads to a method for reaching 2050 climate goals by identifying HPP potential on a variable time basis.

Contents

Acknowledgments	i
Preface	ii
Abstract	iii
Nomenclature	vi
1 Introduction	1
2 Problem Analysis	5
2.1 Literature Review	5
2.1.1 Resource Assessment	5
2.1.2 Airborne Wind Energy	5
2.1.3 Solar Energy	7
2.1.4 Hybrid Power Plants	8
2.1.5 Data and Tools for Resource Analysis	11
2.1.6 Literature Review Summary	14
2.2 Research Gap and Questions	15
2.3 Methodology	16
3 Model and Tool Development	17
3.1 Overview of Hybrid Location Model	17
3.1.1 Data configuration	18
3.2 Resource Analysis Concept	20
3.2.1 Wind	20
3.2.2 Solar	21
3.2.3 Resource Evaluation Scale	22
3.3 Energy Potential Process	24
3.3.1 Airborne Wind Energy Technology	24
3.3.2 Solar PV Panel Technology	26
3.3.3 Energy Potential Evaluation Criteria	27
3.4 Prospective Hybrid Site Configurations	28
4 Case Study - Marseille	30
4.1 Resource Case	30
4.1.1 Wind Speed in Marseille	30
4.1.2 Solar Irradiation in Marseille	33
4.1.3 Resource Correlation Marseille	35
4.2 Energy Case	42
4.2.1 Kite Energy in Marseille	42
4.2.2 PV Energy in Marseille	44
4.2.3 Energy Correlation Marseille	44
4.3 Marseille Scenario Results	46
4.4 Multiple Locations	47

- 5 Conclusion** **52**
- 5.1 Key Outcomes 52
- 5.2 Recommendations and Future Possibilities 53
- References** **54**
- A Appendix A** **57**
- B Appendix B** **63**
- C Appendix C** **66**
- D Appendix D** **80**

Nomenclature

Abbreviations

Abbreviation	Definition
AEP	Annual Energy Production
AWE	Airborne Wind Energy
CF	Capacity Factor
CFSv2	Climate Forecast System Version 2
CMSAF	Satellite Application Facility on Climate Monitoring
DHI	Diffuse Horizontal irradiation
DNI	Direct Normal Irradiation
ECMWF	European Centre For Medium-Range Weather Forecasts
FF	Fill Factor
GHI	Global Horizontal Irradiation
GIS	geographic information systems
GTI	Global Tilted Irradiation (at optimum angle)
GWA	Global Wind Atlas
HAWT	Horizontal Axis Wind Turbines
HPP	Hybrid Renewable Power Plants
LCOE	Levelized Cost of Energy
NREL	The National Renewable Energy Laboratory
NSRDB	National Solar Radiation Database
PCC	Pearsons Correlation Coefficient
RES	Renewable Energy Sources
SAS	Stand Alone Systems
STC	Standard Testing Conditions

Symbols

Symbol	Definition	Unit	
A	Area	m^2	
A_M	Air mass coefficient	-	
C	Aerodynamic coefficient	-	
E	Energy	Wh	
G	Ratio of lift and drag	-	
G	Irradiance	W/m^2	
h	Height	m	
I	Current	A	
p	Surface pressure	Pa	
P	Power	W	
r	Pearson's correlation coefficient value	-	
t	Time	hr	
T	Temperature	K	
V	Voltage	V	
V	Velocity	m/s	
v	Speed	m/s	
z	Geo-potential	m^2/s^2	
η	Efficiency	-	
ρ	Density	kg/m^3	
Subscripts			
D	Drag		
hr	Hourly		
Irr	Irradiance		
L	Lift		
m	Module		
nom	Nominal		
op	Open-circuit		
PV	Photovoltaic		
sc	Short-circuit		
SSR	Solar net surface irradiation		
$surf$	Surface		
sys	System		
u	U-component (eastern direction)		
v	V-component (northern direction)		
w	Wind		
yr	Yearly		
Constants		Numeric Value	
g	Gravitational constant	9.80665	m/s^2
k_B	Boltzmann's constant	1.38065e-23	m^2kg/s^2K
q	Electronic charge	1.60218e-19	C
R_{earth}	Radius of the earth	6367.47	km

List of Figures

1.1	Alternating phases of the pumping cycle and maneuvering [6]	2
1.2	Hybrid power system (solar-wind) [9]	3
2.1	Solar cell example - Recombination [17]	7
2.2	Hybrid classifications [18]	8
2.3	Hybrid plants further classification and configurations [18]	8
2.4	Instantaneous complementary energy source situations in Poland [19]	10
2.5	Global Wind Atlas [27]	13
2.6	Solar GIS [28]	13
2.7	HOMER interface [30]	14
3.1	Model overview	18
3.2	Wind speeds above Europe	21
3.3	Solar radiation components [37]	22
3.4	Correlation explained visually [38]	24
3.5	Comparison of different kite curve-fits	25
4.1	Hourly wind speed in Marseille for lowest and heights points between 2017-2021	31
4.2	3D graph of wind speed above Marseille 2017 to 2021 from daily and yearly perspective	32
4.3	Trend lines for five geometric heights for wind speed above Marseille	33
4.4	3D graph of hourly solar irradiance in Marseille 2017 to 2021 from daily and yearly perspective	34
4.5	Solar irradiance in Marseille 2017-2021	34
4.6	Solar trends for Marseille 2017-2021	35
4.7	Resource trends for Marseille from 2017-2021	36
4.8	Re-scaled and normalized wind speed and solar irradiance trends for Marseille	37
4.9	Correlation plots of resource trends in Marseille Week 51 in 2017	39
4.10	Correlation plots of resource trends in Marseille January 29 2018	41
4.11	Correlation Histograms per time and height in Marseille	42
4.12	Curve-fit with Kitepower	43
4.13	Hourly AWES power production for 2017	43
4.14	AWES kite power trends five years stacked	44
4.15	Hourly PV array power production in Marseille 2017-2021	44
4.16	Hourly power trends in Marseille 2017-2021 stacked	45
4.17	Hourly power trends in Marseille 2017-2021 re-scaled	45
4.18	Energy correlation histograms per height and time in Marseille	46
4.19	Energy scenarios	47
4.20	Map all test locations	48
4.21	Week 27 correlation all locations at 285 m	49
4.22	Week 23 correlation all locations at 285 m	50
A.1	Kite Power Brochure	60
A.2	Solar Panel Specifications	62

B.1	Hourly Wind Speed in Marseille all heights using AWERA curvefit	64
B.2	3D graph of wind speed Marseille 2017 to 2021 using AWERA curvefit	65
B.3	Trend lines for five geometric heights of wind speed above Marseille using AW- ERA curvefit	65
C.1	Visual of annual correlation of resources over five heights from 2017-2021 Mar- seille	79
D.1	ArcGIS	80

List of Tables

3.1	Scale to evaluate the PCC of hybrid energy sites	28
4.1	Yearly average wind speed in m/s above Marseille between 2017-2021	31
4.2	Average monthly wind speed in m/s above Marseille between 2017-2021	32
4.3	Annual energy potential in Marseille sorted by height and time	46
4.4	Summary of test sites	49
4.5	Week 27 correlation table all locations	50
4.6	Week 23 correlation table all locations	51
4.7	Quarterly correlation percentages to meet minimum hybrid requirements	51
C.1	Correlation values between wind speed and solar Irradiance in Marseille (monthly to yearly)	67
C.2	Correlation values between wind speed and solar Irradiance in Marseille (weekly)	68
C.3	Correlation values between wind speed and solar Irradiance in Marseille Q1 (daily)	69
C.4	Correlation values between wind speed and solar Irradiance in Marseille Q2 (daily)	70
C.5	Correlation values between wind speed and solar Irradiance in Marseille Q3 (daily)	71
C.6	Correlation values between wind speed and solar Irradiance in Marseille Q4 (daily)	72
C.7	Correlation values between Kite and PV Energy in Marseille (monthly-yearly)	73
C.8	Correlation values between Kite and PV Energy in Marseille (weekly)	74
C.9	Correlation values between Kite and PV Energy in Marseille Q1 (daily)	75
C.10	Correlation values between Kite and PV Energy in Marseille Q2 (daily)	76
C.11	Correlation values between Kite and PV Energy in Marseille Q3 (daily)	77
C.12	Correlation values between Kite and PV Energy in Marseille Q4 (daily)	78

1

Introduction

Humanity is in the midst of a massive shift of energy sources from fossil fuels to renewable resources, resulting in a green energy transition. This is due to rising climate fears pushing many stakeholders to accelerate it. As a society, we need to advance to a more sustainable future in order to maintain and enhance the viability of enjoyable life on earth. Governments around the world have pledged to achieve net zero emissions and other climate goals by 2050 to show their commitment to the energy transition [1]. The political side of energy is the dependencies governments place on a reliable energy market to satisfy the needs of their constituents while maintaining certain profitability. To hasten the energy transition, there must be an emphasis on the fiscal and reliability side of things as well as social acceptance. A successful energy system should be able to encompass all three targets therein mutually benefiting all persons involved. An acceptable future for energy generation systems means they will rely mostly on natural sources that are constantly replenished to meet the growing global energy demand.

Often wind energy generation is only thought of as conventional horizontal axis wind turbines (HAWT) and farms, with a limited path for future innovation, usually restricted to offshore implementations (i.e. floating wind) and larger capacity turbines. It is known that the higher the altitude the better access to wind resources due to fewer obstructions. However, there must be a limit to the stature of these turbines, if not theoretically then they will meet social resistance [2]. Eventually, a more efficient way of harvesting wind energy will be favourable. Enter airborne wind energy (AWE), an unconventional form of harnessing wind for generation capabilities through the means of kites, with many advantages over HAWT.

AWE is still in the prototyping phase but holds exciting potential as a key renewable resource system (RES). Miles Loyd, often considered an early pioneer of airborne wind energy, discovered the key theory to use kites for energy generation. His calculations led to the concept of crosswind flight and rotational movement to harvest energy. By using the surface area of the kite and its aerodynamic forces, he found that the motion of the kite could be transformed into power via kinetic energy [3]. Meaning it is doing the same thing as the portion of the blade on a wind turbine which converts wind into energy, but at a fraction of its size. The two methods for converting into power are: converting mechanical power into electricity in the air with generators or belaying a tether to the ground and converting there [4]. For simplicity, they will be referred to as fly-gen and ground-gen, respectively. Each utilizes different aerodynamic drag forces to optimize power generation.

Airborne wind energy has the advantage of mobility over HAWT meaning that AWE has

the potential to produce more energy. This flexibility is demonstrated in two ways, the first is through vertical movement by kite adjustment where the power harvesting technique is used by optimizing the kite's height in accordance with wind availability. The second way is by the ability to move the kite to different locations allowing rural places to have a greater chance of accessing renewable energy. By being able to tap into higher heights and steadier/stronger wind currents the energy generation of kite technology is potentially greater than turbines. A way to estimate wind power potential can be found using

$$P_w = \frac{V_w^3 \rho}{2}, \quad (1.1)$$

for several wind power technologies. The wind velocity, V_w , is cubed and multiplied by the air density ρ then halved. By increasing V_w the power density of the wind, P_w , is also increased and when reaching higher altitudes there is a steadier and stronger wind flow, this is where one of the advantages of AWE comes into play. Equation 1.1 outputs a highly idealised potential without the systems losses so it should not be used as the only method in determining potential. AWE technology is also able to continuously adjust vertically in an effort to find the most optimal wind to power the kite.

There are two main phases when operating an AWE kite for energy uses, traction, and retraction, generating and consuming electricity respectively. During traction, the kite is producing power by raising the angle of attack away from the wind while allowing the tether to be pulled taught. The retraction phase (reel-in) is when the angle of attack of the wing is lowered into the wind therein depowering the wing, this consumes energy until the kite reels back out. Loyd's research found

$$P = P_w A \frac{4}{27} C_L G^2, \quad (1.2)$$

to be used specifically for kites. For an optimization for C_L , the lift and drag must be found to complete the above calculation. The ratio $4/27$ is the Betz limit, the maximum theoretic limit for wind and G is the ratio of lift and drag while A represents the surface area [3]. Equation 1.2 is used during the traction phase. The crosswind motion and pumping cycles move in figure 8 loops as it is the most optimal configuration to fly in [5], see Fig 1.1.

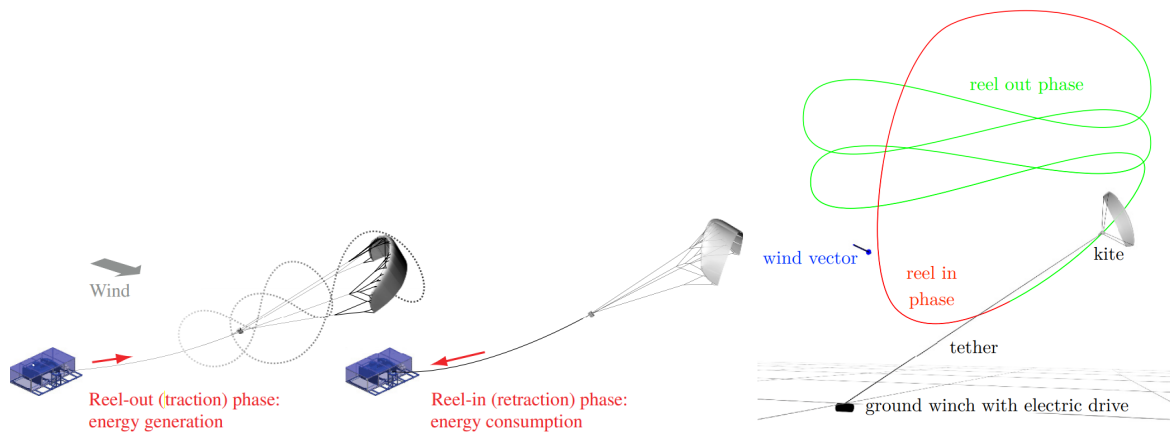


Figure 1.1: Alternating phases of the pumping cycle and maneuvering [6]

Disregarding the socio-geopolitical hurdles, RES's biggest enemies are either the tight timeline for technology to meet 2050 climate goals or the lack of innovative advances [7]. The capacity of renewables is not enough to meet the population's energy demand when

depending on one source, this is due to the mismatch in energy generation. Most RES are heavily impacted by the sun, which is not something humans can control or set limitations on. Though it may seem they are dependable due to the "unlimited" fuel supplied by the sun, there are still discrepancies. These are mostly due to temporal and spatial variations. The wind is considered to be anti-correlated with solar where it roughly sees an apex at night and is also opposite to most energy demand loads [8].

The basics of any energy market are to at least meet the demand at any given time, without having massive price changes. Some current solutions to the intermittency of generation are relying on storage, offset with other energies, and forecasting. Forecasting and other meteorological observations have helped "predict" the solar and wind resources to varying levels of accuracy. These solutions have not reached their peak performance in assisting in covering the mismatch. Storage capabilities and prediction methods are limited due to a lack of knowledge, innovation, and reliance on the current energy supply.

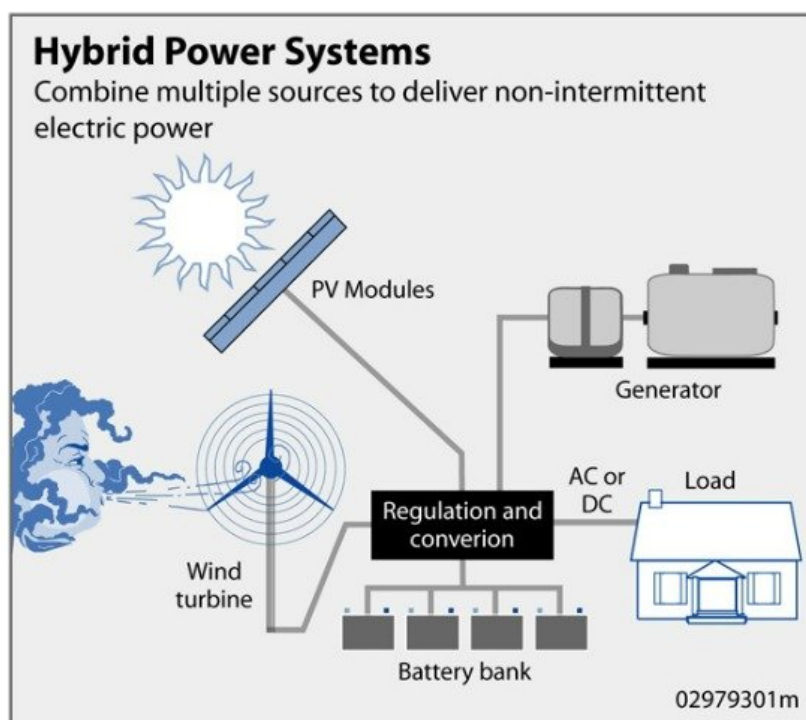


Figure 1.2: Hybrid power system (solar-wind) [9]

Hybrid power is the combining of multiple several types of technology to strengthen the overall output. While stand-alone systems (SAS) are typically off-grid power systems relying on one energy generation technology and supply. Hybrids can be done in several ways including using storage, generators, and other renewable energies. There are already several hybrid options in use the oldest was implemented in the late 1970s in Nova Scotia, a hydro wind system [10]. Other examples are wind-hydrogen, wind-diesel, and newer technology in the form of floating solar arrays.

Therefore, the listed issues motivate this research to discover the potential hybridization between natural sources. Solar and higher wind were selected due to their natural anti-correlation, to analyze an emerging technology with a higher possible potential than turbines, and flexibility [11]. Hybrid renewable power plants (HPP) would be a great solution for the future of energy generation and management if they prove reliable with a steady output. In

this case, the combination of solar and airborne wind energy will be the base resources for the hybrid power plant configuration.

This research aims to evaluate the feasibility of hybrid renewable power plants using airborne wind energy and solar from the resource perspective. If such locations can be identified on a geographic scale from historical data trends, it can pave the way for a reliable sustainable future energy network provided by RES.

This research is relevant to many different areas around the world, the test sites will however be based in Europe, as the comparisons will have fewer external environmental factors influencing results due to geographic proximity. Using MATLAB and Python to model an HPP leads to different potential scenarios that can be evaluated. First, a resource analysis must be done which is tied to the location of a site using the solar and wind data available. The correlation between each is weighed and evaluated. This is followed by an energy analysis where the technology will weigh in on the results. Using a unique location as a case study will lead to the possibility of multiple locations being evaluated at once, allowing for to the creation of the framework for a Hybrid Potential location tool.

The structure of this research is as follows and formulated to use the best research methods, answer the objective, and meet all minimum requirements. The report will be divided by how the project was completed in the above order. Chapter 2 will discuss the outcomes of the literature review focusing on the background information needed. Chapter 3 will present the methods to answer the research question(s) and the model development. 4, will contain the framework developed for the tool and the results of previous chapters, respectively. Finally, Chapter 5 will summarize the relevant conclusions and future recommendations found through the outcome of the research.

2

Problem Analysis

The purpose of this chapter is to provide more context on what research exists and what is needed to evaluate the potential generation of HPPs. It will also outline prior challenges and solutions considered. This portion will reflect the knowledge accumulated during the literature review and what led to the research questions selected.

Section 2.1 covers the extensive research in resource assessments between wind and solar, what data is used and HPP evaluation tools that already exist. The unanswered research questions that have arisen will be found in Section 2.2. Finally, Section 2.3 will outline the methodology used to answer the questions.

2.1. Literature Review

This first section will be the knowledge acquired during the literature review. The largest components of evaluating sites for good HPP potential are the resource assessment of AWE-Solar, hybrid power plant structure needs, and the current tools available for HPP analysis.

2.1.1. Resource Assessment

There have been many studies done on the assessment of different resources for a variety of means. Both solar and wind have variability, are unpredictable, and are difficult to forecast. This is not always true, solar energy can be 100% accurately forecasted, but only at night. This aside another reason for these studies is to alleviate the mismatch between the two most widely used RES. Sometimes these studies are done on a single resource but will be applied in separate ways such as onshore vs offshore wind generation. One of the most common factors in these studies is the importance of surrounding environments and timescales.

2.1.2. Airborne Wind Energy

Wind will be the primary resource and will be more of the focus, as there is little research concerning airborne wind energy. Wind farms on average have a higher capacity than solar farms. They are able to be installed on land and offshore while solar has a slower start to offshore capacity. Society tends to lean more towards the production of energy offshore as it is usually not in the vicinity of their everyday life. However onshore wind generation is still quite common and has the potential to grow. On the opposing side, many people do not appreciate the environmental impacts that large-scale wind turbine installations cause. This includes the disruption to the ecosystem primarily avian life is affected [12].

Energy Estimation

Usually, when a resource assessment is done for wind turbines, the wind power density equation (1.1), fulfils the first estimation for power potential. In order to evaluate the feasibility of hybrids specifically through the use of AWES, this process must go a bit further and should be checked with an outside source. As airborne wind energy is still a recent innovation and there are not many kites commercially available. The methods and calculations to produce energy still vary. The main challenges are the ability to adjust the optimal power harvesting height of the machines and the path they take.

With the limited computation sources, the method for finding the energy potential will be done similarly to how a wind turbine is evaluated. The power curve from the Kite technology is used. However the curve covers a large vertical distance, therefore several assumptions will be used to simplify the calculations. The power will be determined using five separate heights, each height will represent the vertical midpoint for the kite flying range [13]. In reality, the kite will choose the most optimal height to fly at depending on the wind speed and what stage it is at in the pumping cycle. If the model's calculations considered the best wind speed then it is more than likely the kite would always fly at the highest altitude, however, this is not the actual case as the kite will have to be reeled in and out. A simulation covering the traction and detraction case would be a whole different project. The calculations will also not include take-off and landing times and will assume the kite is continuously flying if it meets the minimum cut-in speed. The kite's efficiencies are already factored into the power curve.

Prior Research Higher Wind

The difference in this research is the focus on airborne wind energy which derives its primary "fuel" from higher-altitude winds. There have been several wind assessments to find out if there are more favourable conditions with regard to HAWT. However higher altitudes do not necessarily mean better output. According to a study done "the strongest winds are not necessarily always at the highest altitudes and therefore the best performance for high altitude technologies can be obtained by raising or lowering the kites to the height where the maximum potential exists" [14]. This can be thought of as adjusting the power harvesting device vertically and horizontally. Another reason wind data is more difficult to corroborate is wind speed profiles. Wind velocity cannot be evaluated at exactly one area in space as it is not uniform. Referring back to the method which AWE technologies use to generate electricity shows that a lot of the emphasis is related to the wind power density equation 1.1 which derives its primary focus on the wind velocity however the air density ρ also varies and changes with respect to altitude. Another disruption to these calculations is the obstacles found on the surface. One must find the potential height and pressure and then the energy potential can be calculated. However, the pressure equation is a logarithmic function which is where these velocity profiles originate. Therefore, the wind calculations are not varying in a linear way and through this logarithmic path the curve smooths.

Several studies were conducted to evaluate the difference in potential energy production from altitudes used by wind turbines and those used by AWE technology. While many studies have varied in the actual number of possible watts of energy that can be produced, they are all safely above the energy from HAWT. One of the most recent articles mentions the comparisons in potential done by different groups as well as their own evaluation. The analysis was done on ERA5 hourly data sets throughout Europe over a 7-year period, focused on an altitude range that would act as a max ceiling the kites can reach and a floor above the average hub height of a wind turbine. Overall AWE scored higher in terms of a stable and stronger resource than the heights for HAWT. The energy potential was found to be 40 W/m² for the period of time that the minimum technology requirements were met [15].

2.1.3. Solar Energy

Solar energy in the form of PV panels allows for flexible and relatively smaller-scale energy system installation and is attractive as it relies on an infinite amount of fuel. Solar potential varies by location and generally peaks shortly after 12:00 on a given day. There are also many innovative ideas in the field such as transparent solar cells, flexible panels, and solar tracking. Assessments of solar and wind resource are also done with the intent to help reduce storage capacities. If solar and wind are complimentary enough that and can create a stable base load of energy generation then there is less need for storage to mitigate the variations with respect to time and demand. When the resources are studied together, they are evaluated using historical data of hourly, daily, monthly, seasonal, and yearly time steps. The two are usually most complimentary on a smaller temporal resolution due to the diurnal cycle of solar radiation, but the relationship declines with time [16].

Solar energy is evaluated in many ways with several parameters and refining the raw data has more limitations. Solar PV derives energy from solar irradiance and its conversion relies on the cloud coverage, reflection, and geometry of the angles striking the PV panels. This is often referred to as indirect, direct, and global irradiance which can be further quantified as horizontal or vertical. Solar data is also usually evaluated at the surface of the ground as it takes into consideration all the losses up until that point (e.g., reflection and transmission through the atmosphere).

The conversion from solar irradiance to solar energy through PV panels is called the photovoltaic effect. Incoming solar radiation strikes the boundary layer of semiconductor materials, and an electric current can be generated. The insolation is composed of photons, which are the units of energy stored in light. A PV cell is made from semiconductor materials with a p-n junction.

Once it hits the PV cell, some of the photon energy is absorbed. This results in the production of an electron-hole pair. The pair is called charge carriers. If an external circuit is formed, the voltage difference drives the electrons from the n-side to the p-side of the junction and is collected at the terminals. The electrons flow through the circuit generating an electric potential and are finally recombined with the holes. An example of the photovoltaic effect can be seen in figure 2.1.

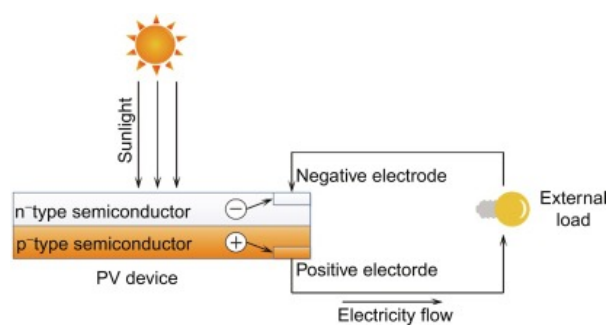


Figure 2.1: Solar cell example - Recombination [17]

Research in the solar energy sector is mostly focused on the efficiency of cells, accessibility, and reducing costs. The current issue that pertains to this research is the power efficiency, which varies with temperature, material composition, and the irradiance that actually hits the cells.

Normally solar panels are evaluated at standard test conditions (STC) which is a temperature of 298.15 K, the amount of irradiance on the panel is 1000 W/m², and a sea level air mass of 1.5. As the temperature rises the cell's efficiency decreases and the opposite is true for colder temperatures. As the irradiance is almost never equal to exactly that of STC and so the efficiency fluctuates with respect to the amount of irradiance hitting the cell.

Despite these differences, solar radiation data is more fine-tuned than wind data. Once the data is modelled, analysed, and calculated though, depending on the technology outputs a capacity factor that can be directed with regards to the area. Generally, the farther from the equator in the latitudinal direction, solar irradiance becomes less abundant.

2.1.4. Hybrid Power Plants

Hybrid power plants are a fairly new practice and as such has not been defined by an industry standard yet. The current most used taxonomy for the classifications of hybrids was proposed by NREL and is either locationally or operationally linked [18]. The three types of hybrids and their benefits are shown in figure 2.2.

Category	Locational Linkage	Operational Linkage	Dominant Anticipated Benefits and Approaches
Co-Located Resources	Yes	No	Decreased costs through shared balance-of-system costs and interconnection
Virtual Power Plants	No	Yes	Increased operational value through coordinated control of optimally sited technologies
Full Hybrids	Yes	Yes	Enhanced net economic benefits through co-optimization of constituent technologies, often involving shared components

Figure 2.2: Hybrid classifications [18]

The HPP configurations can be seen in figure 1.2 and how they are linked to each other, the grid, and operated. A goal of this research is to be able to reach full hybrid status as it is the optimized configuration for economic, energy, and capacity viability.

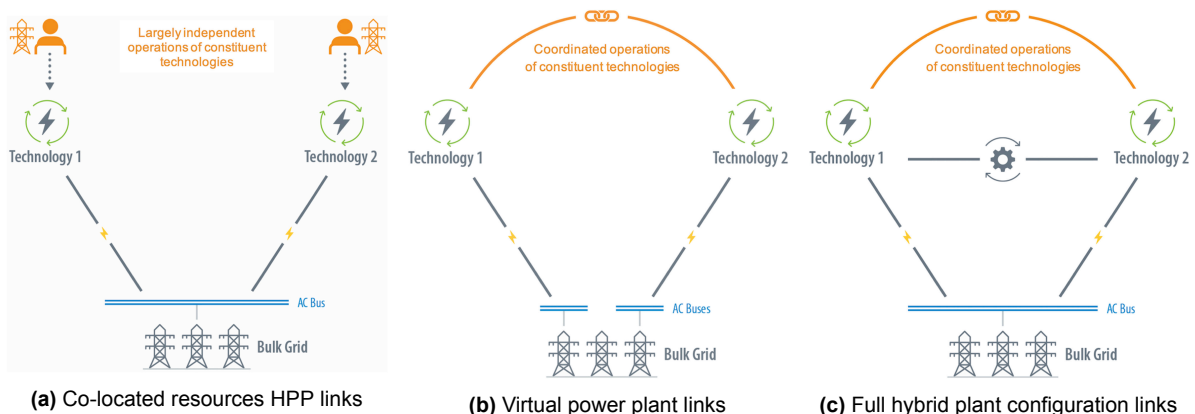


Figure 2.3: Hybrid plants further classification and configurations [18]

Co-located resource configuration is similar to having two SAS but lacks a connection

between them, which would allow for separate entities to own a portion of the plant. This would lead to a loss of efficiency when tracking the complementarity of the shared resources as neither plant would be able to communicate with the other.

VPP's benefit by allowing each technology to operate from optimized locations and are able to send and receive messages from the other. However, the benefits are more from an energy market standpoint and allow for the owner of the plants to reap more benefits with higher negotiating power. Another downside would be fewer cost savings opportunities from operations and maintenance due to distance.

Full hybrid systems share partial benefits from the two previous configurations. Having a centralized operation that also communicates allows for more storage to be integrated, optimized, and efficiently operated. The best-case storage situation is when excess energy is generated and can be used to cover the times when the technologies are operating at a lower capacity or when the correlation drops.

The first step in reaching a full hybrid configuration is through resource assessments for both wind and solar potential to evaluate the mismatch and the correlation of each. The goal of the review in assessments done was to find if there were any that had already answered the question and if not where to start.

In Poland, a study was done on resource compliments and droughts for wind and solar [19]. The data inputted was from the ECMWF hourly at single levels with resolution ($0.25^\circ \times 0.25^\circ$). The wind speed was measured at 100 m above ground level and the solar irradiation used was the horizontal surface irradiation. The solar data was available in terms of shortwave radiation for reaching the surface this was the most the study needed so no further refinement was added. The wind data was translated into the wind power density with no additional steps and a standard value of the air density was used. The swept area from the blades of a wind turbine was also used. The study modelled the results in a spherical grid with the energy demand, generation potential from each resource, and overall correlation.

Figure 2.4 represents four different scenarios in which two renewable energy power plants (red and green lines) exhibit different complementarity. The orange line represents the joint energy generation from the two energy sources (red and green together), whereas the black line indicates a theoretical constant load/demand. If the orange line is above, it indicates an energy generation surplus, and when it is below, energy demand is greater than supply, and energy deficits occur. Each of the lines is generated from idealized sine functions and shows the amount over time, which is why the spherical grid represents the overall time period where the evaluation is done.

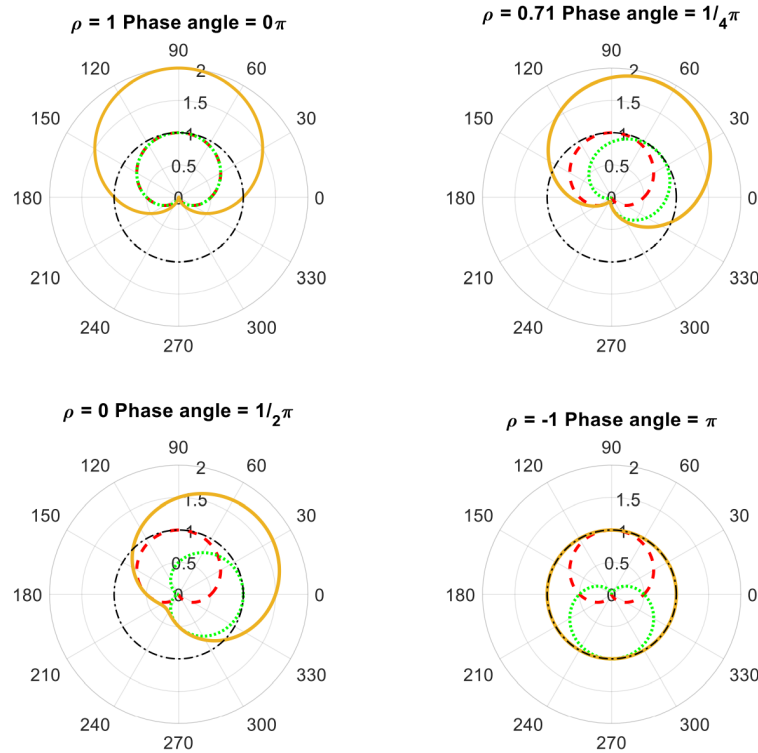


Figure 2.4: Instantaneous complementary energy source situations in Poland [19]

ρ represents the correlation coefficient between the two sources. The upper left case in figure 2.4 shows a case of exact correlated behaviour, which could be two different PV arrays set up in the same location. This means that even if more of the same technology was installed the energy availability would not change over time as they follow the same pattern. The top right and bottom left cases show two different RES as can be seen by the demand (black) and the amount generated (orange), there will be periods where excess energy is generated while other times the demand will not be met. The final case is the most ideal for hybrid justification. If the two sources are perfectly complementary then the demand over time will always be met, the amount of power generated is not a primary factor as more units can be installed to reach a safe install capacity.

These cases are idealized meaning that the energy potential is distributed evenly over the run time of the experiment. In order to keep this assumption accurate an energy storage system must be integrated into the array of PV panels and wind turbines. The energy system is generalized to a PV farm and wind turbine installation without decreasing the capacities of each based on the limitations of a specific technology. Only the best and worst-case instantaneous scenarios were evaluated. This limited scope does not take into consideration the many temporal and spatial challenges. One of the studies' conclusions found resource droughts were more frequent in areas that were characterized by strong wind potential [19]. ERA5 was used as it provided a more accurate insight in comparison to Merra-2. The historical data provided upward trends for solar potential and downward trends for wind (but only in the centre of the country). Overall, the resources were complimentary on an inter-annual scale [19].

Another resource assessment case explored the energy resource complimentary over Europe [20]. A continental view of wind and solar potential was evaluated. The wind data used

had the same parameters as the previous case and was evaluated between 70-110 m. A Vestas wind turbine was used, and the annual energy potential (AEP) was calculated based on its capacities. The same solar data was considered but the study used satellite-based data, as the reanalysis data had more clear sky days than were actually observed. The wind potential had variation when evaluated seasonally (quarterly per year). The solar data derived from the Satellite Application Facility on Climate Monitoring (CMSAF), peaked in terms of a capacity factor in June and July. The overall AEP was not the only factor considered but also the change in the monthly variation, to determine the storage needed. The results determined that the maximum wind potential was offshore in the northern regions. Solar energy faces many changes in both the latitudinal and longitudinal directions. The overall complementarity on the annual scale was observed due to each being out of phase with the other. On the smaller time scales the correlation values peaked in summer.

The final resource assessment was done in Texas which is based on an area similar to the area of Poland, the grid is also more separated from other states [21]. This case was different as it analysed the output and potential from locations around Texas that already had existing wind and solar farms. These sites were also separated into coastal and non-coastal categories as there was a large difference that can be seen in the diurnal and seasonal patterns. The solar data was acquired from the NSRDB from NREL which is a satellite data-driven model outputting the GHI from half-hour increments. The Wind data was derived from the NREL's WIND toolkit. The height considered was 100 m in a 2 km x 2 km resolution and the data was generated power production every 5 minutes. The study wanted results that could be relied on so the metrics for reliability were considered to be able to produce power for nearby demand 87.5% of production hours, which is the same metric a coal power plant runs at. The other metric was to factor in the peak power demand hours. Like similar studies, it relied on the Pearson correlation coefficient to evaluate each site. The study further resulted in complementarity between the two being weaker for coastal sites and stronger for onshore wind production. The results also depended on older technology that had already been installed and the historical demand in nearby areas [21].

2.1.5. Data and Tools for Resource Analysis

There are several different means to measure climate parameters globally. They use a mix of measured, interpolated, forecasted, and simulated means. Measured data is as it seems, directly taking incremental records of specific parameters. The increments can vary temporally or spatially. Interpolated data is based on measured data and uses some correlation factors to further improve spectral data. Models are based on all measured data, simulations (usually historically based), and interpolation with a limit based on the laws of physics. Real-time data is the only way to stay current with measurements, however, like all measured data, it is limited.

Both wind and solar fall under the climate and atmospheric umbrella, meaning they derive most of their data from meteorological means. There are several industries dedicated to monitoring and forecasting atmospheric parameters, as such, there is a lot of data that must be purchased before being able to analyse and calculate the end terms. This thesis topic is currently not funded by the university or any affiliated companies, and all the data used must be openly accessible. Therefore, there are more limitations placed on what type of data we need to acquire in order to perform an analysis. The most favoured in the scientific energy community is ERA5 data, other common data types are collected from Lidar, met mast, DOWA, NOAA, and many more.

Atmospheric data sources

Many resource studies use data from one of the largest meteorological data-sharing organizations called the European Centre for Medium-Range Weather Forecasts (ECMWF) [22]. Most European nations actively contribute their local measurement devices to this massive online database, which also acts as a research institute. It claims to be collecting this data (historically) to create more accurate forecasting and predictions. It has data that is both openly accessible and available for purchase. The data they primarily supply is called ERA5, a meteorological data set using a collection of atmospheric parameters, which monitor the climate changes on earth. It uses a method called reanalysis, which combines model data and the laws of physics to assimilate forecasts and then looped to change the forecast when the time has passed to the accurate situation [23]. This continuous analysis acts as a correlation factor to increase the accuracy of projected forecasts. The archived data can date as far back as the 1950s and up to a 3-month lag.

The Lidar system can measure wind from a distance using light from a laser, similar to that of the detection system which works on the principle of radar. As with all measurement devices, the accuracy can also vary and the distance(time) it can measure is also limited. Lidar is a preferred method for HAWT as it can measure the wind speed before it reaches the turbine blades, which allows for control optimization. It is almost like an early warning detection system. The extent of the laser correlates to the amount of time the system has to calculate changes [24]. When compared to MERRA-2 (another popular reanalysis set), ERA5 was more accurate on all fronts with regard to wind energy [25].

Energy Tools & Evaluation

Modelling and forecasting natural resources is not a new concept, there are many means built with wind and solar potential in mind. These focus on the energy that could be potentially produced for two standard technology. Agencies such as NREL create open-source tools that allow all researchers access to data to use for their own means [26]. Agencies are also employed and have created pay-for software that maps the possibilities as well. Meteorological data varies and with that, the accuracy of the downstream processes is affected sometimes in a snowball way. Most hybrid system software can be split into these categories; technical, economic, design and simulation, and feasibility.

Often the tools and software output results are location-based with an API displaying an atlas. The Global Wind Atlas (GWA) is a free open-source web-based application [27]. It focuses on identifying areas with high-wind velocities that have the potential for wind power generation globally. Figure 2.5 displays a screenshot from the GWA.

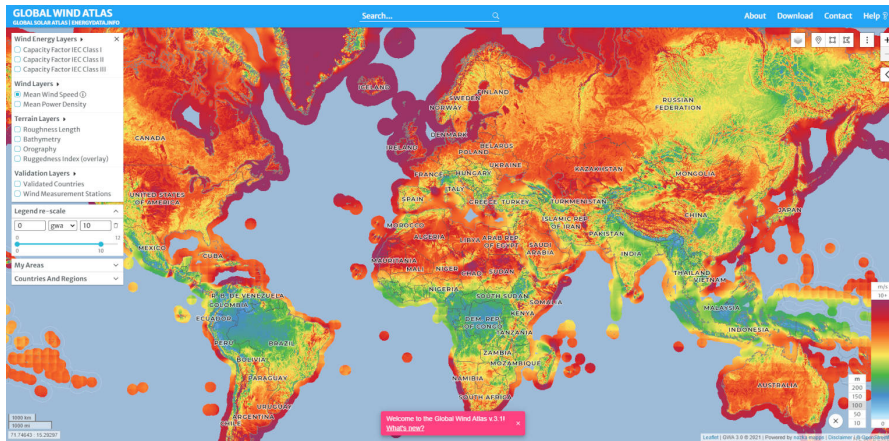


Figure 2.5: Global Wind Atlas [27]

The details of this application are based on 10 years of mesoscale time-series model simulations with ERA5 reanalysis data. The newest version has improved the atmospheric data by optimizing elevation and land cover data in the micro-scale modelling. It also now includes data up to 200 km from all shorelines and has heights of 10, 50, 100, 150 and 200 m and outputs data on spatial, temporal and energy basis.

The GWA has a solar twin, shown in figure 2.6 with a display of solar geographic information systems (GIS), it has the input option of using raw data; global horizontal (GHI), direct normal (DNI), direct horizontal (DHI), global tilted (GTI) irradiance as well as the specific photovoltaic power output. There are many customization options for the size and use of a system to estimate solar-generated electricity potentials based on solar radiation.

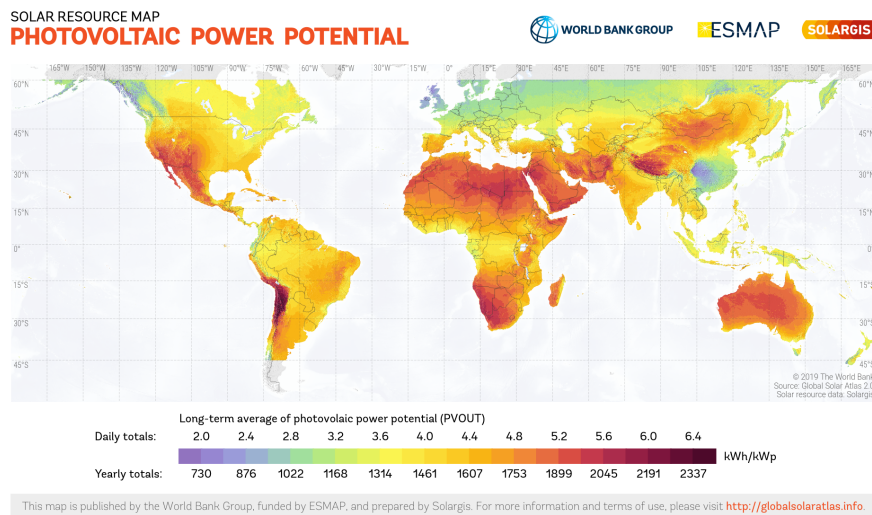


Figure 2.6: Solar GIS [28]

Solargis a global solar data and related solar energy assessment services provider [28]. The tool uses sources from the ECMWF ERA5 data, Climate Forecast System (CFSv2), satellites, and several other meteorological sources. It uses its own set of algorithms to compute the energy output and other data sets needed. There are few unpaid open-source software for hybrid systems and most require a special education membership or are limited by a trial

period.

Software and tools created by agencies from the industry are usually not readily open-source available. The centre for Energy and Environment from NITH in India analysed 17 different hybrid software and toolkits [29], however since then all the free options have been converted into paid or academic options. These tools also mostly focus on sizing and cost analysis for actual hybrid systems. The most well-known one is called Homer, created by NREL its objective is to minimize the net present cost, shown in figure 2.7. Each software has its own limitations such as a small library of technologies, limited source data, and future projections. Of the 17 options only RETScreen outputs energy resource maps and the data affiliated with them.

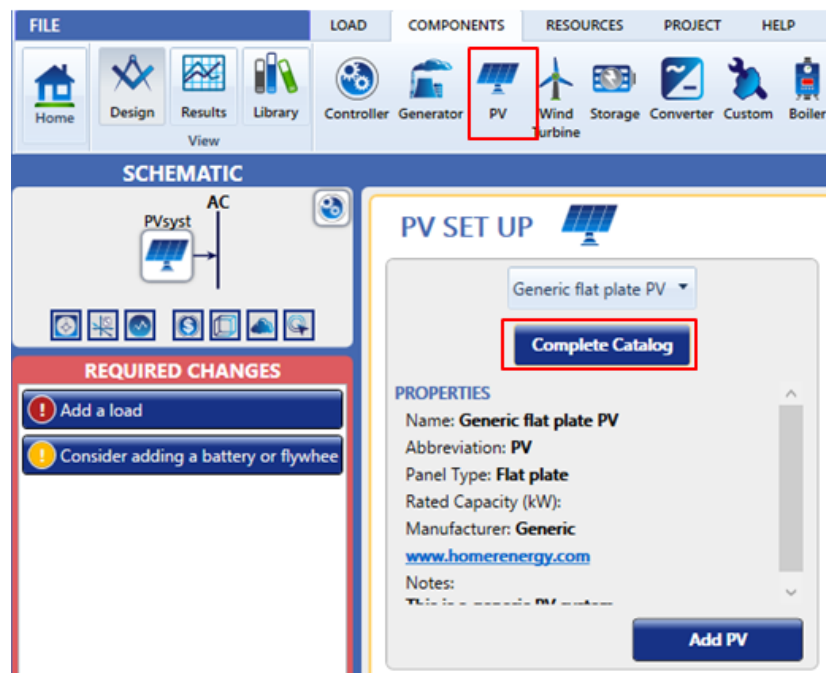


Figure 2.7: HOMER interface [30]

These specialized tools are marketed for the accuracy of specific technologies for RES and not necessarily the resource assessment. They help plan the sizing and design of a hybrid system and place strong importance on the levelized cost of electricity (LCOE), and electricity markets. Tools with industrial backing usually have more validation and can provide a higher degree of accuracy than open-source models.

2.1.6. Literature Review Summary

The challenges that this topic faces are limited knowledge, application, and data configuration. As AWE is a newer technology there have not been a lot of studies regarding its capabilities, much less in combination with other resources, it can also be considered to be in the prototyping/testing phase.

Overall, there have been many studies done on resource assessment with wind and solar. Several of these were done with a stand-alone system assumption and idealized wind values. The wind power density equation was the most used and then statistical analysis and technical specifications was added. All of the evaluations considered wind sites and heights for HAWT

with a max height of 200 m. These studies also focused on the wind aspect a bit more than the solar aspect. Most solar situations converted the raw data, usually in the form of GHI or net surface irradiation into a PV configuration of their choosing. The AWE resource assessment scored wind resources at higher altitudes as more reliable and stronger than the potential at lower heights. The resource correlation for several different areas was more stable during the summer (varied less) and potential with integrated storage systems lead to a conclusion of reliable base-load possibility. The trends for wind changed along the latitudinal direction while solar varied in both directions, the overall variability was remarkably less than the wind.

There was a clear trend with the use of ERA5 data for the wind analysis portion and each study referenced the reliability and accuracy over other counterparts [31]. The solar data was derived either from ERA5 or was satellite driven inputted into personal models. However, those studies were done before the CDS's newest generation of ERA5 reanalysis data. The atmospheric consideration and parameters that the ECMWF provides take into consideration enough to satisfy the historical approximations to actualities.

Finally, most tools available for resource analysis are stand-alone. Meaning the focus on the accuracy of one resource and forgoing the relationship with another. These tools provide a great base for wind turbine site selection and PV potential.

2.2. Research Gap and Questions

The above section summarizes the literature review and what has already been done. However, there is a research gap when analysing the feasibility of AWE-Solar hybrid potential. The majority of the solar wind assessments and tools only consider HAWT technology, hitting a glass ceiling of 200 m in height. By not considering higher heights the correlation between wind and solar is limited. Also, most hybrid energy potential cases are geographically limited to Europe and the US, which leads to missing spaces at the equator and the south half of the world. Currently, an atlas that considers the energy potential of higher-altitude wind and solar does not exist. The tools that do exist often allow for downloadable maps for short instances and limited areas. However, most of the raw data is taken from the same place and the validation for higher accuracy between the wind and solar relationship is not a priority. To bridge this gap in the development of a tool that can search for areas of high resource correlation the data must be validated by a second data type and then compared. If the difference in the comparison is small, then the resources are synchronous.

The research questions were formulated after the literature review uncovered the current research and what gaps there remain.

What factors affect PV-AWE hybrid power plants and to what extent do they influence determining a feasible location?

The sub-questions narrow down the factors and focus on three areas.

1. How does the relationship between solar irradiance and wind speed affect hybrid site locations?
2. What is the difference in energy generation of AWE systems as opposed to other wind technologies, if it exists?
3. How does geography affect the correlation of each technology?

2.3. Methodology

The steps needed to answer this question are described by following the methodology. The first few encompass creating a model of an HPP locator in MATLAB and outputting different scenarios for an optimized energy-to-resource balance.

- Develop an (anti)correlation model of the wind and solar resource potential to confirm resource variability at the location
- Develop energy generation model of airborne wind and solar potential at a location to quantify variability
- Develop a scale to evaluate the hybrid locations based on variability and output
- Evaluate different scenarios based on the results of the model to support different hybrid plant configurations
- Compare AEP model results from a case study with AWERA [32] AEP for the same site to confirm the models' assumptions
- Form a framework for the basis of a tool to evaluate and identify hybrid power plants sites based on resources available

A case study for a single model location will then be inputted and its results measured against a finer-tuned tool to validate the model and data used. These uncertainties must fall within a reasonable range to justify using the model for other situations. Once this is done then the model will be expanded to be able to evaluate HPP potential using both temporal and spatial adjustments. This could lead to the first step in the framework for creating an HPP site resource evaluator tool.

As this research has the potential to be relevant globally, the model will run about 3-5 locations in Europe, with very different geographic environments to create a proof of concept for the framework of an evaluation tool. Chapter 3 will be a deep dive into the development of the model with the inputs along with the outputs and the scenarios they would be categorized under. Chapter 4 will go through a step-by-step calculation of the case study for the test location in Marseilles, and a comparison to other locations. The results and recommendations will be covered in Chapter 5.

3

Model and Tool Development

This chapter explains the development of the model and tool framework when searching for a suitable HPP site. This will lead to the results for the location used as the base scenario and other sites for comparison. The overview can be found in Section 3.1, followed by Section 3.2, where the assessment of the wind and solar potential is found. Once the relationship between resources is uncovered, Section 3.3 calculates the potential energy of each technology based on a control case. Finally, the results will be sorted and a scenario will be ascribed to each hybrid configuration possible in Section 3.4.

3.1. Overview of Hybrid Location Model

This section is meant to give a brief glimpse at the final picture in order to cohesively follow the steps that went into building the model. The outcome is based on the input data running through various calculations and statistical analysis. The flowchart indicates each step in modelling the resource and energy assessment. An explanation of the methods for collecting the data sets and calculating the correlation with each resource follows. These sections provide the technical background details of the data. Figure 3.1 shows the input data and the desired output data needed for the model. This leads to the calculation of the correlation coefficients, which is the key takeaway informing how well the hybrid performs.

The first half of the flowchart calculated how well the wind speed and solar irradiance complement each other using the Pearson correlation coefficients to signify the strength. These sets are then analyzed in various time scales to see if there is an optimized running time for each resource and whether or not they are viable to run continuously. The results are sorted based on a correlation scale and by percentiles. This is further managed in Section 3.2 the resource assessment.

The second part of the model in Section 3.3 explores the energy potential of the location, and whether the results of the resource assessment meet the minimum requirements for a viable location. Using the specifications of the PV technology and AWE capacity along with a control number for each, the resources are looped over the length of time and energy is found. The relationship and correlation are calculated using the same method as the resource portion. This time the scenarios are updated and an energy requirement is added. The rest of this section deals with the set-up of the input variables in the model.

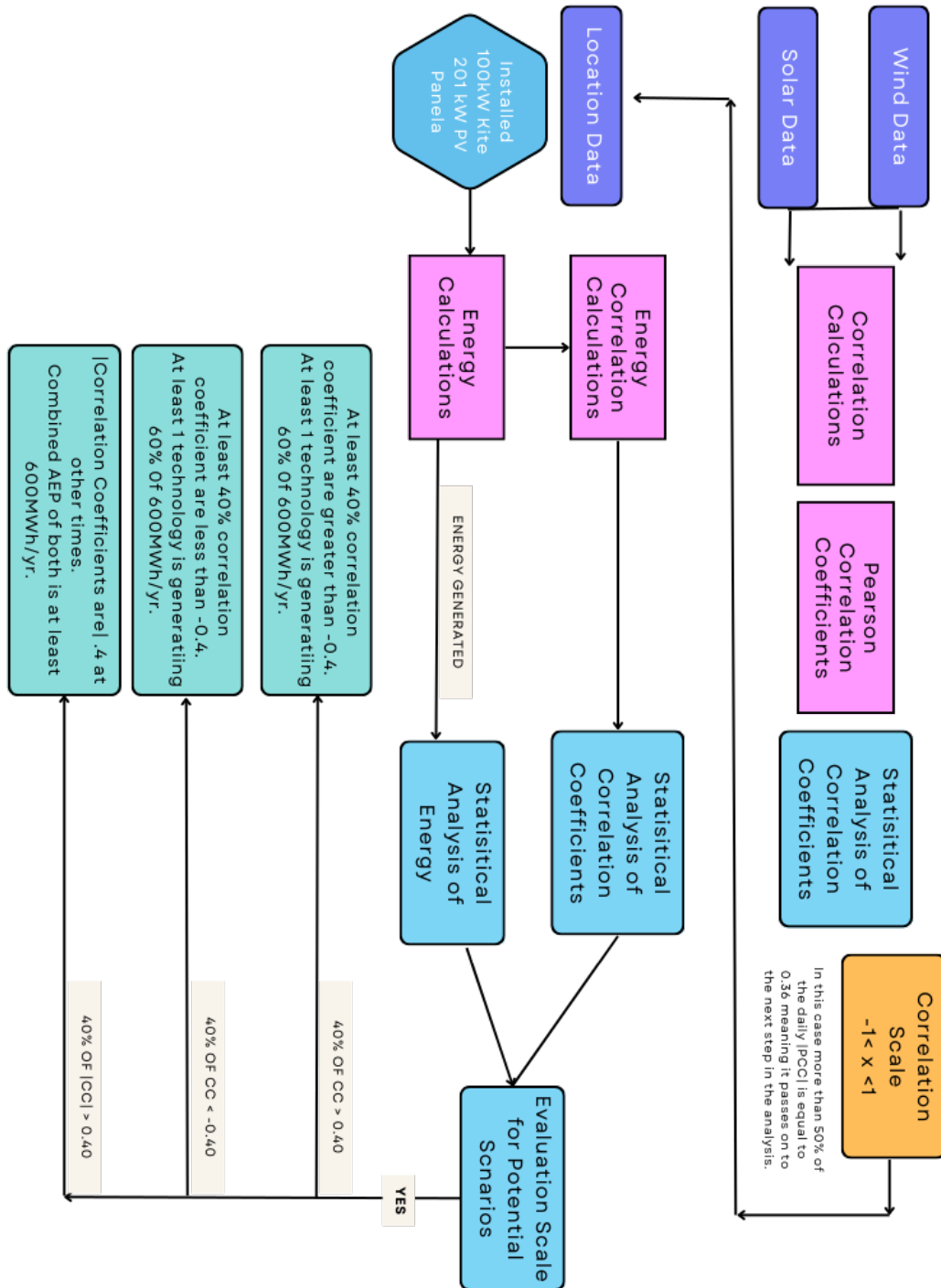


Figure 3.1: Model overview

3.1.1. Data configuration

Both solar irradiation and wind resource follow different natural laws, changing with respect to time, geographic location, altitude, and many other variables. The input data was an ERA5 format available from the online CDS created by the ECMWF. As previously found ERA5 is a leader in the field of atmospheric data where the reanalysis closes the gap in modelling versus real case scenarios.

Using ERA5 for both allows for less disruption between the measurements due to the equipment used and the forecast modelling. The CDS specializes in atmospheric and planetary measurements, computations, and predictions. It uses past, present, and future modelling to develop the closest accurate understanding of the climate one can get. While there are sites available for specialized data in either wind or solar, this ERA5 format is also commonly used for open-source applications, which is beneficial in the creation of an open-source library for hybrid predictions.

The database covers a large number of atmospheric, land and oceanic climate variables usually starting on the hourly level. The data covers the Earth on a 30 km grid and the atmospheric coverage is varied along 137 barometric altitude levels from the surface up to a height of 80 km [33]. It also includes uncertainties for all variables at reduced spatial and temporal resolutions. Therefore, all of the data is shaped locally from the surface level elevation and reflects up to the highest height. ERA5 files can be downloaded from the CDS after inputting a few starting parameters. Those inputs are based on time, location, and specific climate parameters based on the surface or atmospheric levels. They are usually multidimensional arrays using longitude, latitude, levels, and time as its indexed arrays.

The files are downloaded into either GRIB or NetCDF (from GRIB) files. For directly downloading from the online CDS then any system can request and queue online, which is known as fast access. However, specific requests are not available through the online store and must be requested through a Mac or Linux environment using login credit and executing python request files. The slow access allows for model-level parameters to be downloaded, allowing for multiple heights to be requested. The resource potential does not require as many specific technical and operational parameters as the energy technology needs. These files are then loaded into MATLAB for continuation. There were a few service disruptions, which delayed the research due to the physical relocation of the data centre in Italy.

Time

For the selected climate variables, one of the three main variables used was time. The temporal coverage is archived from 1979 to the present day using hourly resolution from 1979 to the present. An underlying 10-member ensemble samples an uncertainty estimate at three-hourly intervals. The selected time period for the analysis was from 2017-2021, using an hourly resolution. During the five-year period, the constraint was set to allow for enough data to evaluate the resources in order to discover the regular patterns as well as discern any anomalies that could happen. Due to the limitations of computational resources, it was also the maximum amount of data that could be used. A smaller temporal resolution (e.g. seconds or minutes) would also lead to an increase in computational time and space with little excess impact on final results therefore was not considered. For wind and solar, it is common to use hourly or above when evaluating years at a time. Smaller resolution is used more for fine-tuning specific applications.

All the temporal data started at the base hourly resolution, and then situations for the time periods (daily, monthly, seasonal, and yearly) were extrapolated through either summation or averaging of hourly values. This displays the variability of the resources over short and longer periods of time, which will influence the HPP's ability to produce energy. It is unlikely that the natural complementarity of the resources is strong enough to maintain a balanced energy generation, without the use of storage (for excess produced) over the course of an entire year. Therefore, different scenarios and plant configurations will be evaluated based on the output of energy found.

Using the data from 2017-2021 allows for a historical and general situation to be extrapo-

lated. A set of most likely wind and solar resource patterns can be found and used for calculation for a mean year, but the outliers and unlikely situations can also be spotted and will be considered.

Location

For the single location case, both sets of files must be constrained to one longitudinal and latitudinal degree with a horizontal resolution of $0.25^\circ \times 0.25^\circ$. This geographic view creates more simplicity when calculating and cuts down on computational power. Using one location as a model site allows for mistakes or marginal errors to be caught before upscaling to multiple areas. Marseille was selected as the singular test site, and determined by a simple visual comparison of the GWA and SolarGIS of Europe, revealing an area with great solar intensity and wind speed. A parallel thesis project at TU Delft used the same site to model a hybrid plant configuration [34].

The longitudinal and latitudinal dimensions are separate arrays forming the multidimensional array of the climate-specific parameter. Each is converted from the spherical coordinates into the land coverage in m^2 . This will not be used until the energy potential evaluation as it refers more to the constraints set by the individual technologies of each renewable resource. For the resource analysis, it is merely to know what location was selected for analysis.

3.2. Resource Analysis Concept

One of the most important factors in the site's decision to install any power plant is dependent on the resources available. Therefore, in order to determine if a site is desirable, a resource assessment must be done. In this case, both the solar and wind potential must be measured and evaluated. Past resource assessments for AWE have all evaluated the potential difference from one another, the reoccurring agreement is that AWE has greater potential above the average HAWT height. The Haliade-X is regarded as one of the largest wind turbines with a capacity of 14 MW and reaches a height of up to 260 m [35], which is still a minimal range for kites. Therefore the wind resource above 100 m will be evaluated and those findings will drive the results of this research.

3.2.1. Wind

The climate-specific parameters for wind are broken into components or height-specific variables. The constraints for the data of interest are different depending on the type of data used. The ERA5 wind data is given in the form of horizontal wind speed in the northern direction v_v m/s and the eastern direction v_u m/s, to convert it to total wind speed,

$$v_w = \sqrt{v_u^2 + v_v^2}, \quad (3.1)$$

is used. The total wind speed v_w , in equation 3.1 is comprised of the directional wind speeds and must be calculated to find the combined value. Initially, this research investigated data using pressure level resolution, the vertical coverage, as the constraint was limited to 37 pressure levels [36]. An underlying ensemble samples an uncertainty estimate at three-hourly intervals. The selected levels for wind speed were, 1000, 975, and 950 hPa, which should refer to about 100, 325, and 530 m above sea level, respectively. The CDS recommends checking the heights in reference to the pressure levels using,

$$h = \frac{z}{g}, \quad (3.2)$$

with the geopotential z , at each level. The geopotential from the pressure levels is used to find the height h , along with g the gravitational constant. Then the altitude is calculated

$$alt = \frac{R_{earth}h}{R_{earth} - h}, \quad (3.3)$$

where R_{earth} is the radius of the earth and the previously found height from equation 3.2. The values all correspond to the ERA5 documentation and equations used in the Earth model. The results show the 1000 hPa hourly data points vary at heights between 90-200 m.

To evaluate the wind by specific height a new data set must be downloaded using the model level bank, which can then be converted to regular altitudes through the barometric and geometric height equations. The selected model levels were 10 heights between 100-500 m. The final ERA5 wind data used are from levels 137 to 124 shown as v_u and v_v in m/s calculated in equation 3.1 to find the magnitude and direction of the wind velocity. This method required more programming knowledge to allow for a smooth request to the CDS database.

The wind power density P_w can be used as an estimate for the resource potential using equation 1.1. The wind data will be correlated with the solar data. The wind has a shear profile from the ground up to the height, therefore the main claim is the wind at a level will represent only the wind speed at that exact height. Figure 3.2 shows the wind speeds of the extracted data at 107 m above Europe.

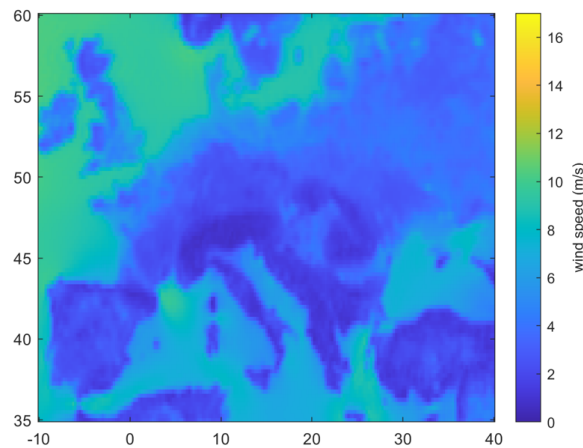


Figure 3.2: Wind speeds above Europe

The shear profile will not be considered as an assumption that the kite will not be moving with respect to the height/area for optimal energy production. The level data will also represent the vertical midpoint of the kite profile for energy generation. For example, 100 m would represent the kite flying between 75-125 m in height, meaning the actual collection from the kite may result in a higher energy yield.

3.2.2. Solar

The use of ERA5 for solar potential is fairly common, but not enough to be considered the worldwide standard. This is due to the fact that the reanalysis process considers more clear cloudless days than actually occur. However, depending on the degree of accuracy one wants this is still a good option. The archives of CDS store more than 40 years of historical data and work on forecasting and improving the collection. The ERA5 parameter used as the second source for the hybrid of this project is solar radiation. More precisely the amount of solar

radiation (also known as shortwave radiation) that reaches a horizontal plane at the surface of the Earth (both direct and diffuse) minus the amount reflected by the Earth's surface (which is governed by the albedo). The database stores the surface net solar radiation G_{SSR} in J/m^2 . This means the amount of radiation reflected and absorbed (from clouds/atmospheric particles/albedo/etc) is already considered, leaving the net amount at the surface level.

The irradiance is accumulated over a particular time period and must be converted before continuous use. In the reanalysis, the accumulation period is take place over the course of one hour ending at the extracted date and time. To convert the irradiance to watts per square meter,

$$G_{Irr} = \frac{G_{SSR}}{t}, \quad (3.4)$$

the accumulated solar irradiation G_{SSR} , should be divided by the accumulation period t , in this case one hour expressed in seconds. The G_{SSR} is the remainder incident on the Earth's surface. The data is downloaded into either GRIB or NetCDF files. ERA5 reanalysis usually shows there to be fewer clear sky days meaning that the solar irradiation is slightly higher than what is considered in a real-life measurement. Figure 3.3 is a diagram of the different components making up solar radiation. For the sake of computational power, the temperature dependency will be disregarded and the assumption of more clear days will result in a higher energy yield.

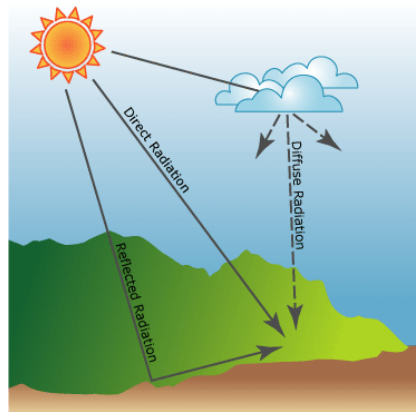


Figure 3.3: Solar radiation components [37]

Solar radiation from the sun travels through the atmosphere where it is normally composed of three components, which are modified by the atmosphere, surface, and topography of the planet. The direct radiation is unimpeded coming directly from the sun. Diffuse radiation is affected by the composition of the atmosphere like clouds or dust particles. The final component is the reflected radiation which is the reflection from the surface components. The sum of the direct, diffuse, and reflected radiation is called total or global solar radiation. For the sake of this research, the net solar surface radiation will be considered global radiation.

3.2.3. Resource Evaluation Scale

There is not the existence of standardized scale to use when evaluating a hybrid energy scenario therefore a new method was created. The overarching goal of this research is locating an area in which a hybrid power plant would be feasibly successful. This means that the resources will be evaluated based on the correlation per time period.

The trends of the wind speed at height levels and solar surface insolation must be found.

The trend lines allow for a quick visual inspection of the trend over time. The MATLAB functions (trendcomp, Trend, detrend) use singular spectrum analysis (SSA), which assumes an additive decomposition of the data. Meaning the data trend is broken up into three parts: long-term, seasonal/oscillatory, and remainder trends. The SSA is used best when the seasonal trend periods are unknown. The trends are broken up equally over time. The parts summed up equal the original data set. The trend lines are shown with respect to the original size of the data, meaning the wind speed over the time evaluated is resized to the trend value with respect to that time period. To compare the trends of wind speed and irradiation the trend line must be re-scaled.

The (anti-)correlation between each resource can be found using the corr/corrcoef function. The correlation coefficient between a pair of values is outputted with the option to pick from different correlation methods, Pearson, Kendall, Spearman. The Pearson method is selected as the correlation is exact when values one and two of the pair come from a normal distribution. This means the covariance of the pair is divided by the standard deviation. The correlation function varies over the time period/value range selected. Beginning with the hourly resolution any time period selected will sum the values and compare them to the rest of the data range. The Pearson correlation coefficient, r , is calculated using the simplified version,

$$r = \frac{n(\sum xy) - (\sum x)(\sum y)}{\sqrt{[n\sum x^2 - (\sum x)^2][n\sum y^2 - (\sum y)^2]}}, \quad (3.5)$$

or more in-depth,

$$r(a, b) = \frac{\sum_{i=1}^n (X_{a,i} - \sum_{i=1}^n \frac{(X_{a,i})}{n})(Y_{b,i} - \sum_{j=1}^n \frac{(Y_{b,j})}{n})}{\sqrt{\sum_{i=1}^n (X_{a,i} - \sum_{i=1}^n \frac{(X_{a,i})}{n})^2 \sum_{j=1}^n (Y_{b,j} - \sum_{j=1}^n \frac{(Y_{b,j})}{n})^2}}. \quad (3.6)$$

X_a and Y_b are the columns of matrices X and Y which are two different variables while n represents the length of each column or length of time. To clarify the Pearson correlation coefficient does not imply a probability of occurrence. The correlation coefficient, r , measures between -1 to 1. A p -value can also be outputted to test the null correlation hypothesis, meaning a value close to .05 is not correlated in any way, the same as when r is close to zero.

A correlation coefficient of one means that for every positive increase in one variable, there is a positive increase of a fixed proportion in the other, meaning the step size of the change is proportional to the data set itself. A correlation coefficient of negative one means that for every positive increase in one variable, there is a negative decrease of a fixed proportion in the other. Zero means that for every increase, there is not a positive or negative increase, the two just are not related. This can be demonstrated visually in figure 3.4.

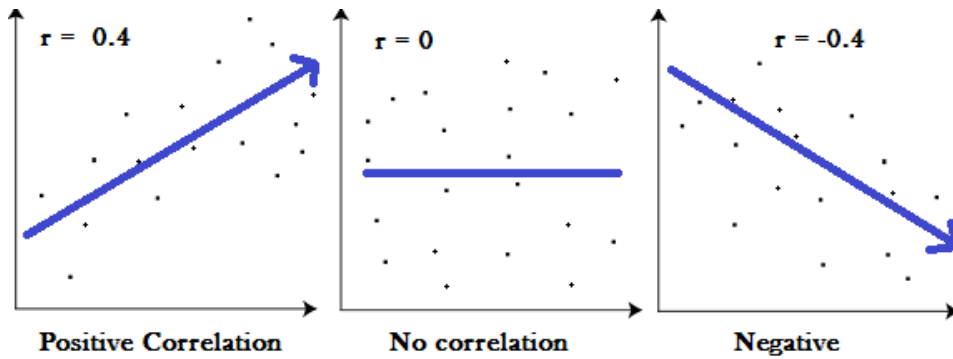


Figure 3.4: Correlation explained visually [38]

r that is higher on the positive side means that the resources are correlated and overlap (abundant or negligible at the same time). This would lead to a scenario that would benefit from an internal storage configuration. Depending on the number of resources there might be too much energy generated at the same time, and it would be better to install a system with storage capabilities.

A hybrid location ideally has a negative r meaning it is anti-correlated. This would lead to one resource peaking while the other is waning, with the hopes of a balanced system over time. This case would solve intermittency and seasonal differences which are the largest problems renewables usually face, the more negative the value the better for the hybrid scenario.

Any situations in which r is close to zero will not have the potential for a hybrid and will not be elevated to the next set. However, just investigating the r is not enough to evaluate a hybrid location. There may exist a case where the resources are directly anti-correlated resulting in a value close to a negative one, but the surrounding area cannot provide significant energy-generating potential. This would result in having to rely on a third resource to provide enough to the grid. In this case, we would need a non-intermittent resource, which is likely to be fossil-fuel based and is not a desired output. This leads to the second part of the analysis for a site, the energy potential.

3.3. Energy Potential Process

Using the results from the resource analysis of both solar and wind, the values must be further analysed in terms of energy for a deeper evaluation of a hybrid site. The biggest difference will be introducing the constraints of each technology into the equations. Figure 3.1, the overview of the model also shows the process for deriving the energy potential.

3.3.1. Airborne Wind Energy Technology

An important factor in the set-up of the test location is the technology selected and the area used. We can choose to cover the entire surface area in kites create a kite farm or select a specific number of kites. The first option would allow for the maximum AWE energy to be used.

The issue with trying to use the amount of energy that can be found per area is that the location of a potential site may not be completely suitable for the construction of kite farms. To avoid this scenario a base of one kite will be considered, the total area needed including the safety buffer is 502,400 m². The Kitepower Falcon 100 has the potential to generate a nominal power output of 100 kW between the harvesting heights of 70-400 m and a wind speed range

of 0-25 m/s. The Kitepower Falcon specifications can be found in Appendix A. The Falcon 100 has a yearly output of 450 MWh/yr meaning the capacity factor is about 51% with no efficiencies, losses, or flight conditions considered. This is a higher capacity factor than that of PV panels, therefore it will be used as the main method of harvesting energy.

As mentioned earlier the wind will be measured at specific height levels and not cover the shear wind profile, nor will the kites move to find the optimal heights for harvesting. So, the kite energy at 100 m will be the midpoint of the 75-125 m height range. The other assumption is once the kite is in the air it will stay there for the entire length of time being calculated. There will be no take-off/landing considered, meaning the kite is estimated to be in flight at all times. Kitepower is also working on an upscaled version of the Falcon 100 with a nominal potential of 500 kW, this model will be available for future scenarios.

The energy will be calculated using the Kitepower power curve from its brochure. A curve fit was created in MATLAB using the brochure's information about cut-in, cut-out, and rated wind speed, which can be seen in figure 3.5b. Below the cut-in speed, the system uses electricity rather than generating it, therefore it is possible to get negative values when running the model. The blue line is the Kitepower brochure's data while the orange line is the generated curve fit. This fitting was validated using the AWERA tool [32]. AWERA was created in another master thesis project using the QSM to calculate a precision of accuracy higher than the curve fit used in this model. Figure 3.5a is the optimized situation for Marseille and a similar curve-fit was created there.

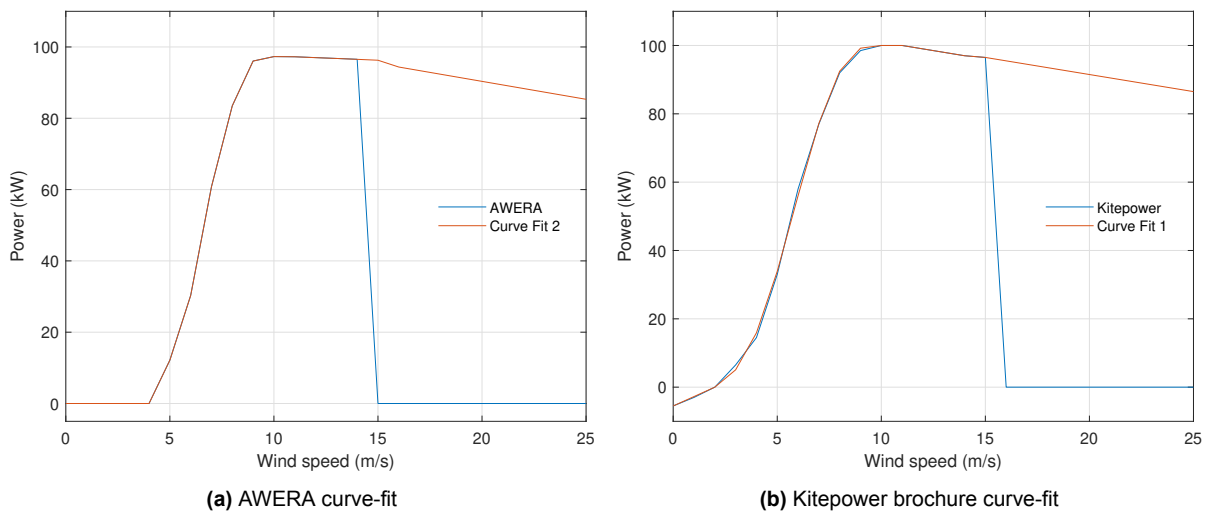


Figure 3.5: Comparison of different kite curve-fits

A side-by-side comparison of each curve and curve-fits are seen in figure 3.5. AWERA calculates power curves using simulations and algorithms to include the QSM for finding the optimal harvesting heights based on wind conditions and locations. As the purpose is to find the most optimized results, the wind speeds are clustered, and the tether/operation height is constantly changing with the base length of 200 m. This is used to create a realistic scenario but also outputs several power curves all containing a frequency of occurrence of each cluster. However, any power curves obtained from AWERA will not realistically translate in this project's calculations as the kite does not move either vertically or horizontally and calculates only at one given height. The biggest difference between the two curves is the initial start of the curves. AWERA is only positive while Kitepower reaches slightly into the negative side for electricity generation.

The annual energy production (AEP) is a key performance indicator for evaluating an energy system. The annual electrical energy production of a facility is calculated as the produced energy minus the consumed energy usually in MWh/yr. In this case, the AEP is calculated as

$$E_{AEP} = \frac{\sum P_{hr}t}{years}, \quad (3.7)$$

the value of the total energy produced over the length of time t . The energy E_{AEP} is calculated based on the amount of energy outputted from the wind speeds over time through the power curve. The measured AEP uses the actual measured values and efficiencies are included, however, it can also be more of an estimate for example over five years it's considered an averaged annual energy production. The ground station of the AWE system has a lifetime of 25 years, and the other components should be replaced regularly. Therefore, the overall system lifetime considered is 25 years which is comparable to HWAT systems. Finding the AEP from AWERA would be a better method of evaluation than the power curves.

3.3.2. Solar PV Panel Technology

Solar technology has most of the same considerations as the kites, but there are many more solar PV technologies currently available compared to the fledgling airborne energy industry. As the more established technology solar panels have reached a somewhat stagnate point in terms of innovation and the ability to change. Two important factors for PV modules are efficiency and performance. Currently, the REC group solar panels are one of the leading brands and most used worldwide. They are very efficient and have one of the best warranties making them the leading choice for many people [39]. The REC Twinpeak Series 4 350W panel from the REC Group will be used for calculations and more information can be found below in Appendix A. The same issue applies to the case study using an objective number of panels or filling the entire area. In order to create more synchronicity with each technology the number of panels will match the safe, available area surrounding the kite farm with an installed power of 201.25 kW.

As PV is a more established technology the product specification sheets for select models show all efficiencies, caps, and limits needed to calculate the power produced. Using the Sandia National laboratory toolbox one can select from a library of solar panels and inverters and a location/time to calculate all necessary information [40]. However, as the solar panel was already selected and is a newer model it does not exist in the Sandia library. Therefore, the global irradiance and values from the specification sheet will be used to calculate the power created.

The solar panels will be placed at a tilt angle of 180° which is simply directly flat on the ground. The net solar radiation will be transformed into global radiation by the end of the resource analysis. Therefore, the PV power will be based on the module components, estimated sun hours, and total irradiance that reaches the panel. First, the open circuit voltage dependent on the irradiance levels is found. Followed by the short circuit current and power production with respect to the same change in irradiance over time.

$$FF = \frac{\eta_m A_{surf}}{V_{oc} I_{sc}}, \quad (3.8)$$

$$V_{oc,Irr} = V_{oc,STC} + \frac{\eta_m K_b T_{STC}}{q} \ln \left(\frac{G_{Irr}}{G_{STC}} \right), \quad (3.9)$$

$$P_{mpp,STC-Irr} = FFV_{oc,STC-Irr} I_{sc,STC-Irr}, \quad (3.10)$$

$$P_{hr} = \eta_{Irr} G_{Irr} A_m, \quad (3.11)$$

$$E_{hr} = \int_t G_{Irr}(t) \eta_{Irr}(t) dt, \quad (3.12)$$

The efficiency is only based on the panel specifications and the irradiance as mentioned in 2.1.3. The power of one panel over the course of one hour is calculated using surface area, irradiance, and efficiency. Then the energy produced is the summation of the hourly power over the course of time. This is the amount of energy produced by one panel, however in this scenario, the solar array will be made up of 575 panels, so the total energy is the sum of the number of panels and the energy from one panel. The total surface area the panels will cover is 1050 m² which is well within the area designated as dual land-use while the Kitepower Falcon 100.

The degradation over the lifetime of the modules is also considered. Other losses like cabling, inverters, and module mismatch are included in the efficiency values with average literature values in place for each. The AEP is calculated based on the energy produced with losses, irradiation, panel type, and the number of modules in the array.

$$E_{yr} = \eta_{sys} A_m \int_t G_{Irr}(t) \eta_{Irr}(t) dt, \quad (3.13)$$

The yearly energy is calculated by summing the irradiance G_{Irr} with the time in hours over time and the efficiency of the panel, finally this is multiplied by the efficiency of the system and the surface area of the module array. The capacity factor is determined from

$$CF_{PV} = \frac{E_{yr}}{P_{nom}t}, \quad (3.14)$$

the yearly energy, E_{yr} produced over the nominal power P_{nom} , multiplied by time t in hours per year. The capacity factor of solar panels is usually quite low compared to other renewable energy technologies and is around 10-20%. The capacity factor is found by dividing the yearly energy generated by the nominal yearly energy.

3.3.3. Energy Potential Evaluation Criteria

The evaluation for the hybrid location will depend on the correlation between the resources and the amount of energy produced. The correlation and trends of the energy produced will be examined for several different time periods. The trend lines of the energy should look similar to the resources of each. The trend lines and correlation coefficients are found the same way as in 3.2.3 above. The energy of each resource can be found in the same units and comparatively evaluated directly. This allows for the identification of which resource has a higher energy output or if they are almost equal. The amount of energy, correlation coefficients, and trends all change based on the time period observed. First, the trend lines are examined to find when the resources are anti-correlated. The situations where the values are closer to -1 or 1 are identified. The amount of energy for those situations is then gathered and based on those three factors a scenario is selected.

3.4. Prospective Hybrid Site Configurations

The three possible situations are based on correlation coefficients, trends, and the amount of energy produced. Correlation coefficients are a difficult concept to grasp and are difficult to evaluate, therefore table 3.1 was created as a scale to evaluate each PCC.

Table 3.1: Scale to evaluate the PCC of hybrid energy sites

Coefficient	Value	Evaluation	Coefficient	Value	Evaluation
Positive	0.0-0.10	Very Poor Correlation	Negative	-0.10 – 0.00	Very Poor Anti-Correlation
Positive	0.10-0.25	Weak Correlation	Negative	-0.25 – -0.10	Weak Anti-Correlation
Positive	0.25-0.50	Moderate Correlation	Negative	-0.50 – -0.25	Moderate Anti-Correlation
Positive	0.50-0.75	Good Correlation	Negative	-0.75 – -0.50	Good Anti-Correlation
Positive	0.75-1.00	Excellent Correlation	Negative	-1.00 – -0.75	Excellent Anti-Correlation

For a strong hybrid case, the daily PCC should be on the negative side of the table and between good and excellent conditions. To evaluate and place each hybrid case both the energy generation and the correlation coefficients are considered together. After they can be classified into the situations seen in the overview figure 3.1. Each situation is classified below composed of energy and correlation outputs.

1. Anti-correlated and abundant energy produced - Hybrid case with minimal storage
2. Correlated and adequate energy produced - more than minimal storage needed
3. Correlation and energy abundance depends on time period - supplement support needed

The above list does not have a situation in which the resources have an r -value that is close to zero. In that case, it would not pass the first criteria of the resource assessment step, meaning there is no value in calculating the energy potential as it is not hybrid feasible under these conditions.

Option 1 - Positively Correlated

The first case means that there is an adequate relationship between the correlation coefficient and energy generation. To specify at least 40% of the daily PCCs are less than -0.40 meaning the minimum threshold for consideration is moderate. The minimum energy needed based on the control case of 575 panels and 1 kite, is 600 MWh/year. This can be further split into sub-cases based on how the energy is generated. If one resource is generating at least 60% or more of 600 MWh then that technology is the primary stakeholder. If both resources are generating energy at about the same levels then this is the prime scenario of equal footing for the hybrid system. All the scenarios will need some form of storage, however, this case requires the smallest amount, mostly for contingencies.

Option 2- Anti-correlated

The second case is the same as the first but in the opposite direction. Therefore, at least 40% of the PCCs are greater than 0.40. If both resources are generating energy with similar output, but are correlated then it tends to be at the same rate. This means the storage system needed stores the excess energy produced at the same time, and it is used to supplement and fill in gaps when the energy generation dips, but demands increase.

Option 3 - Time-dependent correlation

The final case for consideration is when there is not an adequate relationship between correlation coefficients and the minimum 40% of the time is not met being, (greater than an absolute

value period of 0.40), but the minimum energy requirements are fulfilled. However, there may be some periods, i.e. quarterly basis where the correlation coefficients exceed the minimum value needed. With these situations clearly defined the next step is to run a test location.

4

Case Study - Marseille

This chapter focuses on the results obtained for the resource and energy potential models. The location used as a test site was selected based on a visual analysis of the Global Wind and Solar Atlas, identifying an area in Europe in which both solar and wind are abundant. The test site is located on the outskirts of Marseilles, France, and the time period selected for analysis was 2017-2021.

The first Section 4.1 will cover what the resource model outputs and what results mean. Then the in-depth evaluation of the energy model will be performed in Section 4.2. This is followed by Section 4.3 which explains each of the scenarios available and which one Marseille fulfils. Finally, Section 4.4 is a comparison of results from multiple locations.

4.1. Resource Case

As explained in the previous chapter the resource analysis evaluates the wind speeds and solar irradiation to find the correlation and trends between the two. Marseille was selected as the location to test the model as there was an overlap between the wind and solar potential. The coordinates of the unique location in Marseille are from 44° north 5° east to 43° north 6° east with a total calculated surface area of 9e9 m². The wind speed will be inspected at several heights, the same will be done for the solar irradiation. Then the relationship of the correlation over several different time periods will be analysed with an anticipated outcome of anti-correlation values from -0.40 and lower.

4.1.1. Wind Speed in Marseille

To begin the wind speed over the course of the 5-year period (2017-2021) must be extracted at selected heights. As mentioned earlier in 3.1.1 the resolution of the data is in hourly increments. The ERA5 atmospheric parameters for p , u , v , z are used to obtain the wind speeds for the range of model levels 137-124. However, only five levels will be used: 133, 130, 128, 126, and 124, which correspond to the respective geometric heights of 107, 205, 288, 385, and 501 m.

The wind speed at each height is calculated using equation 3.1 as a multidimensional array with dimensions of latitude, longitude, level, and time. The array is reshaped into level x time using the mean with respect to the latitudinal and longitudinal coordinates. Due to the lack of computational power, this provides that the mean over the location is found, rather than the 0.25° x 0.25° horizontal resolution in latitude and longitude. There is no surprise as the heights

increase so do the wind speeds. Below in figure 4.1 the hourly wind speeds for the lowest and highest heights are plotted over time.

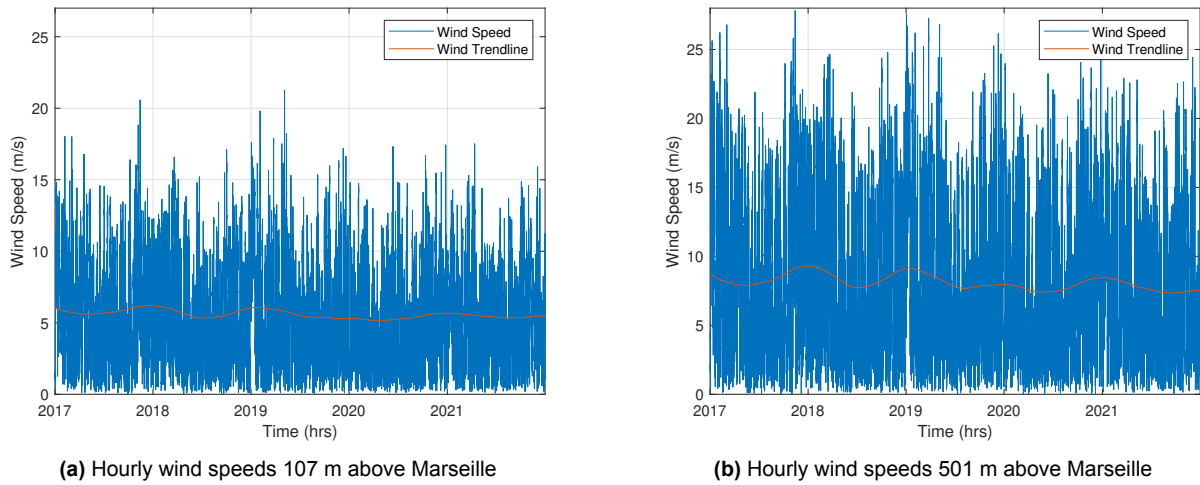


Figure 4.1: Hourly wind speed in Marseille for lowest and heights points between 2017-2021

The plots in figure 4.1 show great variability in each time step. The five-year period allows for a trend to be spotted. Following the curve, the wind speed dips around the halfway point during the year. Summer tends to see lower speeds while winter a bit higher. The difference in wind speed is also noticed along the height when comparing figures 4.1a and 4.1b, there is an increase in wind speed as the height increases.

Using MATLAB, temporal variations begin to emerge. The average wind speed found per hour at each height is shown in table 4.1. The wind speeds in the table were found by taking the hourly mean for 8760 data points to get each year. The 5-year column refers to taking the mean of all five years of data. Table 4.1 shows 2017 results in a higher average wind speed throughout the year and 2020 has a lower average for the wind speed.

Table 4.1: Yearly average wind speed in m/s above Marseille between 2017-2021

Heights (m)	2017	2018	2019	2020	2021	5-yr
107	6.0340	5.5270	5.7912	5.3042	5.5198	5.6351
205	7.1008	6.5952	6.8529	6.2758	6.5233	6.6694
288	7.7249	7.2193	7.4646	6.8303	7.0763	7.2629
385	8.2960	7.7724	8.0153	7.3170	7.5424	7.7884
501	8.7776	8.2343	8.4840	7.7138	7.8970	8.2211

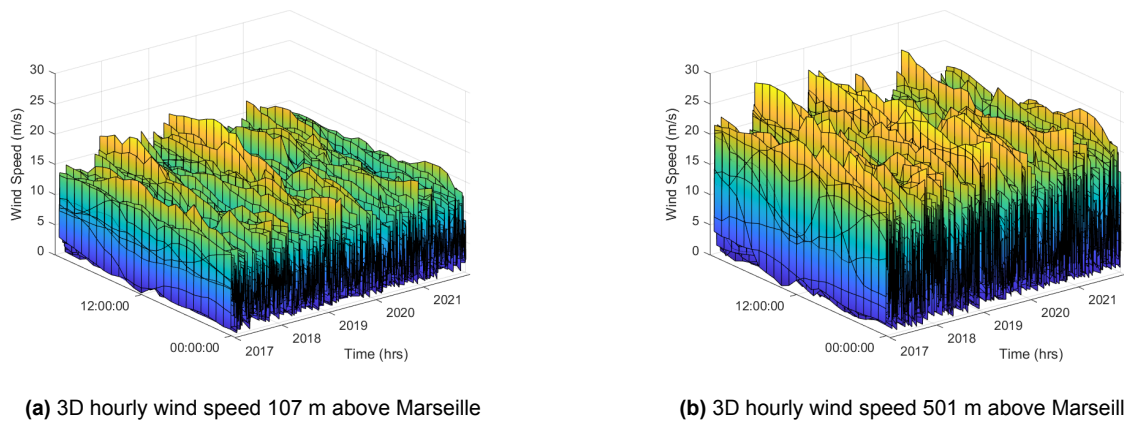
The same trend of increasing wind speed with respect to height is shown in table 4.1. Therefore it is expected that this trend will be in all of the following analyses. The further temporal analysis will be found on a seasonal and biannual basis. Seasonal is defined as quarters: January to March (Winter), April-June (Spring), July-September (Summer), October-December (Fall). For the biannual basis, there are two periods, January-June (1st Half), and July-December (2nd half). Using a monthly interval allows for a closer look at where the maximum and minimum values are found and if they fall in a similar pattern to other years. The average monthly wind speed is found in table 4.2 for all five years.

Table 4.2: Average monthly wind speed in m/s above Marseille between 2017-2021

Height (m)	Jan	Feb	Mar	Apr	May	June	July	Aug	Sept	Oct	Nov	Dec
107	6.8826	5.7607	5.8764	5.5191	5.4313	5.0125	5.1956	5.1066	4.7454	6.1708	6.0518	5.8402
205	8.3794	6.9914	6.9866	6.4494	6.3318	5.7348	5.9226	5.8771	5.5347	7.3407	7.3006	7.1593
288	9.2507	7.7345	7.6233	6.9827	6.8436	6.1293	6.3221	6.2962	5.9884	8.0032	7.9996	7.9607
385	10.0197	8.4279	8.1937	7.4625	7.3006	6.4760	6.6576	6.6345	6.3957	8.5911	8.5978	8.6892
501	10.6828	9.0600	8.6962	7.8692	7.6869	6.7329	6.8886	6.8426	6.7152	9.1006	9.0545	9.3180

When observing the monthly averages, the dip in wind speed happens from June through September which corresponds to the usual summer months in the northern hemisphere. Before seeing the correlation, it is reasonable to assume that the peak for the solar irradiance will happen during summer which is also the lowest period for wind.

The last temporal variation that is important to note is observations shown throughout the day. There is an expected trend to show higher wind speeds during the evening and early morning as opposed to mid-afternoon. These are the diurnal patterns discussed in Chapter 2, which describe observations that happen during a 24-hour cycle.

**Figure 4.2:** 3D graph of wind speed above Marseille 2017 to 2021 from daily and yearly perspective

This pattern is not as easy to discern compared to the solar daily irradiance, but it is still visible. Figure 4.2 shows most of the peaks happen at the edges of the y-axis in the 3D graphs. The x-axis is the time in days over the course of the 5 years, the y-axis represents the time of day in hours from midnight (00:00) to midnight, with the halfway mark at noon (12:00). The final axis is the z-axis showing the wind speed range from 0-30 m/s. The relationship between height and wind speed is also easily discernible in the above graphs.

After noting areas of significance with respect to times, the trenddecomp function is applied to the wind speed levels. This allows the trends associated with the data to be individually found. Each trend output is composed of three parts long-term, seasonal/oscillatory, and the remainder, these trend lines summed up equal the original data, for more information refer to 3.2.3. In this case, the long-term trend will refer to the overall progression/pattern found over the course of five years.

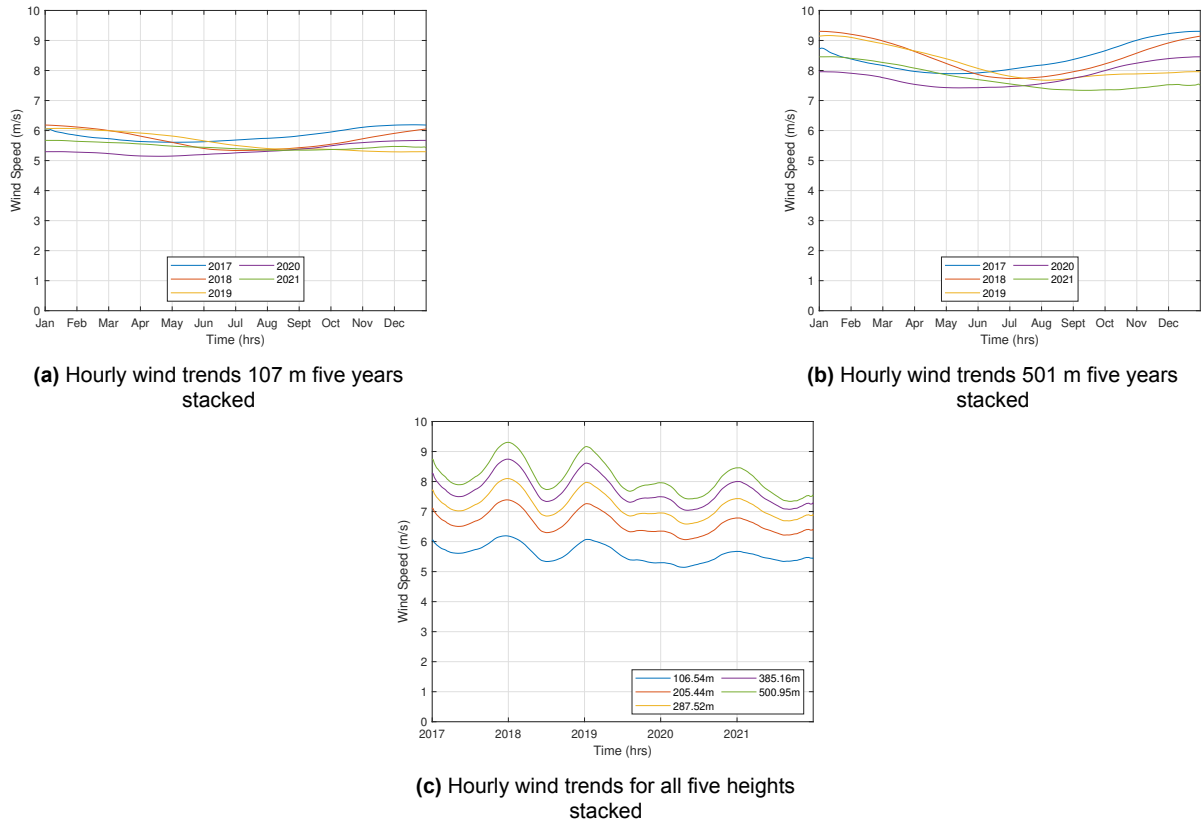


Figure 4.3: Trend lines for five geometric heights for wind speed above Marseille

The trends show the patterns in the data set with respect to time. When looking at figure 4.3c it is clear the wind speeds are higher during the winter months and lower in summer, which holds true to previous observations in table 4.2. Figure 4.3c also shows clearly the relationship between wind speed and height. With plots in figure 4.3a and figure 4.3b it is more difficult to observe differences due to the trend function. Long-term in these cases equals one year and the oscillatory trend is four seasons which is the minimum needed for the long term meaning there would little difference between the two. Differences are much clearer using more than one year of data with this function as there would be multiple inflection points to represent the change in seasons.

Overall in Marseille, the average wind speed reaches 5-9 m/s increasing proportionally with respect to height. There is a clear annual trend separating the winter from the summer, with weaker winds in summer and the lowest on average in July. Based on this there is an expected increase in energy produced with respect to operational height. Once the solar patterns are determined the correlation values between the two can be found.

4.1.2. Solar Irradiation in Marseille

In solar data, set patterns are much more predictable and expected. The sun rises and sets each day and with that about half of the time, there is no solar radiation expected. The diurnal patterns for areas near the poles are unusual as they have periods of extreme sun hours or extreme night for times surrounding the solstices. Each pole gets about 24 hours of pitch darkness every “day” for about 10 weeks per year during its winter period. While the same can be said about the summer period. Therefore, looking at the poles over the course of a year it almost balances out, however on a smaller scale like monthly intervals there is a major

difference from the rest of the world. The closer to the equator, the more predictable the diurnal pattern is for the estimated sun hours. For Marseille, it is expected to see no solar irradiance when the sun is down for the hours between 18:00-06:00 on average.

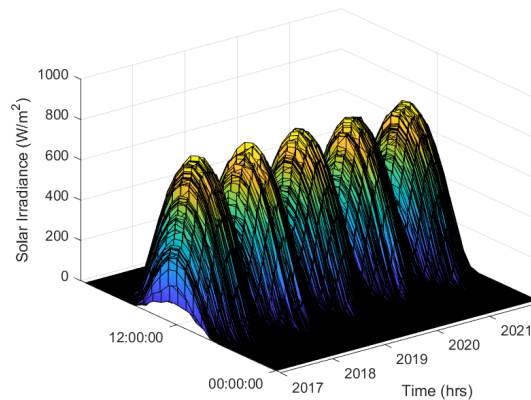


Figure 4.4: 3D graph of hourly solar irradiance in Marseille 2017 to 2021 from daily and yearly perspective

Figure 4.4 shows the diurnal pattern with solar irradiance equal to zero in the evening to early morning and a maximum occurring around 12:00. There is also an annual peak in the summer months. The 3D graph shows that the irradiance is roughly more predictable and equal on an annual basis throughout the 5-year period. Figure 4.5a illustrates figure 4.4 in 2D, where it accounts only for the x and z axis and the sum of the daily solar irradiation.

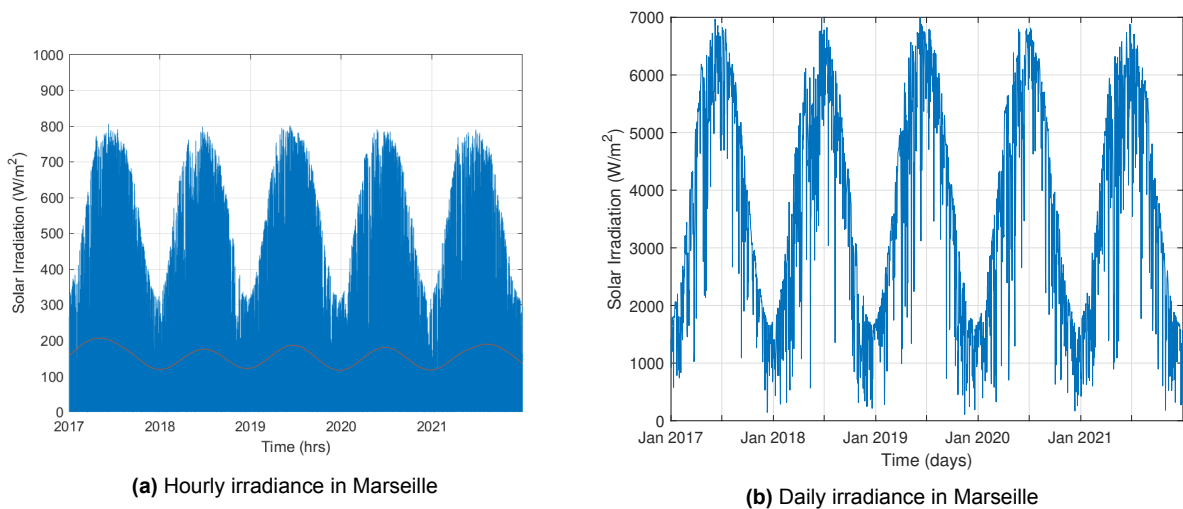


Figure 4.5: Solar irradiance in Marseille 2017-2021

The variation of the solar irradiance can be easily observed in figure 4.5a. The amount of solar irradiance each year varies slightly, but not as much as the wind speed. Figure 4.5b shows the sum of the hourly solar irradiance per day. The sum is important because, unlike the wind, the irradiance used in PV can be collected. Whereas wind technology relies on the change in wind speeds to generate energy. There are also a few days where there is a significantly lower irradiance with respect to the annual trend, one which can be seen in late 2018, these are due to clouds obstructing the sun. These are expected but difficult to forecast

the effect on the irradiance levels. The amount of solar peaks in the summer and dips in winter remains to be the opposite behaviour of the observed wind speeds.

The solar trend line shows the same conclusions as the previous plots. Figure 4.6 indicates the peak during the year is in the summer and much less irradiance is available in the winter. However, depending on the other weather patterns the data may show a shifted peak from the norm.

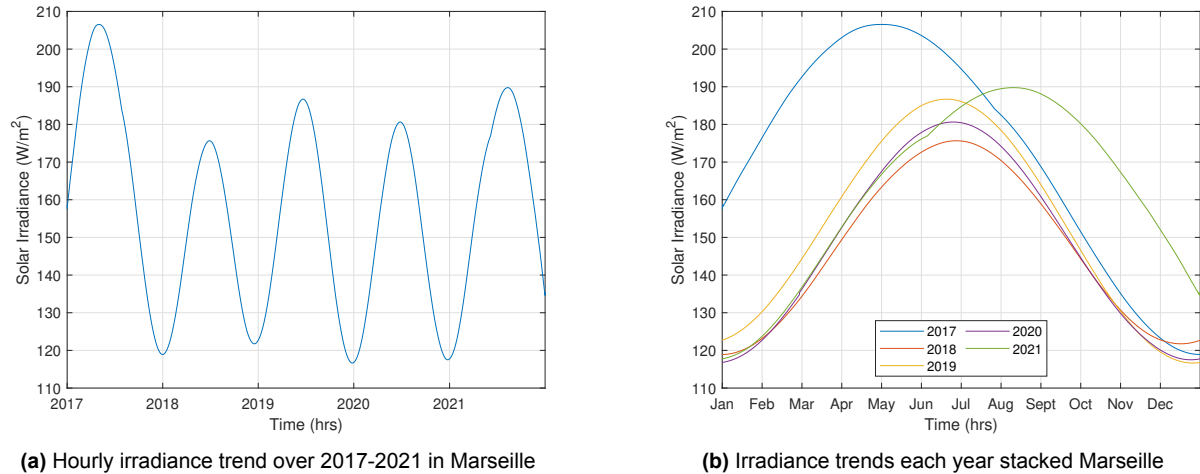


Figure 4.6: Solar trends for Marseille 2017-2021

In figure 4.6b, the 2017 trend shows a greater peak closer to May and the 2021 trend is shifted to the right. This shows how difficult it would be to accurately model and forecast energy predictions. Though when both 2017 and 2021 are averaged together they show a curve peaking closer to the other three years in mid-June/July. Therefore, the energy potential on an annual basis would be still in line with predictions, but not for smaller intervals.

Overall the solar irradiance behaves opposite to the wind speed. The resolution of both is hourly which is suitable for the research means of this project, any higher fidelity would need an increase in computing capabilities. From these observations there is an expected anti-correlation between the two resources on an annual basis. With the strongest Pearson coefficient values in the summer and winter.

4.1.3. Resource Correlation Marseille

It is essential that the first step in evaluating the correlation between resources is finding out if there is any change in correlation. If there were no indicators that the resources would be correlated, then the following evaluations would be essentially useless. Finding each of the long-term trend lines allows for a first look at the possibility of correlation and the ballpark of what the calculated values represent. It is easier to see early conclusions when both are shown together.

Figure 4.7 shows both resource data sets plotted with the same x-axis and normalized. The MATLAB function normalizes defaults to have a mean zero and a standard deviation of one. The normalization method used here is a range, where the data is scaled to an interval of [a b], where $a < b$. Equation 4.1 shows the normalization method used. X is the original data, a,b are the limits of the normalized data.

$$X_{rescaled} = a + \frac{X - \min_X}{\max_x - \min_x} (b - a), \quad (4.1)$$

Figure 4.7a shows the long-term trend lines of each resource plotted with a shared x-axis. Figure 4.7b shows the trend lines normalized which appear to be shifted downwards.

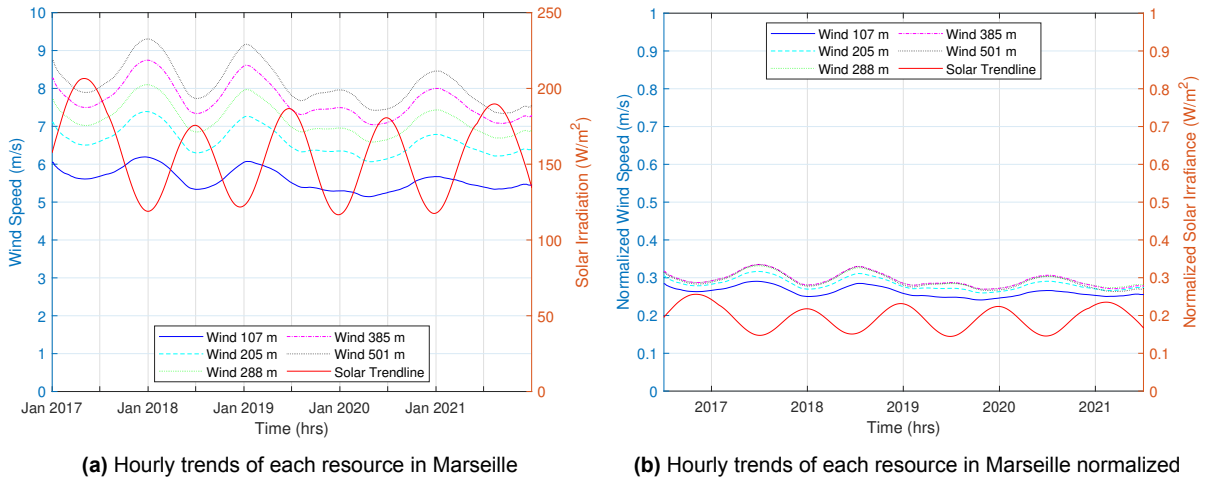


Figure 4.7: Resource trends for Marseille from 2017-2021

Normalizing the data is not enough to show the relationship between both resources. Trends between two different sets of data are easier to spot when each has been re-scaled. Re-scaling is different from normalizing as the range and dependencies change. In MATLAB the re-scale and normalize functions are the same for the default option, however, they can be adjusted to better suit the needs of the data.

Re-scaling changes the distance between the min and max values in a data set by stretching or squeezing the points along the number line. The z-scores of the data are preserved, so the shape of the distribution remains the same. While the normalize and re-scale functions can both re-scale data to any arbitrary interval, re-scale also permits clipping the input data to a specified minimum and maximum values [41].

$$B = L + \left[\frac{A - X_{inputmin}}{X_{inputmax} - X_{inputmin}} \right] (U - L), \quad (4.2)$$

Figure 4.8 is re-scaled using the formula in equation 4.2, L is the default value of zero as is U defaulted to 1. Input min is the selected minimum value of the entire data set and input max is the selected maximum value of each resource set. Re-scaling allows for the comparison of two different variables on equal grounds.

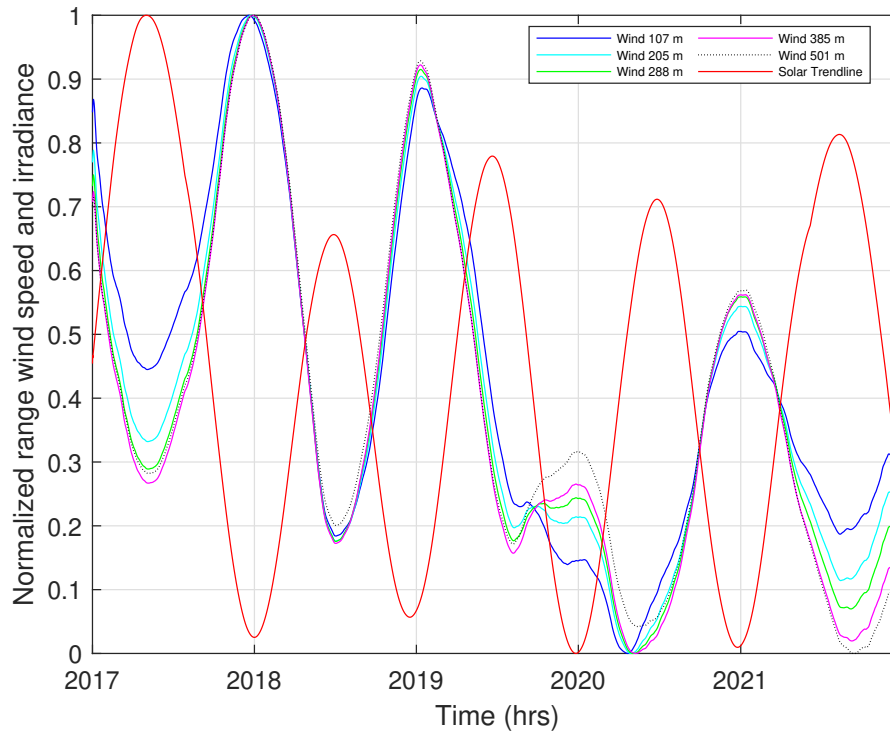


Figure 4.8: Re-scaled and normalized wind speed and solar irradiance trends for Marseille

Here the plotted trends show the annual variation of each resource, in relation to each other. The predicted anti-correlation is more visibly prevalent on this scale. It is safe to assume that the majority of the time the resources are anti-correlated. Visually this is shown as one line peaking near one and the other dipping around zero. The line must continue to increase or decrease opposite to the line it is compared to. Based on the trends, the correlation coefficients between the solar and wind will be highest between the heights 385-501 m. The most negative Pearson value is expected at the beginning of 2018 and the worst correlation is expected between summer 2019 and summer 2020.

To investigate the correlation coefficients fully it is necessary to start with a broad scope and zoom in on interesting areas. The correlation values can be found in several tables in Appendix C. Table C.1 holds Pearsons' correlation coefficients from the monthly up to yearly time interval between the wind speed and solar irradiance. Table C.2 refers to the calculated PCC values on a weekly basis. Finally, the smallest calculated PCC value is on a daily interval found in table C.3. Each of these table values was calculated using the same hourly resolution.

The correlation coefficients are calculated based on the number of hours in the interval of time stated by the header of each column. For example, the PCC value for the year is 43800 wind data points compared with another 43800 data points for solar into one value. As the intervals decrease in time the more precise the correlation coefficients are.

As can be seen in table C.1 the values all range between -0.25 to 0.10 which means they are poor or weak (anti)correlation. When the PCCs are greater than $|\cdot 25|$ then they reach moderate status and can be used for potential hybrid planning. The tables are colour-coordinated to show the visual range of correlation. Dark red indicates values close to the ideal negative anti-correlation value, while bright green refers to high correlation. White values are representative of poor correlation in either direction or are not correlated in any way. From seasonal basis and higher there is only one positive value 0.0117 which shows closer to the null corre-

lation theory rather than being positively correlated. On the monthly interval, there are a few areas that indicate correlation, but the majority of values are still anti-correlated.

This can be seen in table C.1, where the correlation coefficients are calculated using the hourly resolution summed over the course of the time period found in the heading of the table. The year column represents the hourly values summed over the year and each height has one correlation coefficient representing the whole time period. The year column shows an increasing anti-correlation as the heights increase however the max varies mostly between the fourth and fifth height, it can also be seen that 2018 has the highest anti-correlation and 2020 with the lowest. The yearly correlation coefficients are between -0.1583 to -0.0597 which is low by correlation standards, from an absolute value of 0.25 and above the correlation is strong enough to start planning around. As predicted the PCC value is stronger with smaller intervals of time. However, none of the time intervals in table C.1 are strong enough to be considered helpful to determine the hybrid potential.

In Appendix C the weekly values can be found in table C.2 ranging from -0.5638 to 0.3093. This point on the PCC values shows a strong enough relationship between solar irradiation and wind speed, to contribute positively to a hybrid power plant. The trends show there is an increase in the absolute correlation value as the wind height increases, however, the heights of 288, 385, and 501 m trade-off are top spots on each occasion. This means that the optimized height technique that AWES employ can take advantage and change the height to match the best correlation. Figure 4.9 graphically demonstrates how the correlation value is found. The wind speed for a select period of time is plotted against the solar irradiance for the same time. Then the opposite scatter plot is found. The r value as shown on the left of each scatter plot is equal to the value of the least square regression fit.

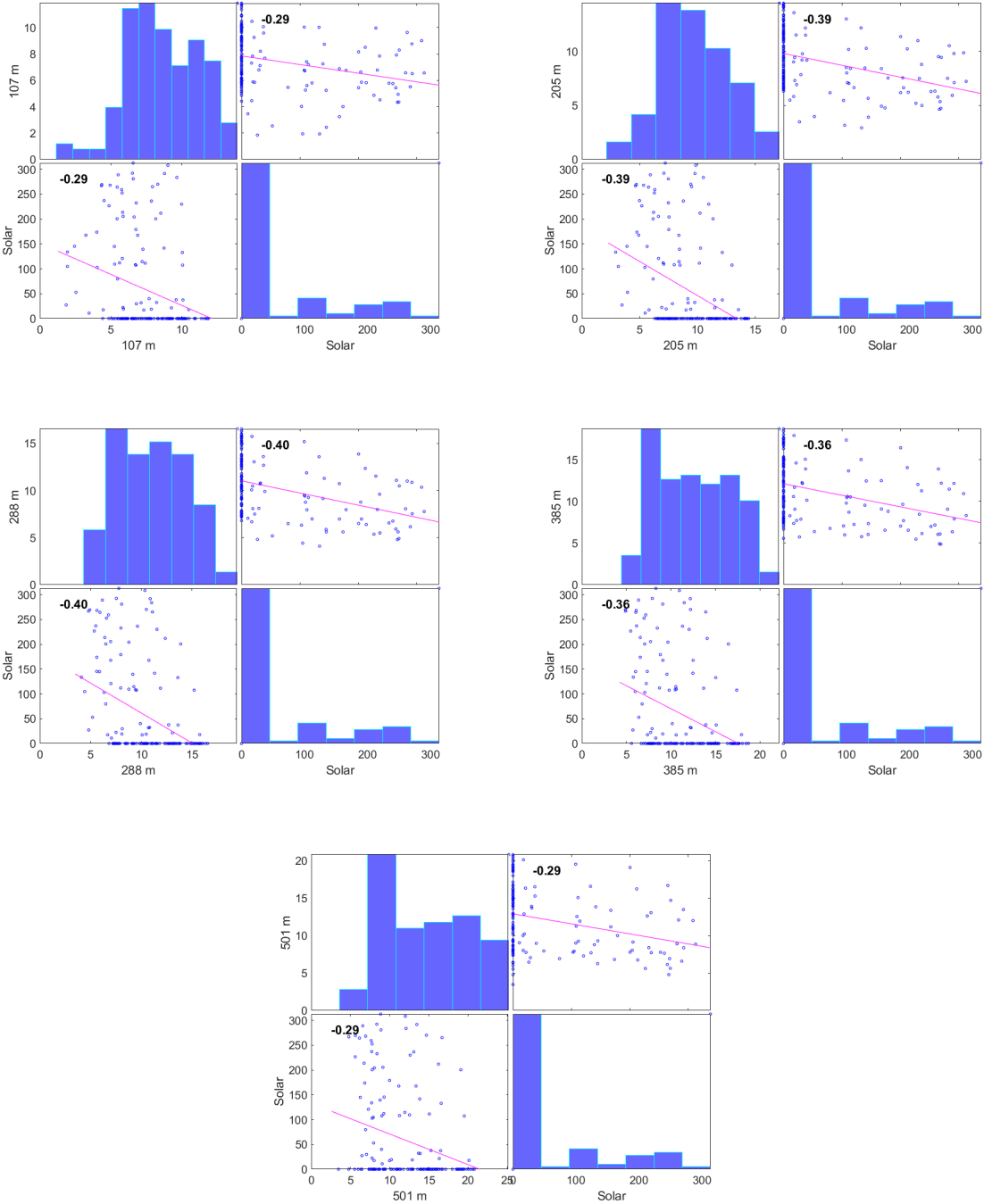


Figure 4.9: Correlation plots of resource trends in Marseille Week 51 in 2017

Each scatter plot has 168 points representing the hourly values of either the irradiance or wind speed. The correlation coefficient value should be the same when comparing the same two variables. To check the values are correct simply refer to table C.2 find the 51st week in 2017 and verify the value are the same for each height.

To further investigate we zoom in on the smallest scale correlation possible which is over the course of 24 hours. The final resource table in Appendix C shows the daily correlation

values, table C.3. This table has the most impressive range of -0.9758 to 0.9284. A heatmap displayed in figure C.1 is provided for better understanding. As there are 5 heights over 5 years to correlate per day means there will be a minimum of $5 \times 5 \times 365$ values in that table. Therefore breaking the table down into a heatmap helps as a visual aid in understanding the relationship between the resources.

The example used to demonstrate the correlation of a daily resolution is found in figure 4.10. Looking at table C.3 one of the strongest anti-correlated days was on January 29th, 2018.

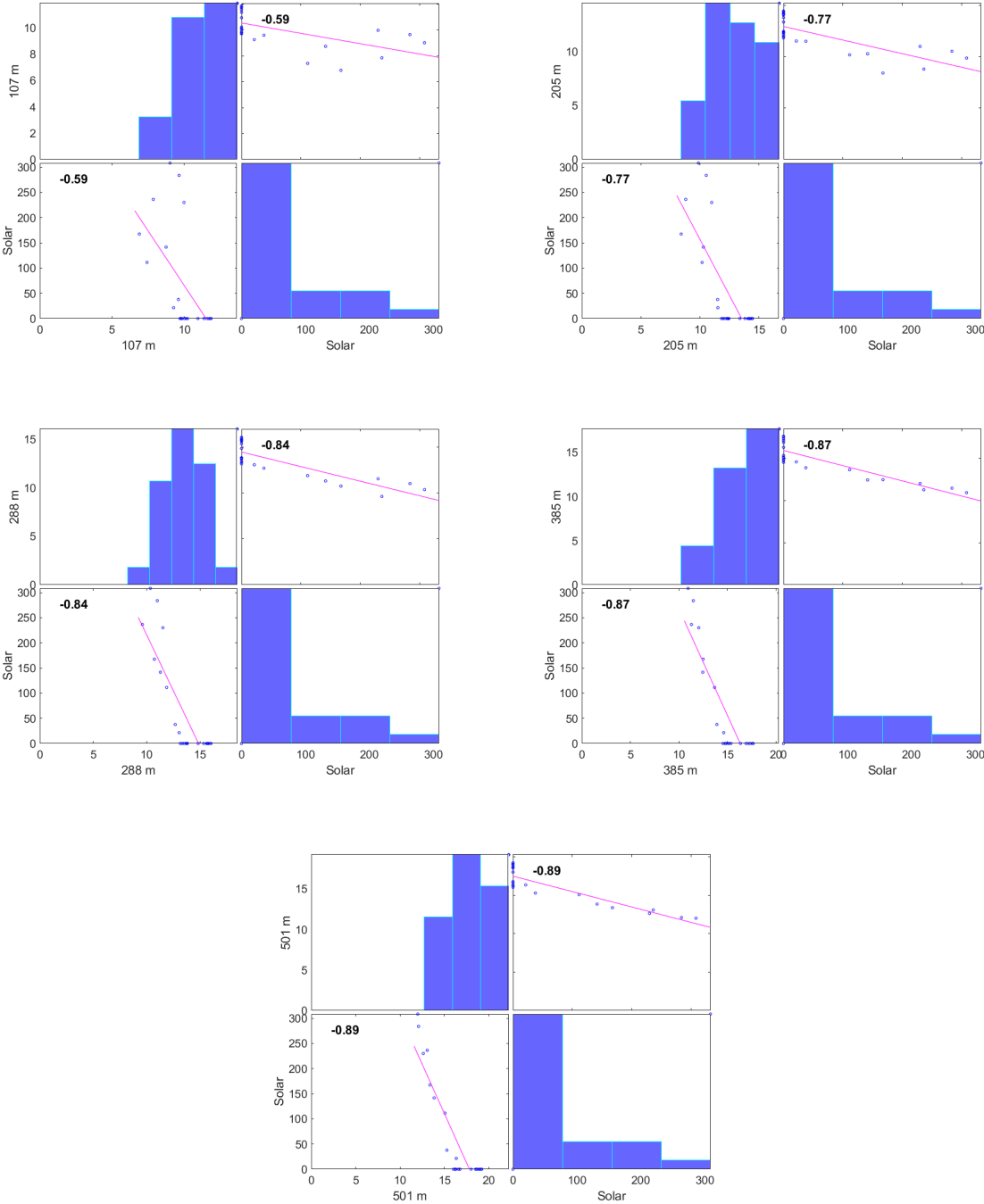


Figure 4.10: Correlation plots of resource trends in Marseille January 29 2018

Unlike the weekly example, this plot is derived from only 24 data points, as such the R-value has increased. To further investigate the resource correlation figure 4.11 is a histogram that sorts the daily values into bins on both a temporal and height basis.

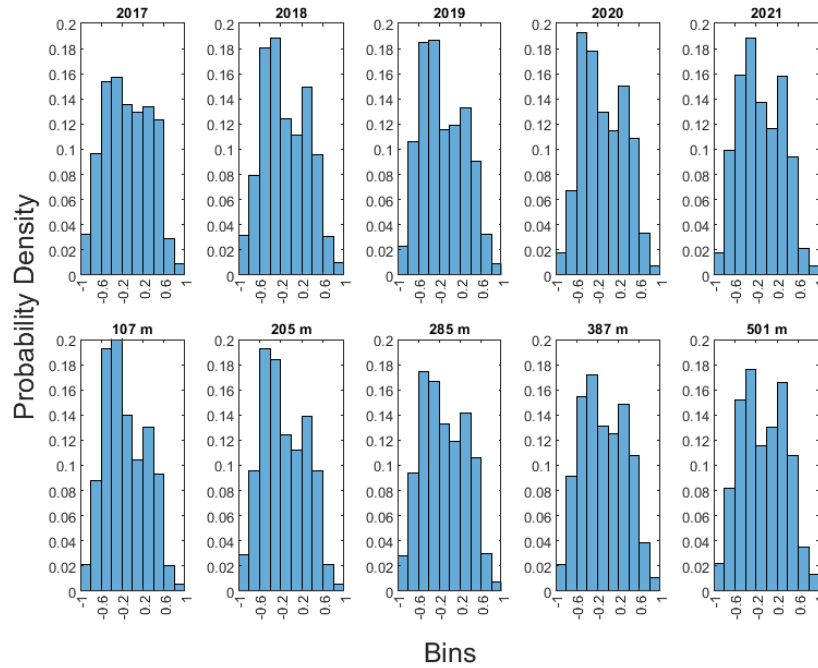


Figure 4.11: Correlation Histograms per time and height in Marseille

The bins form the correlation range from perfectly anti (-1) to perfectly correlated (1). The bins are skewed to left indicating a majority of anti-correlated values. As can be seen more than 85% of the time the correlation is greater than the absolute value of 0.1 in all instances. However, about 60% of the time the correlation coefficient is negative and only 20% are positive, meaning there is more anti-correlation between the sun and wind resources during the day.

In order to determine if the location has enough resource justification to move to the energy analysis, it must meet a minimum threshold. The minimum requirement: * the majority of the |correlation coefficients| is greater than or equal to 0.25. In this case more than 50% of the daily PCC is equal to |0.36| meaning it passes on to the next step in the analysis. The resource analysis section is not considering the amount of energy generated therefore the correlation coefficients can be of lower value. Once the energy scenario is evaluated the correlation coefficients and the amount of energy produced to determine which scenario fits each location.

4.2. Energy Case

For the energy case, the amount of installed must be set in order to compare the two. This group of calculations has an installed capacity of 100 kW for the AWES and an overall installed capacity of 201.25 kW of PV panels. The installed capacity for solar energy comes from 575 modules with a maximum power of 350 Wp.

4.2.1. Kite Energy in Marseille

To calculate the amount of energy derived from the AWE technology, the power curve and wind speeds are used. The power curve for the Kitepower Falcon 100 model is found in Appendix A, this is the technology used for the wind aspect of this research. To check the replicated curve a curve fit is done before the real wind speeds are used for power calculations. Once the curve is fitted and validated, the power curve can be used to start calculating the actual

power at an hourly frequency. Using the hourly resolution wind speed data set, increasing in time the wind speed uses figure 4.12 to find where it intersects with the curve at the instance in time with the power produced in watts.

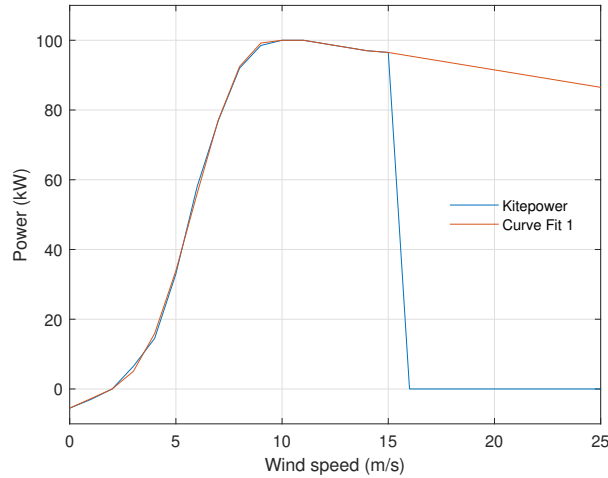


Figure 4.12: Curve-fit with Kitepower

As can be seen from figure 4.12, the curve looks similar to wind turbine power curves. There is a sharp incline from the cut-in wind speed of 3 m/s to roughly 9 m/s. This is where most of the wind data from Marseille falls in after there is a slight decline from the rated wind speed all the way to cut-out wind speed. The wind speed per hour is inputted then where it intersects with the curve is the power that wind speed generates. Currently, the Kitepower Falcon 100 kW has a cut-out of 16 m/s but is planned to have a future cut-out of 25 m/s. Figure 4.13a shows the power produced at each instance in time over the course of 2017.

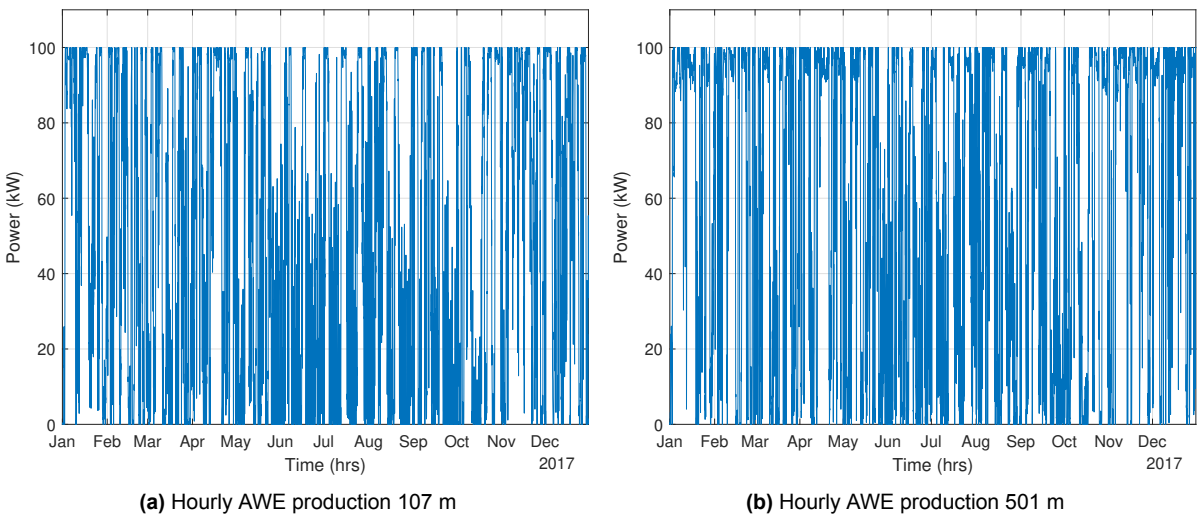


Figure 4.13: Hourly AWES power production for 2017

The power produced dramatic changes over time. Figure 4.14 shows the trends over the 5-year period for the energy generated from the AWE technology. The difference in heights shows an obvious increase proportional to the increase in height. The 107 m height is much lower than the cluster of the other four heights, this can be due to the exponential change in difference due to the surface roughness as height increases.

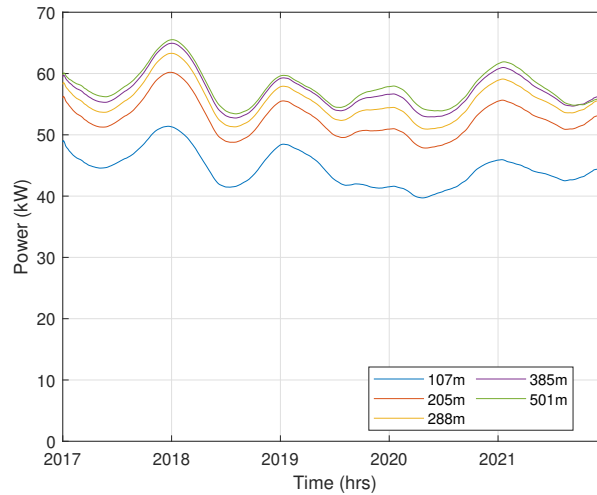


Figure 4.14: AWES kite power trends five years stacked

The trends show that there is very little difference between the 385 m and 501 m height, therefore for future comparisons, it would be best to stick between the heights of 200-300 m. Figure 4.14 also shows a decreased energy generation in the summer months. The average energy produced per year was between 365-530 MWh/yr across all five heights.

4.2.2. PV Energy in Marseille

The PV panel power production can be found in figure 4.15 shows a very similar figure to one of the raw solar irradiances. From both, it can be seen that there is a peak in production during summer. The installed capacity is 201.25 kW, however, the max power generated is around 130 kW which is slightly more than half.

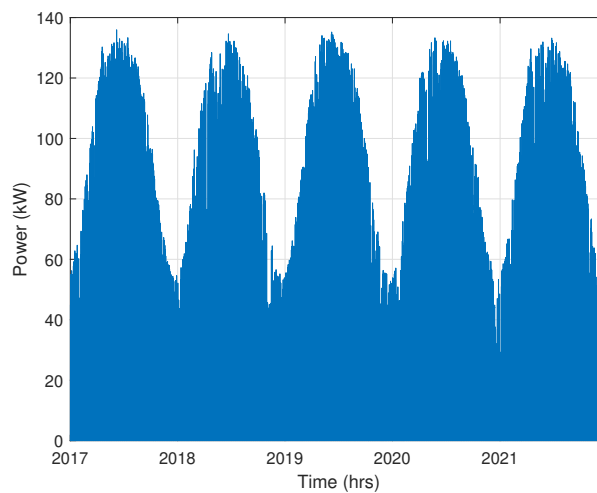


Figure 4.15: Hourly PV array power production in Marseille 2017-2021

The amount of land these panels cover is 1,050 m². The average AEP by the PV installation was around 223 MWh/yr. On average it supplies around 30% - 36% of the total energy.

4.2.3. Energy Correlation Marseille

The energy trends for each renewable technology can be found in figure 4.16, from this the amount of energy produced by the PV panels is much lower than the AWE. These trends show

that the current installed power for PV panels should be at least doubled to match the amount outputted from the wind side. However, this does not show clearly how the energy of each correlate, as the trends can change with more installed power, shifting vertically on the graph.

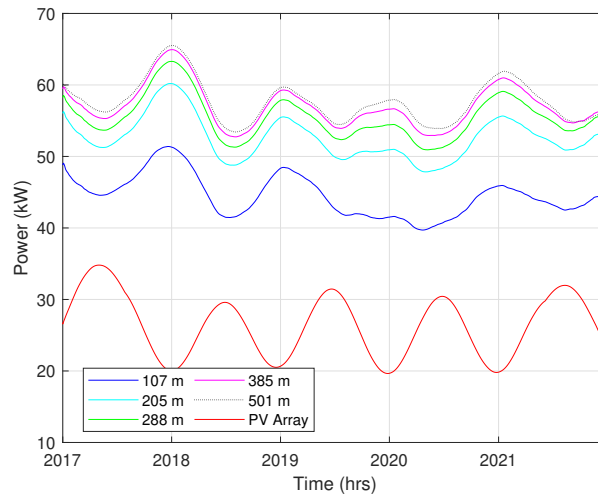


Figure 4.16: Hourly power trends in Marseille 2017-2021 stacked

The re-scaled trends shown in figure 4.17 depict a typical sinusoidal function for the PV panel and a less smooth curve for the wind technology. This means that solar PV generation can be more accurately predicted with weather and historical data. The PV power can be considered the more stable power-generating aspect of the hybrid configuration.

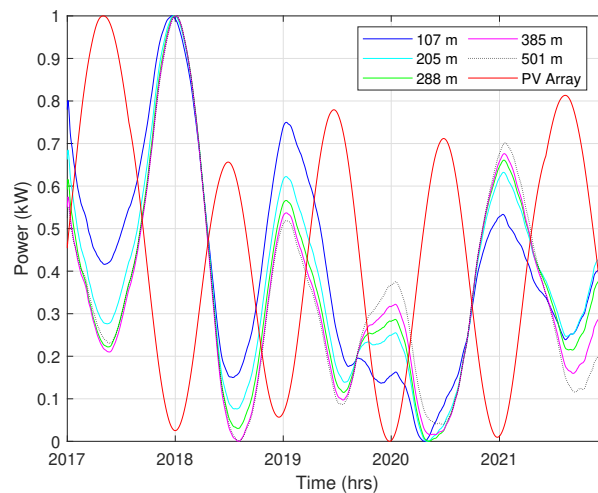


Figure 4.17: Hourly power trends in Marseille 2017-2021 re-scaled

The interesting aspect in figure 4.17 is that the airborne energy generated at the 385 m height is more anti-correlated with the solar power during summer while winter is between the extremes of 107-501 m. The following figure 4.18 shows the PCC of generated energy sorted into bins.

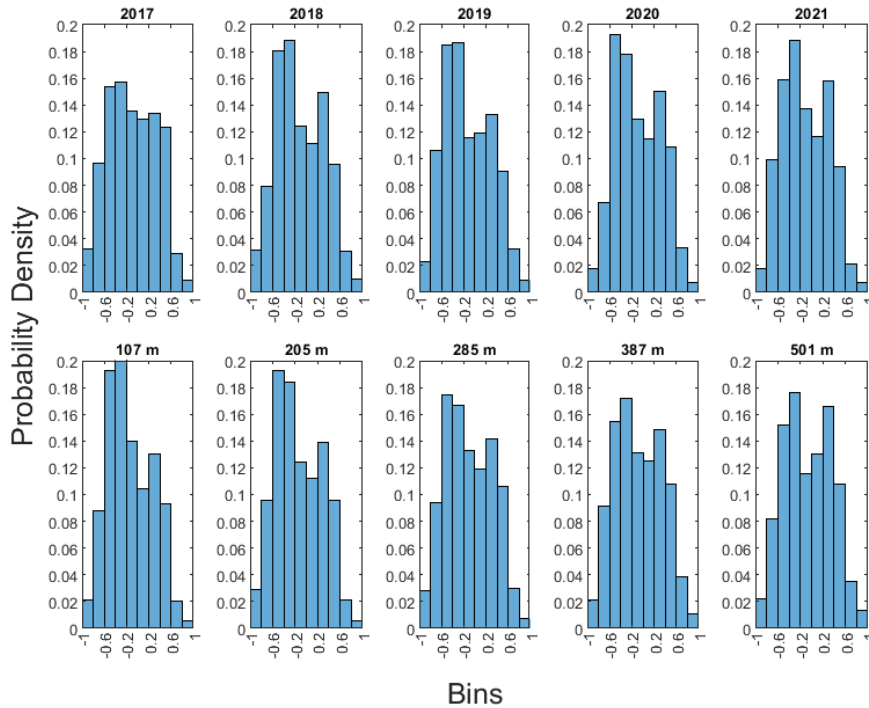


Figure 4.18: Energy correlation histograms per height and time in Marseille

The bins show a positively skewed distribution with the majority of PCC values on the anti-correlated side between -0.2 to -0.5, however, it is not as extreme as figure 4.18.

4.3. Marseille Scenario Results

To recap the case study standards, the AWE installed capacity was 100 kW about a third of the total, the PV installation capacity was 201.25 kW, and the minimum amount of energy generated should be 600 MWh/yr. This condition is based on it being roughly 0.01% of the total region’s energy production from combustion technology in 2020.

Table 4.3: Annual energy potential in Marseille sorted by height and time

	AEP (MWh/yr)					
	Kite 107m	Kite 205m	Kite 285m	Kite 387m	Kite 501m	PV Array
2017	432.28	496.75	517.27	528.44	531.77	232.20
2018	385.18	457.44	483.54	498.55	506.68	214.55
2019	397.01	464.13	488.36	501.83	505.49	229.25
2020	364.38	437.22	464.52	481.68	490.71	220.02
2021	391.01	472.20	497.78	508.77	511.38	220.01
Average	393.97	465.55	490.29	503.86	509.21	223.21
Combined	617.18	688.75	713.50	727.06	732.41	

To determine which scenario Marseille fits in the flowchart in figure 4.19 is used. The minimum for the |PCC| is reached with at least 40% of equal or greater value to 0.40 on the daily scale. Along with this, the minimum threshold of generated energy is reached. Roughly one-third of the values are greater than 0.40 and two-thirds less than 0.40. Therefore the Marseille location is just short of the option for the most promising hybrid location, but for various timescales smaller than a year it would work well.

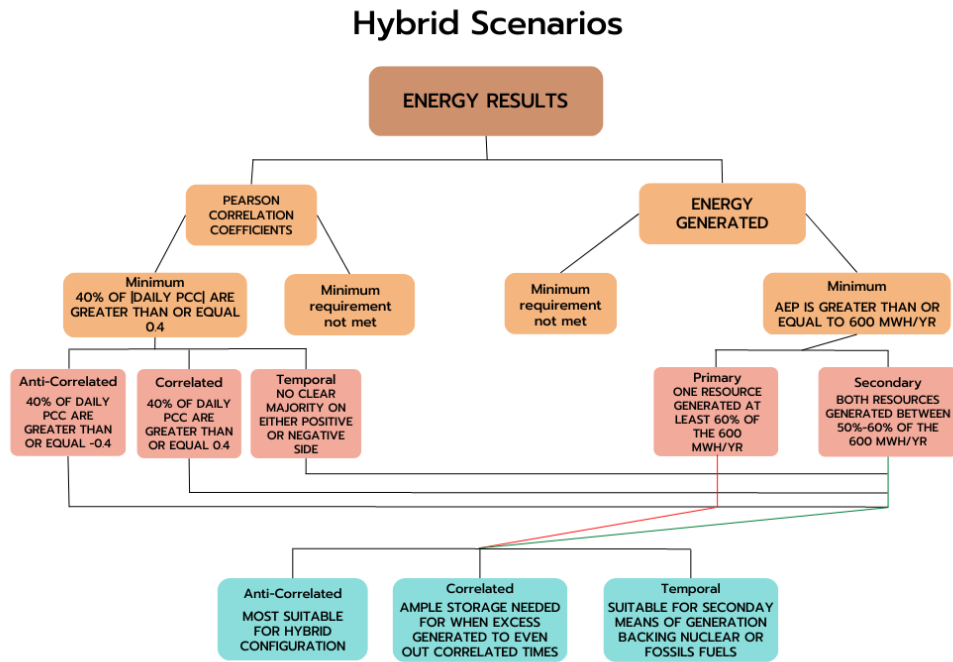


Figure 4.19: Energy scenarios

The scenarios that best-fit hybrids in Marseille are most likely to occur in Q1 (Winter) and (Q3 Summer). When looking even narrower some weeks in those quarters show PCC values less than -0.40 more than 60% of the time. Meaning on weekly basis the optimal solution is anti-correlated which is the best fit for hybrids.

4.4. Multiple Locations

To get an even comparison of the energy generated by the different types of technology multiple locations were evaluated. With the results of the comparisons, the feasibility of the model can be more strongly verified.

The locations selected were all in Europe, to keep errors limited, but with very different environments and geographic distances. The locations selected are Athens, Graz, Gdansk, Kyiv, and, Reykjavik the results of the resource and energy assessments will be compared to the more in-depth analysis of Marseille. The locations can be seen in figure 4.20. There are several coastal regions with two in the Mediterranean Athens and Marseille, Gdansk is set by the black sea, and finally, Reykjavik is on the Atlantic. Graz and Kyiv are landlocked at the elevations of 353 m and 179 m separately, Graz also sits at the base of a small mountain range with heights reaching almost 1750 m. They are all located near large populations with higher-than-average energy demands.

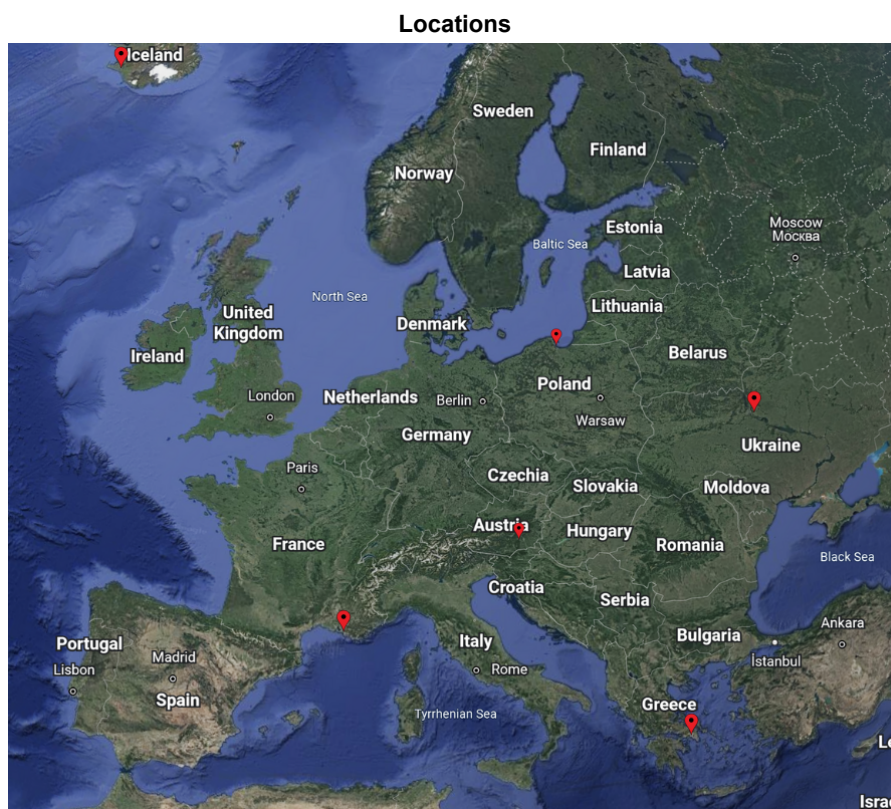


Figure 4.20: Map all test locations

These will be our five other test sites to compare with the results obtained from the Marseille case. The comparisons are simplified by using data from 2018 and the AWES heights set at 205 and 285 m, to show a realistic flight situation. It is expected that Marseille will still have the highest affinity for generation between resources due to the wind and solar map. However, the relationship between the correlation coefficients could change significantly. This will help uncover some patterns that are not based solely on attributes around Marseille.

Resource Availability

Of the other test sites Athens and Marseille have the highest potential for solar, this is due to the longitudinal coordinates being the closest to the equator. Gdansk, Graz, and Kyiv all are similar in solar, and Reykjavik with the lowest. While on the other hand, all locations besides Athens and Graz have similar higher wind potential. Graz's low wind potential could be due to the surrounding geographical landscape (the Graz highlands). Preliminary findings suggest that the solar potential is based on the latitudinal and longitudinal, while wind relies more on the geographic landscape even at heights above 100 m.

Energy Availability

The energy generated by locations varies significantly by type of technology however when summed they are similar. The regions that are expected to have lower potential due to latitude are shown clearly. A summary of the resources, energy, and estimated potential can be found in table 4.4.

Table 4.4: Summary of test sites

Location	Wind (m/s)	Solar (W/m ²)	Kite (MWh/yr)	PV (MWh/yr)	Energy (MWh/yr)
Athens	3.63	169.19	171.34	289.73	461.07
Gdansk	8.37	110.90	623.07	169.64	792.71
Graz	5.64	120.87	389.94	178.35	568.29
Kyiv	7.47	107.80	560.56	159.06	719.62
Marseille	7.22	145.38	483.54	214.55	698.09
Reykjavik	8.33	61.87	569.91	91.25	661.16

This table does not show the significance of correlation yet, as it is the key component that cannot be altered, unlike the amount of energy generated. A few examples of good and bad correlation weeks follow.

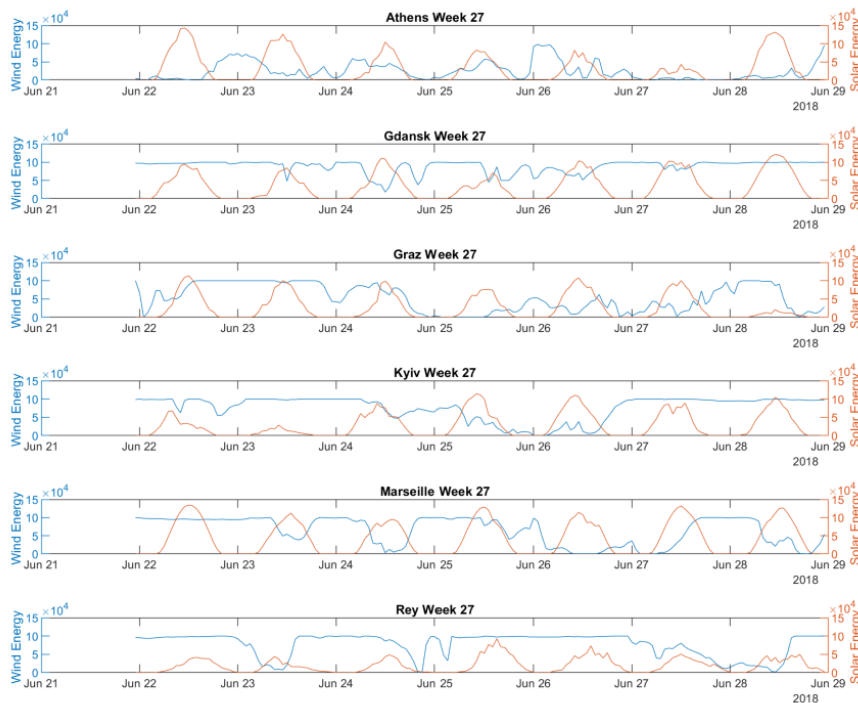


Figure 4.21: Week 27 correlation all locations at 285 m

Week 27 of 2018 is graphed in figure 4.21. Athens and Graz have an even amount of positively and negatively correlated days, Kyiv is close but still has a few more negative. Gdansk, Reykjavik, and Marseille have more anti-correlated days during the week.

Table 4.5: Week 27 correlation table all locations

		Week 27						
	Height (m)	21/06/2018	22/06/2018	23/06/2018	24/06/2018	25/06/2018	26/06/2018	27/06/2018
Athens	205	-0.6328	-0.5854	-0.3514	0.5530	0.7893	-0.4327	0.5136
	288	-0.6505	-0.5079	-0.4094	0.4666	0.7841	-0.4549	0.3227
Gdansk	205	-0.3630	0.3455	-0.4465	-0.6332	-0.2611	-0.5641	-0.7945
	288	-0.4194	0.1645	-0.4626	-0.6594	-0.2312	-0.5865	-0.7503
Graz	205	-0.4050	0.0816	0.0895	0.4137	-0.1481	-0.0826	-0.3084
	288	-0.4313	0.0203	-0.0067	0.4226	-0.2045	-0.1979	-0.3870
Kyiv	205	-0.9316	0.2432	0.6195	-0.0079	0.1217	-0.0904	-0.4320
	288	-0.9126	0.2443	0.7247	-0.1033	0.1655	-0.0947	-0.4533
Marseille	205	0.1826	-0.2639	-0.7592	0.1727	0.2341	0.1248	0.2681
	288	0.2212	-0.3646	-0.6830	0.0369	0.2307	-0.0624	0.0513
Reykjavik	205	-0.4418	-0.4853	-0.9049	-0.9530	0.3024	-0.5757	-0.0091
	288	-0.4359	-0.4059	-0.8879	-0.9459	0.2215	-0.5972	-0.0029

These can also be represented as the correlation values in a table with a colour-coded scheme for the negative and positive sides in table 4.5 The generation of both technologies over the course of week 23 of 2018 is shown below this is considered a bad week across the locations. Athens, Kyiv, and Marseille all show stronger positively correlated days during the week. While Gdansk, Graz, and Reykjavik all have stronger anti-correlated days during the week.

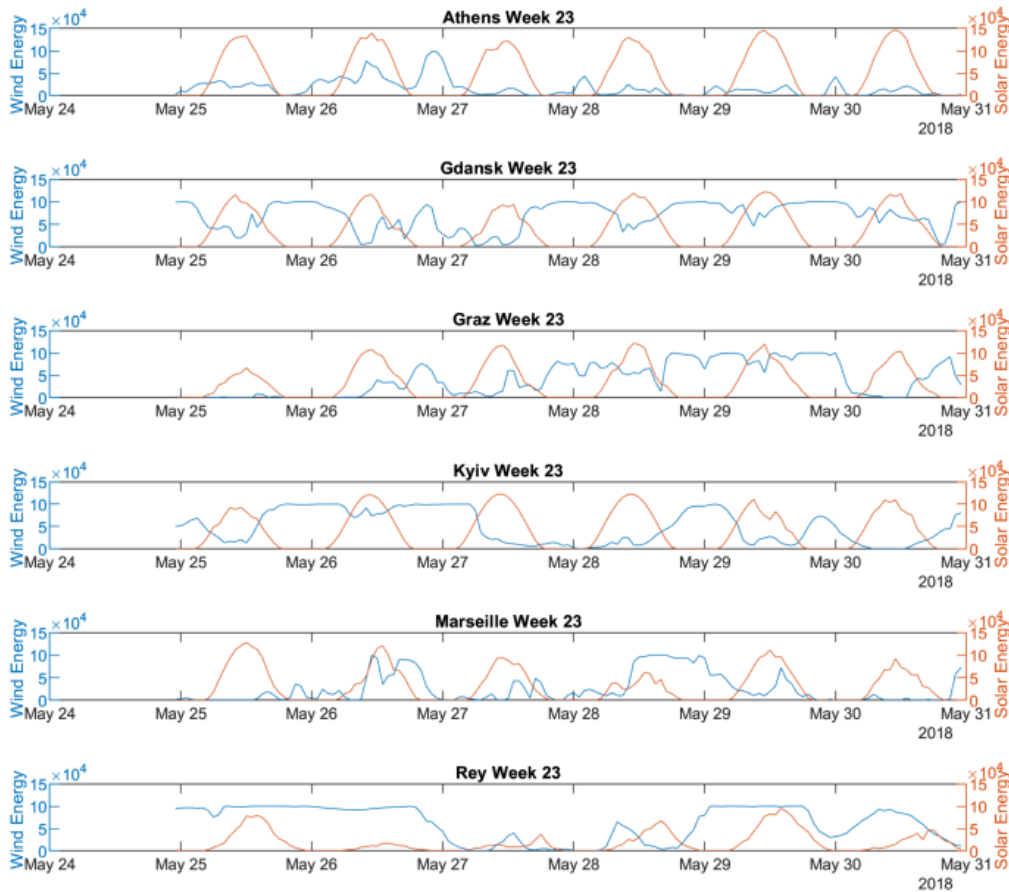


Figure 4.22: Week 23 correlation all locations at 285 m

Table 4.6: Week 23 correlation table all locations

		Week 23	3					
	Height (m)	24/05/2018	25/05/2018	26/05/2018	27/05/2018	28/05/2018	29/05/2018	30/05/2018
Athens	205	0.6493	0.5839	0.1773	0.0498	0.4848	0.4608	0.6495
	288	0.5799	0.5698	0.0298	-0.0937	0.3177	0.3712	0.5090
Gdansk	205	-0.8035	-0.9072	-0.7641	-0.5732	-0.9588	-0.6906	-0.1612
	288	-0.8077	-0.8246	-0.7458	-0.5320	-0.9680	-0.7127	-0.1044
Graz	205	-0.0228	0.3442	0.0879	-0.3023	-0.3490	-0.3779	-0.7697
	288	-0.0183	0.2652	0.0685	-0.2753	-0.4528	-0.5412	-0.7653
Kyiv	205	-0.8014	-0.7773	-0.8495	-0.3571	-0.3196	-0.7437	-0.9173
	288	-0.7888	-0.7429	-0.8696	-0.3546	-0.3134	-0.6970	-0.9234
Marseille	205	-0.3010	0.4081	0.1668	-0.1913	0.1469	0.4614	0.3386
	288	-0.3469	0.4224	0.1537	-0.1288	0.0443	0.2181	0.0035
Reykjavik	205	-0.1598	-0.4462	0.5021	0.1616	0.2823	0.2863	-0.1435
	288	-0.0625	-0.3989	0.5149	0.2093	0.3572	0.0734	-0.1695

A short statistical analysis of the PCCs is displayed in table 4.7. The final results were split by quarters based on solstice dates as those accurately show the whole year in a compressed view. The amount of anti-correlated days that are smaller than -0.40 range between 16% up to nearly 45%, while correlated above 0.40 from 7% to 31%. Q4 has the lowest anti-correlated potential on average and Q3 is the highest with Q1 in a close second.

Table 4.7: Quarterly correlation percentages to meet minimum hybrid requirements

Location	Q1		Q2		Q3		Q4	
	<-0.40	0.40 <	<-0.40	0.40 <	<-0.40	0.40 <	<-0.40	0.40 <
Athens	27.78%	15.00%	26.63%	20.65%	18.48%	30.98%	22.53%	14.84%
Gdansk	37.22%	7.22%	36.96%	7.61%	32.07%	16.30%	17.58%	15.93%
Graz	31.67%	13.33%	35.87%	14.13%	38.59%	9.24%	18.13%	13.19%
Kyiv	38.89%	7.78%	29.89%	11.41%	44.57%	13.59%	24.73%	14.29%
Marseille	38.33%	12.78%	26.09%	14.67%	39.13%	11.41%	21.43%	12.64%
Reykjavik	23.33%	11.11%	28.80%	24.46%	30.43%	15.76%	15.93%	14.29%

While all the locations differ significantly geographically, the correlation coefficients all stay in a similar range. Based on table 4.7 Gdansk, Kyiv and Marseille meet the minimum correlation requirements for a hybrid-suited location in Q1. Q3 also shows the same anti-correlation strength in Graz, Kyiv, and Marseille. The overall energy generation varies slightly for all locations except for Athens, which is significantly lower than the average. However of the locations with strong PCC availability, only Graz does not meet the energy generation minimum of 600 MWh/yr, this can be remedied by installing more capacity for either or both resources. Marseille has the strongest solar generation of the three final locations, with most of the configurations relying on the wind as the primary generator. The configurations are considered as co-located as there is a geographical link between generators. The method of evaluation does not consider an operational link between the solar panels and the kite, therefore the plant is not yet a full hybridisation. Full hybridisation means that the generation techniques affect each other, and would be explored more in the functional sizing of a hybrid plant.

5

Conclusion

The purpose of this research was to determine the critical factors and to what extent they affect the selection of a feasible location for an AWE-PV hybrid power plant. Generating a model in MATLAB uncovered the relationship between the resources and energy potential as well as the correlation of a co-located system. One location served as a test case to evaluate the whole system in depth, followed by a comparison with other sites to determine the influence of differing geography.

5.1. Key Outcomes

The results from the Marseille case concluded that wind speed and solar irradiance were more often negatively correlated, with more than 50% of the daily PCC values throughout the year being less than -0.36. The optimal times are in the first and third quarters of the year. The other locations also showed similar trends with Q1 and Q3 having a higher overall amount of desired PCC for the daily values between wind and solar during 2018. Using the solstices rather than the calendar to mark the quarterly time periods creates a connection between the temporal constraint with the behaviour of one of the two measured natural resources. The aim was to minimize the unrelated variance between resources over different time periods. The seasonal variation was the largest timescale exhibiting a reasonable amount of anti-correlated instances however the weekly and daily time periods allowed for much higher PCC values, in both the positive and negative directions. The association between the energy generated and PCC turned out to be almost unrelated, therefore the deciding factor for hybrid locations relied primarily on the relationship between the correlation of resources over time.

The research done before the creation of the model found that airborne wind technology is a newer industry concept and therefore has not been considered in a multi-technology use situation.

Marseille showed that with the control configuration, the amount of energy generated meets the minimum requirements for all heights. AWES is generating at least 60% of the time over all five years and is the primary generator with solar acting as a supplementing power. To create an ideal situation the plant location should install more solar to create a balance of generation between the two resources.

It is also still debated whether AWE systems or wind turbines have a higher generating potential. However, there are many undisputed benefits that AWE hold over HAWT systems, therefore exploring futuristic set-ups such as hybrids would benefit from further research. The

average hub height for HAWT is 94 m [42], therefore the 100 m results will represent other wind energy technologies. There is a large difference in trends of wind speed between the 100 m height and the others. There is an exponential difference in the energy potential from the operational heights of 100 m to 200 m, after that the increase is more linear. When comparing the two maximum heights there is less than 2% difference between the AEP's and the two lowest heights on average have more than a 15% increase.

When evaluating the results over all the sites, only two locations met the minimum energy requirements in Q1 and Q3, Marseille had the closest generation output of solar and wind energy, while Kyiv had a larger percentage of anti-correlated instances and energy generated. Gdansk also had a higher overall energy output compared to Marseille, but a lower correlation relationship during Q1 and Q2. In general, the number of resource correlated instances was slightly higher on an annual basis as opposed to the amount of energy correlation instances.

When evaluating the resource correlation and energy potential of the sites, related behaviours were attributed to geography differences. The northern and southernmost test sites, Reykjavik and Athens, had the lowest correlation relationships and were unable to meet the minimum energy demands. Athens was unable to generate enough combined energy to meet the minimum threshold with the smallest AWE energy potential. However, it had the closest rate of generation and the amount contributed by each technology of all the sites, meaning it was nearest to a balanced 50-50 energy generation. The Reykjavik site showed great promise for kite farms, but the low amount of solar made it an ineffective method of energy generation, which might allow for a future hybrid system consisting of kite farms and hydro-power. A tentative conclusion would be hybrid locations around Europe depend on a strong anti-correlated relationship and higher energy output with minimal storage to said configuration would be best suited to latitudinal ranges in the centre of the northern hemisphere.

5.2. Recommendations and Future Possibilities

To take this research a step further the model created in MATLAB should be rewritten into python to ensure smoother integration between the ERA5 database. This can also allow for the data to be used and inputted at a rate of three months behind the present, allowing for the use of data bypassing the challenges of downloading it. This would also allow for the exploration of past European areas.

A regression curve can also be introduced as a means of forecasting future generating potential and the correlation. This would be more accurate in the prediction of future sites as opposed to an averaged curve for modelling based on a few years of data. It would make identifying the best height for generation potential clearer and closer than to the 100th place.

The current model uses the 100 kW Falcon, however, in the future a 500 kWh kite will be finalized for commercial use and then it must be upscaled to take the new technology into consideration.

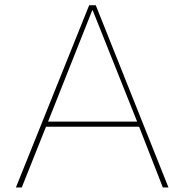
The final step that was not completed during this project was creating a user-friendly map with the geo-data showing the potential and energy generation. This was briefly explored using the ArcGIS software, however, just the raw data had already overloaded the computing capacity of the resources used. Screenshots from the attempt can be found in D. An alternative method could be to use google earth and a cloud service instead.

References

- [1] International Energy Agency. *Net Zero by 2050 - A Roadmap for the Global Energy Sector*. Tech. rep. Oct. 2021.
- [2] Andrew Lee. *Limit to size of wind turbines set by 'social acceptance not technology' say industry chiefs | Recharge*. Dec. 2020. URL: <https://www.rechargenews.com/wind/limit-to-size-of-wind-turbines-set-by-social-acceptance-not-technology-say-industry-chiefs/2-1-924243>.
- [3] Miles Loyd. "Crosswind kite power (for large-scale wind power production)". In: *Journal of Energy* 4.3 (1980), pp. 106–111.
- [4] Antonello Cherubini et al. "Airborne Wind Energy Systems: A review of the technologies". In: *Renewable and Sustainable Energy Reviews* 51 (Aug. 2015), pp. 1461–1476.
- [5] Tarek N. Dief et al. "System identification, fuzzy control and simulation of a kite power system with fixed tether length". In: *Wind Energy Science* 3.1 (May 2018), pp. 275–291.
- [6] Rolf Van Der Vlugt, Johannes Peschel, and Roland Schmehl. "Design and Experimental Characterization of a Pumping Kite Power System". In: *Airborne Wind Energy*. Springer. Chap. 23, pp. 403–425.
- [7] REN21 Secretariat. *Renewables 2022 Global Status Report*. Tech. rep. Paris, 2022.
- [8] Phil Coker et al. "Measuring significant variability characteristics: An assessment of three UK renewables". In: *Renewable Energy* 53 (May 2013), pp. 111–120.
- [9] Department of Energy. *Hybrid Wind and Solar Electric Systems*. URL: <https://www.energy.gov/energysaver/hybrid-wind-and-solar-electric-systems>.
- [10] Nova Scotia Power. *Wreck Cove marks 40 years of renewable energy*. 2018. URL: <https://www.nspower.ca/about-us/press-releases/details/2018/05/16/wreck-cove-marks-40-years-of-renewable-energy>.
- [11] Chris Vermillion et al. *Electricity in the air: Insights from two decades of advanced control research and experimental flight testing of airborne wind energy systems*. Jan. 2021.
- [12] Zach Fitzner. *The environmental impacts of solar and wind energy • Earth.com*. May 2018. URL: <https://www.earth.com/news/environmental-impacts-solar-wind-energy/>.
- [13] Mark Schelbergen et al. "Clustering wind profile shapes to estimate airborne wind energy production". In: *Wind Energy Science* 5.3 (Aug. 2020), pp. 1097–1120.
- [14] Cristina L. Archer and Ken Caldeira. "Global assessment of high-altitude wind power". In: *Energies* 2.2 (2009), pp. 307–319.
- [15] Philip Bechtle et al. "Airborne wind energy resource analysis". In: *Renewable Energy* 141 (Oct. 2019), pp. 1103–1116.
- [16] F Monforti et al. "Assessing complementarity of wind and solar resources for energy production in Italy. A Monte Carlo approach". In: *Renewable Energy* 63 (Mar. 2014), pp. 576–586.

- [17] Tiantian Zhang and Hongxing Yang. "High Efficiency Plants and Building Integrated Renewable Energy Systems". In: *Handbook of Energy Efficiency in Buildings: A Life Cycle Approach* (Jan. 2019), pp. 441–595.
- [18] C. A. Murphy, A. Schleifer, and K. Eureka. "A taxonomy of systems that combine utility-scale renewable energy and energy storage technologies". In: *Renewable and Sustainable Energy Reviews* 139 (Apr. 2021), p. 110711. ISSN: 1364-0321. DOI: 10.1016/J.RSER.2021.110711.
- [19] Jakub Jurasz et al. "Complementarity and 'resource droughts' of solar and wind energy in poland: An era5-based analysis". In: *Energies* 14.4 (Feb. 2021).
- [20] Mario Marcello Miglietta, Thomas Huld, and Fabio Monforti-Ferrario. "Local Complementarity of Wind and Solar Energy Resources over Europe: An Assessment Study from a Meteorological Perspective". In: *Journal of Applied Meteorology and Climatology* 56.1 (Sept. 2016), pp. 217–234.
- [21] Joanna H. Slusarewicz and Daniel S. Cohan. "Assessing solar and wind complementarity in Texas". In: *Renewables: Wind, Water, and Solar* 5.1 (Dec. 2018).
- [22] Copernicus Climate Change Service (C3S). *ERA5: data documentation*. 2022. URL: <https://confluence.ecmwf.int/display/CKB/ERA5%3A+data+documentation#ERA5:datadocumentation-Dataupdatefrequency>.
- [23] Noelia Oses et al. "Analysis of copernicus' era5 climate reanalysis data as a replacement for weather station temperature measurements in machine learning models for olive phenology phase prediction". In: *Sensors (Switzerland)* 20.21 (Nov. 2020), pp. 1–22.
- [24] Alexis Mariaccia et al. "Assessment of ERA-5 Temperature Variability in the MiddleAtmosphere Using Rayleigh LiDAR Measurements between 2005 and 2020". In: *Atmosphere* 13.2 (Feb. 2022).
- [25] Jon Olason. "ERA5: The new champion of wind power modelling?" In: *Renewable Energy* 126 (Oct. 2018), pp. 322–331.
- [26] Katherine Dykes et al. *Opportunities for Research and Development of Hybrid Power Plants*. Tech. rep. 2020.
- [27] DTU Wind Energy et al. *Global Wind Atlas 3.0*. URL: <https://globalwindatlas.info>.
- [28] Solargis. *Solar radiation modeling* | Solargis. URL: <https://solargis.com/docs/methodology/solar-radiation-modeling>.
- [29] Sunanda Sinha and S. S. Chandel. "Review of software tools for hybrid renewable energy systems". In: *Renewable and Sustainable Energy Reviews* 32 (Apr. 2014), pp. 192–205.
- [30] HOMER Energy. *HOMER Pro - Microgrid Software for Designing Optimized Hybrid Microgrids*. URL: <https://www.homerenergy.com/products/pro/index.html>.
- [31] Alexandre Boilley and Lucien Wald. "Comparison between meteorological re-analyses from ERA-Interim and MERRA and measurements of daily solar irradiation at surface". In: *Renewable Energy* 75 (Mar. 2015), pp. 135–143.
- [32] Lavinia Thimm. *Wind Resource Parametrisation and Power Harvesting Estimation using AWERA-the Airborne Wind Energy Resource Analysis tool*. Tech. rep. University of Bonn, Mar. 2022.
- [33] H. Hersbach et al. *ERA5 hourly data on single levels from 1959 to present*. June 2018. URL: <https://cds.climate.copernicus.eu/cdsapp#!/dataset/reanalysis-era5-single-levels?tab=overview>.

- [34] Sweder Reuchlin. "Modelling and Sizing of a Hybrid Power Plant using Airborne Wind Energy". PhD thesis. 2022.
- [35] Haymarket Media Group. *10 big wind turbines*. Sept. 2018. URL: <https://www.windpowermonthly.com/10-biggest-turbines>.
- [36] H. Hersbach et al. *ERA5 hourly data on pressure levels from 1959 to present*. 2018. URL: <https://cds.climate.copernicus.eu/cdsapp#!/dataset/reanalysis-era5-pressure-levels?tab=overview>.
- [37] ESRI. *Modeling solar radiation*. URL: <https://desktop.arcgis.com/en/arcmap/10.7/tools/spatial-analyst-toolbox/modeling-solar-radiation.htm>.
- [38] Stephanie Glen. *Correlation Coefficient: Simple Definition, Formula, Easy Calculation Steps*. 2021. URL: <https://www.statisticshowto.com/probability-and-statistics/correlation-coefficient-formula/>.
- [39] REC Group. *REC TwinPeak 4 Series*. Singapore.
- [40] Sandia National Laboratories. *PVLIB Toolbox for Matlab*. URL: https://pvpmc.sandia.gov/PVLIB_Matlab_%0AHelp/.
- [41] The MathWorks Inc. *Rescale - MATLAB 2022(A)*. 2022.
- [42] Liz Hartman. "Wind Turbines: the Bigger, the Better". In: *Office of Energy Efficiency & Renewable Energy (Aug. 2022)*. URL: [https://www.energy.gov/eere/articles/wind-turbines-bigger-better#:~:text=Report%3A%202022%20Edition.-,Hub%20Height,\(308%20feet\)%20in%202021..](https://www.energy.gov/eere/articles/wind-turbines-bigger-better#:~:text=Report%3A%202022%20Edition.-,Hub%20Height,(308%20feet)%20in%202021..)



Appendix A

Discover the Great Advantages of Kitepower

Integrate Kitepower into your micro-grid with solar PV and batteries to reap the benefits of smart hybrid energy generation.

Avoid idle generators & save diesel off-the-grid

When integrating Kitepower in combination with batteries, diesel generators can be switched off completely. Hybridizing with Kitepower results in less diesel consumption for more clean energy, culminating in considerable financial savings even for areas that don't experience consistent high wind speeds.

Find out more about Kitepower's competitive advantages when compared to solar PV or traditional wind turbines.

	Mass t	Area m ²	Energy throughout 24 hrs		Hurricane Proof	Installation Time
	220	50	✓	✓	✗	weeks
	70	2000	✓	✗	✗	days
	15	50	✓	✓	✓	hours



Electricity Generation 24/7

Produce electricity during day, night, on cloudy and rainy days



High Energy Production

Higher capacity factor than solar PV and wind turbines



Easy to Transport

All equipment fits in one 20ft container



Deployable in Harsh Environments

Ideal for remote locations



Plug & Play

Install it in less than 24hrs and operate it out-of-the-box

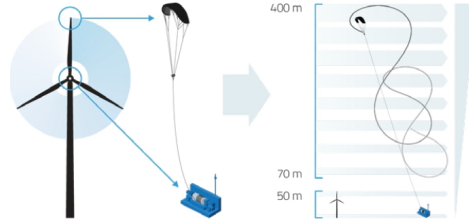
Introducing The Kitepower Falcon

Taking Only the Best from Wind Turbines

PROBLEM

Conventional wind energy systems rely on electricity generation by means of wind turbines installed on the ground. Wind turbines, therefore, require resource-intensive towers and heavy foundations thus imply a demanding transportation and installation process while ultimately being able to only harness less frequent winds at lower altitudes.

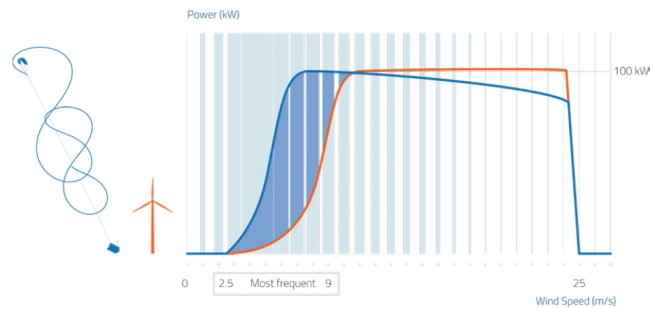
Difficult logistics limit the geographical versatility of wind turbines while their constrained height limit their efficiency. This results in unsustainable diesel supplies needed for most of the remote off- and micro-grid applications across the globe.



SOLUTION

Kitepower develops cost-effective alternatives to existing wind turbines by using kites to generate electricity.

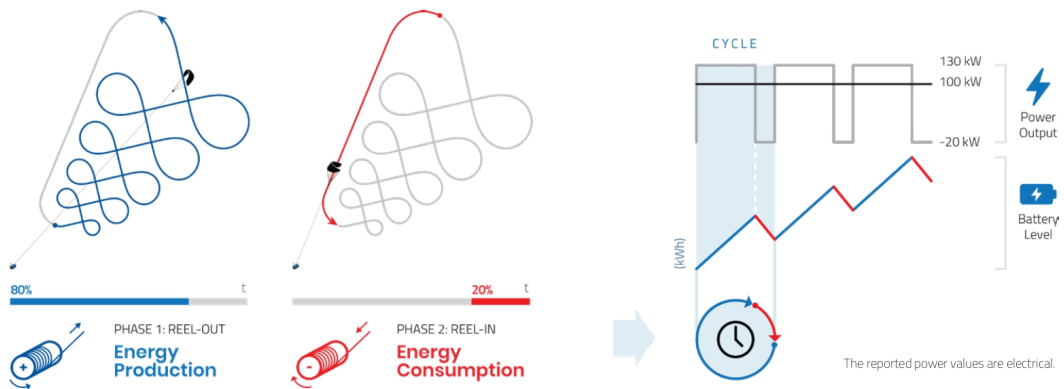
Kitepower systems do not require resource-intensive towers nor heavy foundations and is thus easy to transport and deploy. The system is able to harness stronger and more persistent winds at higher altitudes, allowing for higher capacity factors than traditional wind turbines and solar PV while being easier to transport, install and maintain. Moreover a Kitepower system is also able to start generating electricity with lower winds speeds than the ones required by windmills.



Introducing The Kitepower Falcon

Continuous Pumping Cycle Operation

The electricity generation works in two phases, which repeated in continuous cycles result in positive net energy output.



During the first energy production phase the kite is flown in a cross-wind figure of eight pattern to achieve a high pulling force and reel out the tether from the winch in the ground station.

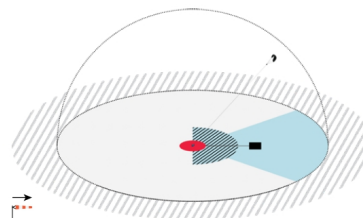
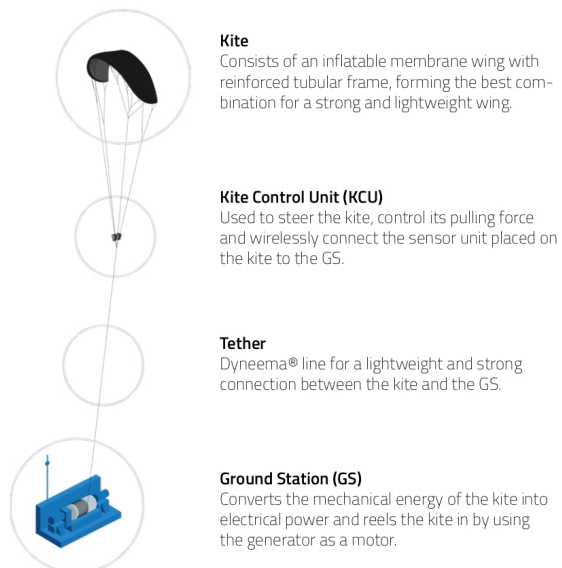
When the max tether length is reached, the kite's profile is adjusted in order to reel-in the tether with low force, using a small fraction of the energy produced in the previous phase.

The Kitepower Falcon:

- Has a single cycle duration of 100 seconds
- Produces 130 kW 80% of the cycle's time when in Reel-out
- Consumes 20 kW 20% of the cycle's time when in Reel-in

Introducing The Kitepower Falcon

System Components & Space Requirements



Zone	Dimensions	Dual Land-use ¹
Restricted Zone	30 m (r)	
Flight Zone	300 m (r)	✓
Potential Flight Zone	300 m (r)	✓
Safety Buffer	400 m (r)	✓
Landing Zone	100 m (r)	
Launching Corridor	150x2 m	
Launch Pad	24x12 m	

Obstacles' height within operational envelope:
1m allowance every 10m of distance from the GS

¹ Land can be used for alternative activities while Kitepower is deployed.
(r) = Radius



The Kitepower Falcon



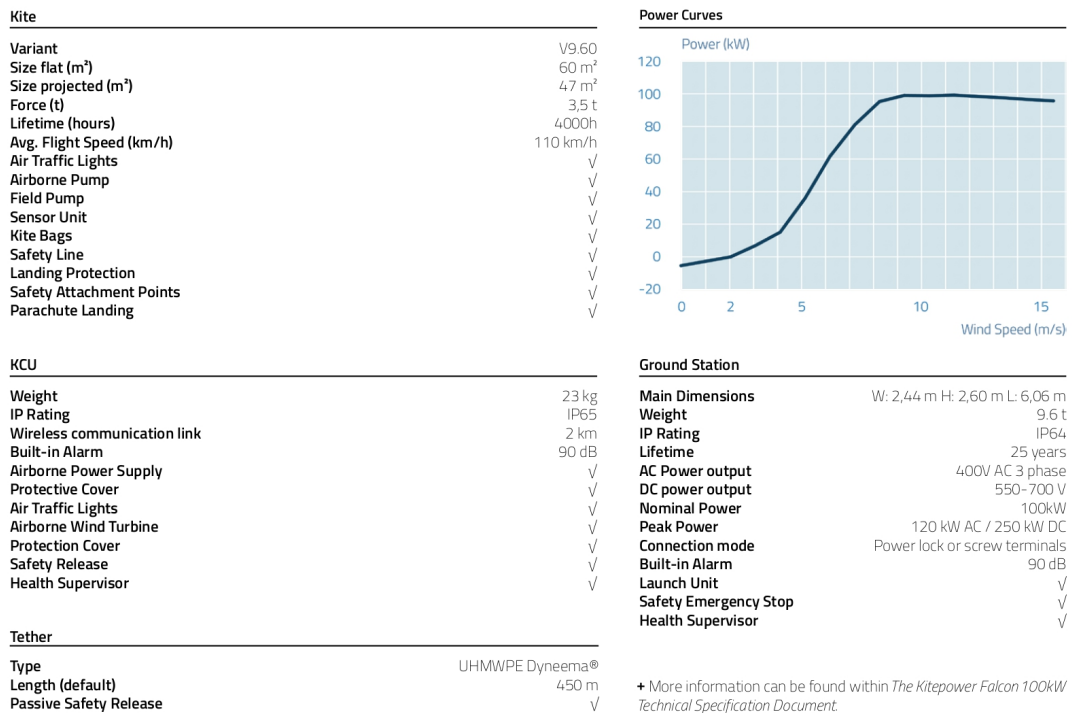
Technical Summary

General Information

Nominal Power Output ¹	100 kW
Yearly Power Output	450 MWh/year
Rated Wind Speed	7 m/s
Cut-in wind Speed	2 m/s
Max Operating Wind Speed	15 m/s
Min Launching Speed	5 m/s
Airborne Wind Range	0-25 m/s
Max Flight Altitude	300 m
Ground Space Required ² (radius)	300 m

¹ Power output potential might differ depending on the kite variant

² The ground space must be free of obstacles



© 2020 Kitepower Airborne Wind Energy - A Eneate BV Company. All rights reserved.

This document was created by Kitepower on behalf of Eneate BV and contains copyrighted material, trademarks and other proprietary information. This document or parts thereof may not be reproduced, altered or copied in any form or by any means without the prior written permission of Eneate BV. All specifications are for information only and are subject to change without notice. Eneate BV does not make any representations or extend any warranties, expressed or implied, as to the adequacy or accuracy of this information. This document may exist in multiple language versions. In case of inconsistencies between language versions the English version shall prevail. Certain technical options, services and system models may not be available in all locations/countries.

Figure A.1: Kite Power Brochure

SOLAR'S MOST TRUSTED



REC TWINPEAK 4 SERIES

PREMIUM SOLAR PANELS WITH SUPERIOR PERFORMANCE

REC TwinPeak 4 Series solar panels feature an innovative design with high panel efficiency and power output, enabling customers to get the most out of the space used for the installation.

Combined with industry-leading product quality and the reliability of a strong and established European brand, REC TwinPeak 4 Series panels are ideal for residential and commercial rooftops worldwide.



**MORE POWER
OUTPUT PER M²**



**FEATURING REC'S PIONEERING
TWIN DESIGN**



**100%
PID FREE**



**SUPER-STRONG
FRAME**



ELIGIBLE

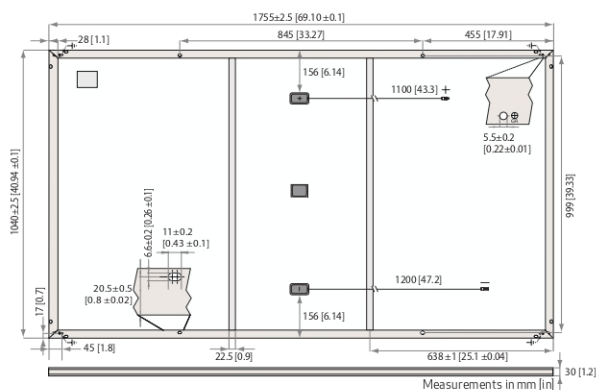
REC TWINPEAK 4 SERIES

PRODUCT SPECIFICATIONS



GENERAL DATA

Cell type:	120 half-cut mono c-Si p-type cells, 6 strings of 20 cells in series
Glass:	3.2 mm solar glass with anti-reflective surface treatment in accordance with EN 12150
Backsheet:	Highly resistant polymer
Frame:	Anodized aluminum (black) with silver support bars
Junction box:	3-part, 3 bypass diodes, lead-free IP68 rated, in accordance with IEC 62790
Connectors:	Stäubli MC4 PV-KBT4/KST4 (4 mm ²) in accordance with IEC 62852, IP68 only when connected
Cable:	4 mm ² solar cable, 1.1 m + 1.2 m in accordance with EN 50618
Dimensions:	1755 x 1040 x 30 mm (1.83 m ²)
Weight:	20.0 kg
Origin:	Made in Singapore



ELECTRICAL DATA

Product Code*: RECxxxTP4

	355	360	365	370	375
Power Output - P _{MAX} (Wp)	350	355	360	365	370
Watt Class Sorting - (W)	0/+5	0/+5	0/+5	0/+5	0/+5
Nominal Power Voltage - V _{MPP} (V)	33.3	33.5	33.9	34.3	35.0
Nominal Power Current - I _{MPP} (A)	10.58	10.60	10.62	10.65	10.72
Open Circuit Voltage - V _{OC} (V)	40.3	40.5	40.6	40.8	41.2
Short Circuit Current - I _{SC} (A)	11.10	11.19	11.26	11.32	11.45
Panel Efficiency (%)	19.1	19.4	19.7	20.0	20.5
Power Output - P _{MAX} (Wp)	264	268	272	276	280
Nominal Power Voltage - V _{MPP} (V)	31.0	31.3	31.7	32.1	32.5
Nominal Power Current - I _{MPP} (A)	8.54	8.56	8.58	8.60	8.63
Open Circuit Voltage - V _{OC} (V)	38.0	38.1	38.2	38.2	38.4
Short Circuit Current - I _{SC} (A)	9.06	9.10	9.13	9.18	9.26

Values at standard test conditions (STC: air mass AM1.5, irradiance 1000 W/m², temperature 25°C), based on a production spread with a tolerance of P_{MAX}, V_{OC} & I_{SC} ±3% within one watt class. Nominal module operating temperature (NMOT: air mass AM1.5, irradiance 800 W/m², temperature 20°C, wind speed 1 m/s). * Where xxx indicates the nominal power class (P_{MAX}) at STC above.

MAXIMUM RATINGS

Operational temperature:	-40 ... +85°C
Maximum system voltage:	1000 V
Maximum test load (front):	+7000 Pa (713 kg/m ²)*
Maximum test load (rear):	-4000 Pa (407 kg/m ²)*
Max series fuse rating:	25 A
Max reverse current:	25 A

* See installation manual for mounting instructions.
Design load = Test load / 1.5 (safety factor)

WARRANTY

	Standard	REC Pro Trust
Installed by an REC Certified Solar Professional	No	Yes
System Size	All	<25 kW 25-500 kW
Product Warranty (yrs)	20	25
Power Warranty (yrs)	25	25
Labor Warranty (yrs)	0	25
Power in Year 1	98%	98%
Annual Degradation	0.5%	0.5%
Power in Year 25	86%	86%

See warranty documents for details. Conditions apply

CERTIFICATIONS

IEC 61215-2:2016, IEC 61730-2:2016, UL 61730	
IEC 62804	PID
IEC 61701	Salt Mist
IEC 62716	Ammonia Resistance
ISO 11925-2	Ignitability (Class E)
IEC 62782	Dynamic Mechanical Load
IEC 61215-2:2016	Hailstone (35mm)
ISO 14001, ISO 9001, IEC 45001, IEC 62941	



TEMPERATURE RATINGS*

Nominal Module Operating Temperature:	44.6°C (±2°C)
Temperature coefficient of P _{MAX} :	-0.34 %/°C
Temperature coefficient of V _{OC} :	-0.26 %/°C
Temperature coefficient of I _{SC} :	0.04 %/°C

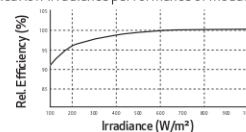
* The temperature coefficients stated are linear values

DELIVERY INFORMATION

Panels per pallet:	33
Panels per 40 ft GP/high cube container:	858 (26 pallets)
Panels per 13.6 m truck:	924 (28 pallets)
Panels per 53 ft truck:	924 (28 pallets)

LOW LIGHT BEHAVIOUR

Typical low irradiance performance of module at STC:



Available from:

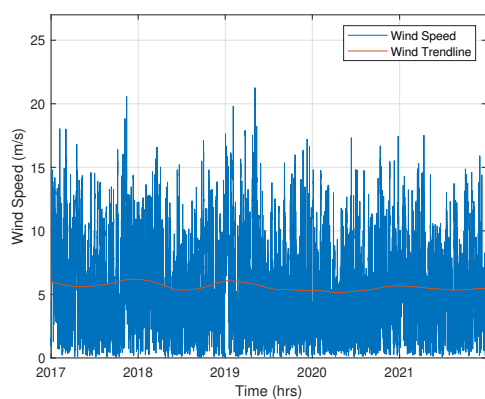
Founded in 1996, REC Group is an international pioneering solar energy company dedicated to empowering consumers with clean, affordable solar power. As Solar's Most Trusted, REC is committed to high quality, innovation, and a low carbon footprint in the solar materials and solar panels it manufactures. Headquartered in Norway with operational headquarters in Singapore, REC also has regional hubs in North America, Europe, and Asia-Pacific.



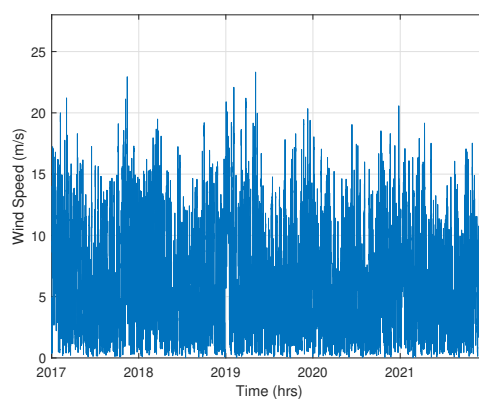
Figure A.2: Solar Panel Specifications

B

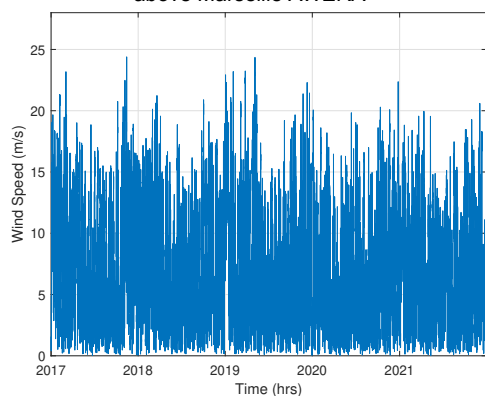
Appendix B



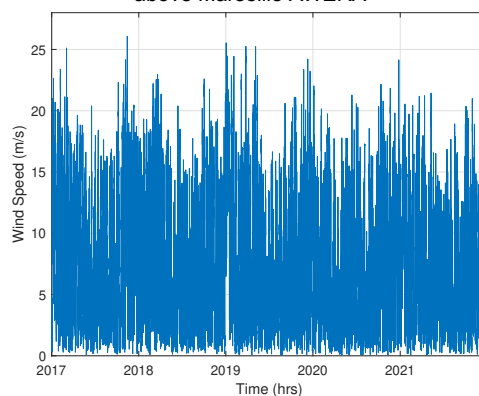
(a) Hourly wind speed from 2017-2021 at 107 m above Marseille AWERA



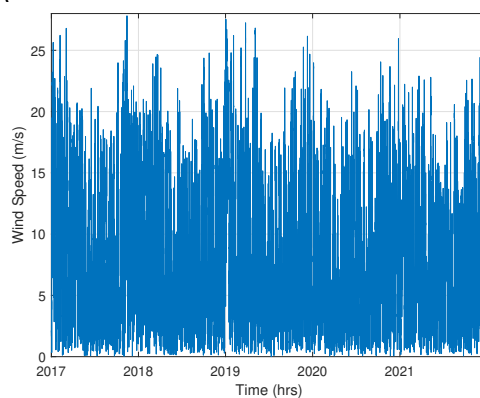
(b) Hourly wind speed from 2017-2021 at 205 m above Marseille AWERA



(c) Hourly wind speed from 2017-2021 at 288 m above Marseille AWERA



(d) Hourly wind speed from 2017-2021 at 385 m above Marseille AWERA



(e) Hourly wind speed from 2017-2021 at 501 m above Marseille AWERA

Figure B.1: Hourly Wind Speed in Marseille all heights using AWERA curvefit

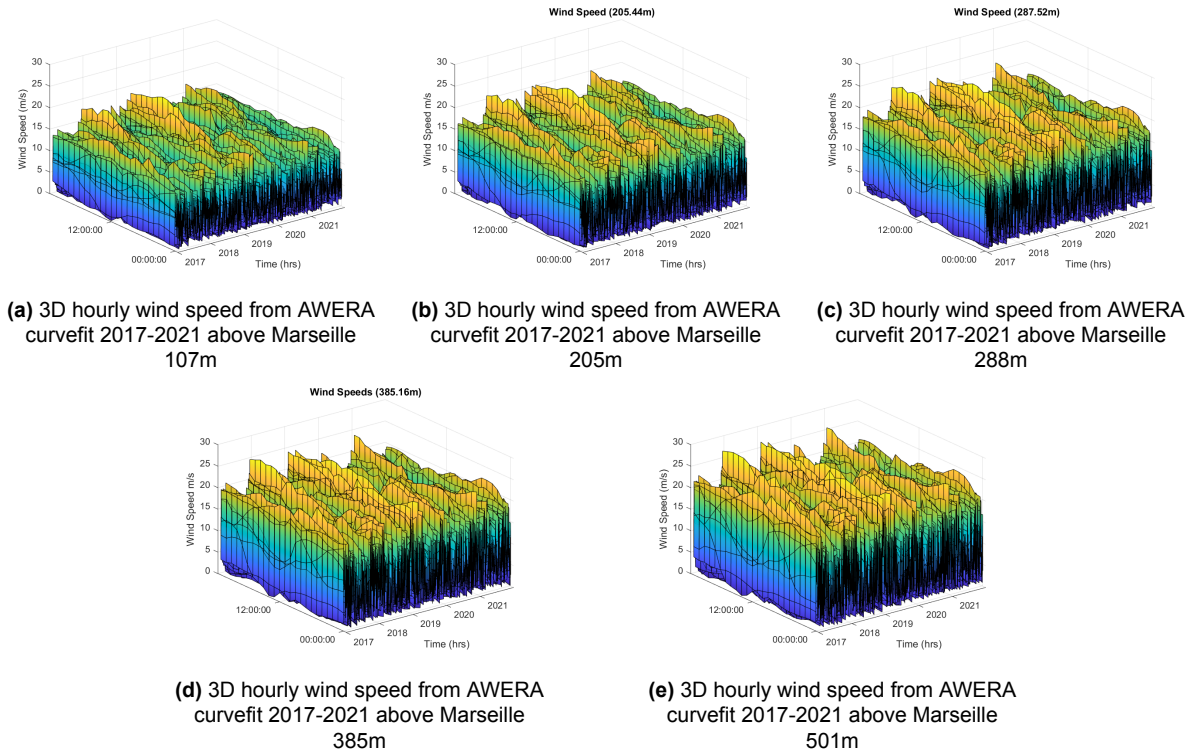


Figure B.2: 3D graph of wind speed Marseille 2017 to 2021 using AWERA curvefit

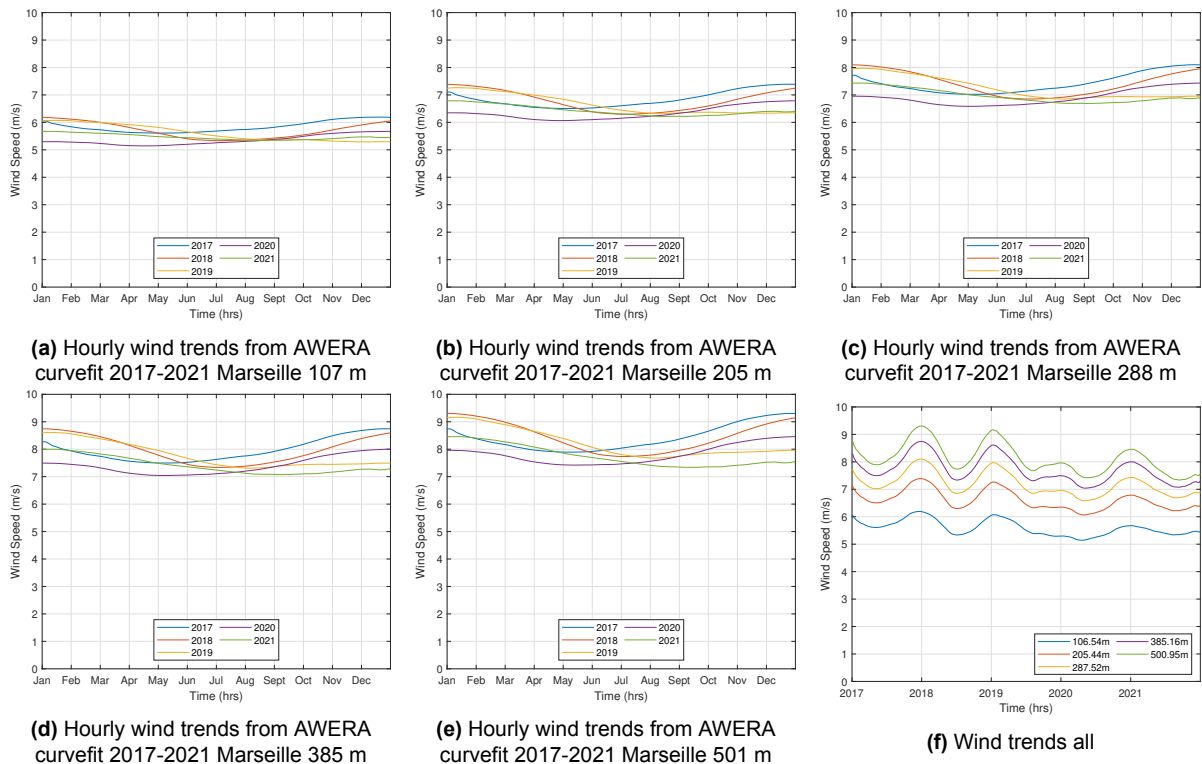


Figure B.3: Trend lines for five geometric heights of wind speed above Marseille using AWERA curvefit

C

Appendix C

Table C.1: Correlation values between wind speed and solar Irradiance in Marseille (monthly to yearly)

	Height (m)	Jan	Feb	Mar	Apr	May	Jun	Jul	Aug	Sep	Oct	Nov	Dec	Winter	Spring	Summer	Fall	1st Half	2nd Half	Year
2017	107	0,0048	-0,0267	-0,0547	-0,0569	0,0039	-0,1435	-0,0535	0,0007	-0,0269	-0,0785	-0,0530	-0,1186	-0,0749	-0,0784	-0,0209	-0,0946	-0,1051	-0,0959	-0,1009
	205	-0,0472	-0,0977	-0,1347	-0,0834	-0,0085	-0,1423	-0,0731	0,0063	-0,0052	-0,0754	-0,0623	-0,1599	-0,1395	-0,0908	-0,0223	-0,1099	-0,1434	-0,1120	-0,1279
	288	-0,0520	-0,1240	-0,1692	-0,0926	-0,0039	-0,1285	-0,0770	0,0215	0,0084	-0,0660	-0,0620	-0,1640	-0,1596	-0,0886	-0,0160	-0,1100	-0,1533	-0,1131	-0,1334
	385	-0,0447	-0,1340	-0,1871	-0,0936	0,0060	-0,0981	-0,0758	0,0399	0,0255	-0,0483	-0,0567	-0,1537	-0,1644	-0,0777	-0,0053	-0,1009	-0,1521	-0,1073	-0,1301
	501	-0,0372	-0,1254	-0,1861	-0,0843	0,0140	-0,0601	-0,0707	0,0479	0,0448	-0,0312	-0,0502	-0,1406	-0,1556	-0,0621	0,0039	-0,0894	-0,1430	-0,1007	-0,1223
2018	107	-0,0290	0,0617	-0,0519	-0,1738	-0,0847	-0,0588	-0,1228	-0,1013	-0,0544	-0,0740	-0,0398	0,0297	0,0117	-0,1013	-0,0898	-0,0198	-0,1096	-0,1141	-0,1100
	205	-0,1134	-0,0391	-0,1451	-0,1905	-0,0788	-0,0775	-0,1156	-0,1420	-0,0551	-0,0683	-0,0493	0,0090	-0,0844	-0,1136	-0,1021	-0,0289	-0,1580	-0,1332	-0,1437
	288	-0,1400	-0,0852	-0,1775	-0,1932	-0,0741	-0,0799	-0,1052	-0,1555	-0,0428	-0,0610	-0,0562	0,0184	-0,1228	-0,1155	-0,1000	-0,0291	-0,1749	-0,1367	-0,1539
	385	-0,1458	-0,1124	-0,1920	-0,1957	-0,0762	-0,0783	-0,0933	-0,1637	-0,0244	-0,0527	-0,0563	0,0310	-0,1424	-0,1180	-0,0933	-0,0263	-0,1839	-0,1358	-0,1580
	501	-0,1354	-0,1199	-0,1935	-0,1989	-0,0816	-0,0764	-0,0834	-0,1670	-0,0010	-0,0468	-0,0537	0,0394	-0,1465	-0,1219	-0,0833	-0,0243	-0,1875	-0,1329	-0,1583
2019	107	-0,0283	-0,1407	-0,1016	-0,0780	-0,0349	-0,1340	-0,0340	-0,1359	0,0219	-0,0567	-0,1056	-0,1592	-0,1339	-0,0860	-0,0579	-0,0909	-0,1251	-0,1004	-0,1058
	205	-0,1031	-0,1844	-0,1965	-0,1061	-0,0501	-0,1156	-0,0454	-0,1193	0,0086	-0,0392	-0,1004	-0,1576	-0,1989	-0,0970	-0,0638	-0,0839	-0,1637	-0,1134	-0,1334
	288	-0,1289	-0,1962	-0,2346	-0,1156	-0,0550	-0,1021	-0,0487	-0,0976	0,0039	-0,0283	-0,0842	-0,1449	-0,2225	-0,0994	-0,0612	-0,0722	-0,1780	-0,1145	-0,1420
	385	-0,1299	-0,1882	-0,2533	-0,1187	-0,0612	-0,0824	-0,0521	-0,0752	0,0022	-0,0152	-0,0643	-0,1340	-0,2281	-0,0991	-0,0572	-0,0585	-0,1829	-0,1143	-0,1447
	501	-0,1152	-0,1633	-0,2562	-0,1192	-0,0663	-0,0590	-0,0534	-0,0557	0,0065	0,0007	-0,0450	-0,1310	-0,2194	-0,0971	-0,0519	-0,0455	-0,1805	-0,1145	-0,1435
2020	107	-0,0974	0,1046	-0,0339	-0,1330	-0,0979	-0,0821	-0,0315	-0,0871	0,0225	-0,0073	-0,1139	-0,0219	-0,0034	-0,0516	-0,0180	-0,0335	-0,0530	-0,0630	-0,0597
	205	-0,1154	0,0119	-0,1110	-0,1135	-0,1257	-0,0970	-0,0413	-0,1067	0,0217	-0,0039	-0,1091	-0,0526	-0,0732	-0,0635	-0,0310	-0,0423	-0,0935	-0,0849	-0,0902
	288	-0,1037	-0,0091	-0,1355	-0,0840	-0,1309	-0,0982	-0,0411	-0,1098	0,0250	0,0026	-0,1026	-0,0523	-0,0900	-0,0607	-0,0329	-0,0397	-0,1017	-0,0898	-0,0966
	385	-0,0802	0,0019	-0,1448	-0,0552	-0,1394	-0,0911	-0,0387	-0,1069	0,0226	0,0086	-0,1015	-0,0370	-0,0879	-0,0665	-0,0343	-0,0345	-0,1003	-0,0914	-0,0968
	501	-0,0605	0,0222	-0,1405	-0,0262	-0,1574	-0,0753	-0,0326	-0,0950	0,0065	0,0146	-0,1122	-0,0130	-0,0130	-0,0771	-0,0356	-0,0299	-0,0957	-0,0919	-0,0948
2021	107	0,0279	-0,0462	0,0432	-0,0258	-0,0873	-0,1896	-0,0560	-0,0476	-0,1664	-0,1571	0,0274	-0,0511	-0,0068	-0,0922	-0,0384	-0,0610	-0,0690	-0,0838	-0,0756
	205	-0,0622	-0,1241	-0,0405	-0,0315	-0,1001	-0,1942	-0,0733	-0,0748	-0,1822	-0,1542	0,0301	-0,0440	-0,0957	-0,1004	-0,0635	-0,0609	-0,1159	-0,1058	-0,1099
	288	-0,0748	-0,1512	-0,0776	-0,0294	-0,1048	-0,1814	-0,0651	-0,0810	-0,1789	-0,1463	0,0406	-0,0154	-0,1276	-0,0986	-0,0654	-0,0498	-0,1309	-0,1047	-0,1165
	385	-0,0549	-0,1560	-0,1042	-0,0246	-0,1067	-0,1653	-0,0540	-0,0793	-0,1673	-0,1410	0,0538	0,0097	-0,1390	-0,0938	-0,0617	-0,0397	-0,1355	-0,0993	-0,1155
	501	-0,0222	-0,1306	-0,1201	-0,0134	-0,1014	-0,1452	-0,0414	-0,0688	-0,1557	-0,1307	0,0612	0,0208	-0,1323	-0,0824	-0,0539	-0,0322	-0,1296	-0,0930	-0,1089

Table C.2: Correlation values between wind speed and solar Irradiance in Marseille (weekly)

Year	Height (m)	Week 1	Week 2	Week 3	Week 4	Week 5	Week 6	Week 7	Week 8	Week 9	Week 10	Week 11	Week 12	Week 13	Week 14	Week 15	Week 16	Week 17	Week 18	Week 19	Week 20	Week 21	Week 22	Week 23	Week 24	Week 25	Week 26	
2017	107	-0.0290	-0.0122	0.0295	-0.1055	0.0252	0.1218	-0.0734	0.0449	-0.0557	0.0981	-0.0628	-0.0608	-0.1456	-0.0955	-0.1423	-0.1289	0.0695	-0.1809	-0.0216	0.0121	-0.0808	0.0192	-0.1581	-0.1464	-0.2278	-0.1665	-0.1034
	205	-0.0691	-0.1156	-0.0199	-0.1430	-0.0100	0.0433	-0.1445	-0.0480	-0.0886	-0.0191	-0.1274	-0.1710	-0.2506	0.0052	-0.1293	-0.1741	-0.0789	-0.1919	0.0286	-0.0015	-0.1383	-0.0086	-0.0889	-0.1383	-0.2604	-0.1034	
	288	-0.0695	-0.1485	-0.0144	-0.1209	-0.0196	0.0165	-0.1754	-0.0887	-0.0960	-0.0633	-0.1633	-0.2234	-0.2732	0.0553	-0.1134	-0.1949	-0.0538	-0.2051	0.0662	-0.0167	-0.1489	-0.0369	-0.1177	-0.1489	-0.2824	-0.1063	
	385	-0.0518	-0.1616	-0.0080	-0.0805	-0.0205	0.0126	-0.1932	-0.1126	-0.0976	-0.0688	-0.1989	-0.2482	-0.2698	0.0875	-0.0889	-0.2058	-0.2026	-0.2164	0.1068	0.0505	-0.1567	-0.0183	0.0259	-0.0845	-0.2858	-0.1044	
	501	-0.0308	-0.1653	-0.0180	-0.0349	-0.0111	0.0219	-0.1807	-0.1177	-0.0899	-0.0819	-0.2226	-0.2412	-0.2479	0.1014	-0.0582	-0.2033	-0.2117	-0.2166	0.1388	0.1008	-0.1776	-0.0070	0.0787	-0.0530	-0.2482	-0.0789	
2018	107	-0.0195	-0.0349	0.2759	-0.1852	-0.0644	0.0264	0.0617	0.0140	-0.1304	-0.1527	-0.2266	0.0675	0.0973	-0.1974	-0.2402	-0.2438	-0.1431	-0.0103	-0.2787	0.0092	-0.1738	-0.0106	-0.1708	-0.0306	-0.1303	-0.1337	
	205	-0.2500	-0.0476	-0.2254	-0.0594	-0.0941	-0.2173	-0.1411	-0.1568	-0.2698	-0.1342	-0.2007	-0.1654	-0.2120	-0.3404	-0.0259	-0.2993	-0.0202	0.1560	-0.1414	-0.1619	-0.2454	-0.1885	0.0942	-0.1670	-0.2248	-0.0617	
	288	-0.2821	-0.1244	-0.2315	-0.0947	-0.1230	-0.2264	-0.1541	-0.1742	-0.2934	-0.1735	-0.2579	-0.1924	-0.1561	-0.3167	-0.0272	-0.2743	-0.0702	0.1696	-0.1340	-0.1611	-0.2686	-0.2074	0.1851	-0.1895	-0.1843	-0.1075	
	385	-0.2541	-0.1816	-0.1366	-0.0899	-0.1601	-0.1763	-0.1132	-0.1020	-0.2748	-0.1995	-0.3097	-0.1669	-0.1669	-0.2016	-0.2782	-0.0347	-0.1769	-0.1385	0.1828	-0.0958	-0.2228	-0.3197	-0.2229	0.2668	-0.1871	-0.0556	-0.1178
	501	-0.2787	-0.1700	-0.1916	-0.1049	-0.1425	-0.2109	-0.1464	-0.1539	-0.2923	-0.1925	-0.2937	-0.1912	-0.1816	-0.2969	-0.2300	-0.1078	-0.1752	-0.1215	-0.1715	-0.1765	-0.2220	-0.2950	-0.2240	0.2485	-0.1971	-0.1204	-0.1242
2019	107	-0.0002	-0.3713	0.0248	-0.1521	0.2398	0.0665	0.2197	-0.0748	0.0900	0.0138	0.0818	-0.1054	0.0187	-0.2233	-0.2611	-0.0198	-0.1422	0.0332	-0.2057	-0.0644	-0.2576	-0.1221	0.0132	-0.0250	-0.0852	-0.1337	
	205	-0.0150	-0.3646	-0.0346	-0.1270	0.1927	0.0025	0.0934	-0.1842	-0.0151	-0.1343	-0.0163	-0.1252	-0.0773	-0.1663	-0.2391	-0.0028	-0.1861	0.1039	-0.1862	-0.1284	-0.3151	-0.1862	0.0735	-0.0279	-0.1401	-0.1981	
	288	-0.0164	-0.3431	-0.0257	-0.0712	0.1764	0.0098	0.0479	-0.2091	-0.0512	-0.1788	-0.0652	-0.1068	-0.0945	-0.1218	-0.2173	0.0583	-0.1869	0.1452	-0.1673	-0.1447	-0.3292	-0.2079	0.1101	-0.0297	-0.1499	-0.2363	
	385	-0.0159	-0.3152	-0.0051	-0.0021	0.2011	0.0419	0.0358	-0.1874	-0.0653	-0.1976	-0.1039	-0.0900	-0.0802	-0.0732	-0.1723	0.1188	-0.2286	0.1406	-0.1476	-0.1486	-0.3387	-0.2071	0.1335	-0.0190	-0.1428	-0.2701	
	501	-0.0293	-0.2834	0.0151	0.0619	0.2238	0.0759	0.0528	-0.1597	-0.0563	-0.1900	-0.1292	-0.0693	-0.0481	-0.0114	-0.1108	-0.1479	-0.2653	0.0950	-0.1439	-0.3466	-0.2219	0.1391	0.0047	-0.1180	-0.2845		
2020	107	-0.1795	0.2097	-0.0136	0.0305	-0.0018	0.0345	0.1095	-0.1249	-0.1011	0.0223	0.2651	-0.0629	-0.0841	-0.1054	0.1130	-0.1306	-0.2476	-0.1312	-0.2386	0.2978	-0.1069	-0.3881	-0.2649	-0.2907	-0.2074	0.0779	
	205	-0.2304	0.0169	-0.1054	-0.0745	-0.0849	-0.0733	0.0292	-0.2065	-0.1310	-0.0680	0.0867	-0.1705	-0.1374	-0.0741	0.0902	-0.1620	-0.2879	-0.0689	-0.2049	0.2405	-0.1021	-0.3861	-0.1771	-0.2663	-0.2605	-0.0151	
	288	-0.2085	-0.0029	-0.1397	-0.0960	-0.0860	-0.1186	0.0103	-0.2483	-0.1299	-0.1016	-0.0096	-0.2339	-0.1413	-0.0273	0.0722	-0.1588	-0.3265	-0.0354	-0.1967	0.2140	-0.1322	-0.3713	-0.1139	-0.2555	-0.2689	-0.0584	
	385	-0.1667	0.0412	-0.1447	-0.0888	-0.0506	-0.1222	0.0195	-0.2839	-0.1318	-0.1302	-0.0758	-0.2795	-0.1319	-0.0430	0.0638	-0.1394	-0.3507	-0.0096	-0.1954	0.1970	-0.1545	-0.3440	-0.0527	-0.2411	-0.2746	-0.0308	
	501	-0.1376	0.0804	-0.1290	-0.0612	0.0006	-0.0835	0.0739	-0.2891	-0.1427	-0.1362	-0.1174	-0.2681	-0.1110	-0.0850	0.0502	-0.1312	-0.3288	0.0398	-0.2031	0.1879	-0.1685	-0.3085	-0.0084	-0.2273	-0.2695	-0.0332	
2021	107	-0.2028	-0.0220	-0.1159	-0.0895	-0.0256	0.1825	-0.0966	0.0749	-0.0022	-0.0112	-0.1168	-0.0684	-0.1833	-0.0527	-0.1723	-0.1341	-0.0170	0.0096	-0.1207	-0.0942	-0.1031	-0.0838	0.0391	-0.1488	-0.2862	-0.1153	
	205	-0.1409	-0.0282	-0.1441	-0.1194	0.0229	0.2339	-0.0993	0.0108	-0.0151	0.0520	-0.0758	-0.0956	-0.2180	-0.0007	-0.1187	-0.1048	-0.0618	-0.0473	-0.0918	-0.0909	-0.1071	-0.1358	0.0371	-0.2094	-0.3870	-0.1435	
	288	-0.1014	-0.0218	-0.1427	-0.1700	0.0601	0.2668	-0.0883	-0.0197	-0.0097	0.0940	-0.0651	-0.1089	-0.2450	0.0082	-0.0787	-0.0744	-0.0733	-0.0652	-0.0735	-0.0843	-0.0843	-0.0748	-0.1580	0.0347	-0.2216	-0.3953	-0.1473
	385	-0.0690	-0.0079	-0.1293	-0.2000	0.0855	0.3007	-0.0645	-0.0444	-0.0050	0.1380	-0.0374	-0.1029	-0.2784	0.0089	-0.0307	-0.0184	-0.0736	-0.0680	-0.0479	-0.0781	-0.0279	-0.1745	0.0404	-0.2240	-0.3582	-0.1529	
	501	-0.0471	0.0156	-0.1180	-0.2114	0.0809	0.3093	-0.0400	-0.0684	0.0013	0.1698	-0.0253	-0.0837	-0.2782	-0.0006	0.0254	0.0311	-0.0694	-0.0288	-0.0680	-0.0740	0.0160	-0.1848	0.0493	-0.2183	-0.2874	-0.1735	
2022	107	-0.2646	-0.1102	0.0162	-0.0963	-0.1033	-0.1831	-0.1511	-0.0512	-0.0293	-0.0422	-0.1817	-0.1400	0.0049	-0.0141	-0.1294	-0.0311	-0.0690	-0.1230	-0.0030	0.0053	-0.2401	0.0868	-0.0743	0.1271	0.0206	-0.0442	
	205	-0.1764	-0.0624	-0.0250	-0.1907	-0.0733	-0.1503	-0.1874	-0.1350	-0.0923	0.0277	-0.1621	-0.1718	-0.0480	0.0155	-0.0883	-0.1176	-0.0876	-0.1192	0.0215	-0.0008	-0.2313	0.0644	-0.1197	0.0971	-0.0094	-0.0588	
	288	-0.1162	-0.0268	-0.0456	-0.2228	-0.0569	-0.1179	-0.1991	-0.1757	-0.1216	0.0627	-0.1104	-0.1640	-0.0709	0.0255	-0.0498	-0.1252	-0.0751	-0.1322	0.0274	-0.0016	-0.2244	0.0620	-0.1404	0.1072	-0.0161	-0.0288	
	385	-0.0622	0.0037	-0.0620	-0.2290	-0.0450	-0.0875	-0.2125	-0.2050	-0.1432	0.0810	-0.0399	-0.1416	-0.0793	0.0321	-0.0083	-0.1390	-0.0535	-0.1449	0.0403	-0.0015	-0.2214	0.0698	-0.1572	0.1232	0.0076	-0.0289	
	501	-0.0299	0.0175	-0.0626	-0.2179	-0.0340	-0.0603	-0.2206	-0.2275	-0.1542	0.0896	0.0172	-0.0952	-0.0731	0.0447	0.0139	-0.1611	-0.0320	-0.1653	0.0522	0.0054	-0.2224	0.0809	-0.1638	0.1340	0.0298	-0.0228	
2023	107	-0.1079	0.0167	-0.2146	-0.1278	-0.1757	-0.3040	-0.0597	-0.2668	-0.0176	-0.0542	-0.1440	-0.1239	-0.1580	-0.0376	-0.1974	-0.1909	-0.0627	-0.1735	0.0219	0.0292	-0.1170	-0.3044	-0.2414	-0.0060	-0.1890	-0.2209	
	205	-0.0068	0.0432	-0.1974	0.0373	-0.1261	-0.2631	-0.0718	-0.2743	-0.0454	0.0058	-0.1287	-0.1733	-0.0046	0.0240	-0.1242	-0.1876	-0.0980	-0.1580	0.0915	0.0391	-0.1166	-0.3586	-0.2305	0.0024	-0.2266	-0.1862	
	288	0.0470	0.0641	-0.1840	-0.0076	-0.0888	-0.2521	-0.0727	-0.2743	-0.0436	0.0394	-0.1248	-0.1824	-0.0719	0.0596	-0.0785	-0.1928	-0.1047	-0.1310	0.1309	0.0507	-0.0880	-0.3601	-0.2289	0.0234	-0.2424	-0.1501	
	385	0.0520	0.0961	-0.1573	-0.0826	-0.0768	-0.1942	-0.0380	-0.2663	-0.0033	0.0914	-0.1549	-0.1599	-0.1350	0.1811	-0.0028	-0.2055	-0.1022	-0.0517	0.1862	0.0636	-0.0213	-0.2886	-0.2816	0.0387	-0.2453	-0.1044	
	501	0.0600	0.0802	-0.1705	-0.0476	-0.0670	-0.2097	-0.0649	-0.2667	-0.0311	0.0693	-0.1367	-0.1795	-0.1127	0.0896	-0.0392	-0.1968	-0.0950	-0.0937	0.1579	0.0615	-0.0537	-0.3270	-0.2514	0.0379	-0.2513	-0.1155	
2024	107	-0.0171	-0.1722	-0.1616	0.2244	-0.0319	-0.5638	-0.1138	0.0279	0.1166	0.0696	-0.1437	-0.0414	-0.0251	-0.1560	0.0479	-0.1211	-0.0090	-0.1216	-0.1157	0.0080	-0.1085	-0.2689	-0.0818	-0.0717	-0.1543	0.0187	
	205	0.0448	-0.1670																									

Table C-5: Correlation values between wind speed and solar irradiance in Marseille Q3 (daily)

Year	Height (m)	Day 182	Day 183	Day 184	Day 185	Day 186	Day 187	Day 188	Day 189	Day 190	Day 191	Day 192	Day 193	Day 194	Day 195	Day 196	Day 197	Day 198	Day 199	Day 200	Day 201	Day 202	Day 203	Day 204	Day 205	Day 206	Day 207	Day 208	Day 209	Day 210	Day 211	Day 212	
2017	107	-0.0917	0.0971	-0.0682	-0.3788	-0.6438	-0.5281	-0.7300	-0.7654	-0.3005	-0.8607	-0.8984	-0.6076	0.6276	0.3391	0.0682	-0.3790	-0.4995	0.0102	0.2682	-0.4719	-0.4330	-0.0776	0.2815	-0.1757	0.8872	0.6226	-0.7469	0.0432	-0.3863	0.6976	0.8331	
	205	0.0341	0.2782	0.0881	-0.2890	-0.0625	-0.7690	-0.6400	-0.3015	-0.1816	-0.8954	-0.6793	0.9230	0.2141	-0.1209	-0.3603	-0.4050	-0.1949	0.0581	0.1961	-0.5614	-0.4669	-0.0066	0.7151	-0.3547	0.7882	0.8155	-0.8004	-0.2118	-0.5411	0.8974	0.4282	
	288	0.0881	0.4184	0.1674	-0.2325	-0.3859	-0.4413	-0.7516	-0.5936	-0.1334	-0.7636	-0.6490	-0.3981	0.2326	0.1048	-0.1860	-0.3371	-0.5438	-0.0589	0.1835	-0.5034	-0.3303	-0.1790	0.3434	-0.3630	0.9330	0.1183	-0.7900	-0.2773	-0.0450	0.8874	0.3114	
	385	0.0823	0.3759	0.1693	-0.2323	-0.3853	-0.4413	-0.7516	-0.5936	-0.1334	-0.7636	-0.6490	-0.3981	0.2326	0.1048	-0.1860	-0.3371	-0.5438	-0.0589	0.1835	-0.5034	-0.3303	-0.1790	0.3434	-0.3630	0.9330	0.1183	-0.7900	-0.2773	-0.0450	0.8874	0.3114	
	501	0.0925	0.3759	0.1693	-0.2323	-0.3853	-0.4413	-0.7516	-0.5936	-0.1334	-0.7636	-0.6490	-0.3981	0.2326	0.1048	-0.1860	-0.3371	-0.5438	-0.0589	0.1835	-0.5034	-0.3303	-0.1790	0.3434	-0.3630	0.9330	0.1183	-0.7900	-0.2773	-0.0450	0.8874	0.3114	
2018	107	0.6905	-0.7151	0.7691	-0.5705	0.6216	-0.3312	0.4674	-0.2638	-0.6627	0.2689	0.2689	-0.4040	-0.7249	0.1063	0.5425	0.6245	0.6245	-0.3469	0.0538	0.3855	0.2215	0.6846	0.4669	0.4669	-0.4851	-0.2926	-0.2932	0.8576	0.2026	0.1276		
	205	-0.5409	-0.5889	-0.7025	-0.4465	-0.5313	-0.0325	-0.1509	-0.2334	-0.1340	-0.1526	0.2833	-0.6333	0.1275	-0.1602	-0.4592	-0.5241	0.2312	0.3247	-0.5895	0.1219	0.7842	-0.5532	-0.1960	0.2830	0.6522	-0.6032	-0.6032	-0.6344	-0.3241	-0.1981		
	288	-0.5303	-0.4388	-0.6049	-0.3918	-0.2623	-0.1379	-0.0530	-0.1744	-0.0624	-0.3055	0.2133	-0.3303	0.3136	-0.2421	-0.1866	-0.1146	-0.0634	-0.1679	-0.2620	-0.5042	-0.1979	-0.2620	-0.5042	-0.1979	-0.2620	-0.5042	-0.1979	-0.2620	-0.5042	-0.1979	-0.2620	-0.5042
	385	-0.5278	-0.1436	-0.4284	-0.3885	-0.1842	0.2711	0.0065	-0.1396	-0.0567	-0.1784	0.2436	-0.2321	0.4536	-0.1863	-0.1863	-0.1863	-0.1863	-0.1863	-0.1863	-0.1863	-0.1863	-0.1863	-0.1863	-0.1863	-0.1863	-0.1863	-0.1863	-0.1863	-0.1863	-0.1863	-0.1863	
	501	-0.5203	-0.2389	-0.3346	-0.4518	-0.3294	0.4176	0.2538	-0.1731	-0.0871	-0.1330	0.2320	-0.4840	-0.4840	-0.1534	-0.0365	-0.0365	-0.0365	-0.0365	-0.0365	-0.0365	-0.0365	-0.0365	-0.0365	-0.0365	-0.0365	-0.0365	-0.0365	-0.0365	-0.0365	-0.0365	-0.0365	
2019	107	-0.4778	0.6797	0.4077	0.1651	-0.7152	-0.7689	-0.5587	0.3261	-0.4647	-0.5805	-0.6896	-0.6896	-0.6896	-0.6896	-0.6896	-0.6896	-0.6896	-0.6896	-0.6896	-0.6896	-0.6896	-0.6896	-0.6896	-0.6896	-0.6896	-0.6896	-0.6896	-0.6896	-0.6896	-0.6896	-0.6896	
	205	-0.3248	0.7295	0.3982	0.2932	-0.3659	-0.6524	-0.5844	-0.3555	-0.3559	0.7337	-0.7039	0.3110	0.7771	-0.3366	0.8898	-0.3794	0.4748	0.3369	0.6844	-0.3829	-0.4422	-0.4422	-0.4422	-0.4422	-0.4422	-0.4422	-0.4422	-0.4422	-0.4422	-0.4422	-0.4422	
	288	-0.2346	0.6989	0.3869	0.3261	-0.3659	-0.6524	-0.5844	-0.3555	-0.3559	0.7337	-0.7039	0.3110	0.7771	-0.3366	0.8898	-0.3794	0.4748	0.3369	0.6844	-0.3829	-0.4422	-0.4422	-0.4422	-0.4422	-0.4422	-0.4422	-0.4422	-0.4422	-0.4422	-0.4422	-0.4422	
	385	-0.2346	0.6989	0.3869	0.3261	-0.3659	-0.6524	-0.5844	-0.3555	-0.3559	0.7337	-0.7039	0.3110	0.7771	-0.3366	0.8898	-0.3794	0.4748	0.3369	0.6844	-0.3829	-0.4422	-0.4422	-0.4422	-0.4422	-0.4422	-0.4422	-0.4422	-0.4422	-0.4422	-0.4422	-0.4422	
	501	-0.2346	0.6989	0.3869	0.3261	-0.3659	-0.6524	-0.5844	-0.3555	-0.3559	0.7337	-0.7039	0.3110	0.7771	-0.3366	0.8898	-0.3794	0.4748	0.3369	0.6844	-0.3829	-0.4422	-0.4422	-0.4422	-0.4422	-0.4422	-0.4422	-0.4422	-0.4422	-0.4422	-0.4422	-0.4422	
2020	107	-0.4378	-0.2832	0.1158	-0.3369	0.4928	0.2723	0.1501	-0.2632	-0.7649	-0.6693	0.2646	-0.0469	-0.1205	-0.7108	-0.4251	-0.6320	-0.7030	-0.8522	0.4778	-0.0565	-0.4715	0.1981	0.8197	0.7338	-0.1146	0.1296	0.2822	0.3942	0.4410	0.5372		
	205	-0.4102	-0.0999	0.1249	-0.2447	0.4776	0.1397	0.1831	-0.2213	-0.3203	0.3145	-0.2306	-0.1325	-0.2067	-0.6511	-0.1639	-0.5966	-0.4923	-0.6394	-0.7639	-0.7788	-0.6818	-0.1382	-0.4777	-0.2835	0.7352	0.6044	-0.1907	0.1414	-0.2021	0.3826	0.4683	
	288	-0.4302	-0.0093	0.1901	-0.1516	-0.4955	0.2650	0.2097	-0.2267	-0.1919	-0.6209	0.3361	-0.1313	-0.1128	-0.1639	-0.5966	-0.4923	-0.6394	-0.7639	-0.7788	-0.6818	-0.1382	-0.4777	-0.2835	0.7352	0.6044	-0.1907	0.1414	-0.2021	0.3826	0.4683	0.4683	
	385	-0.4737	0.1564	0.2476	-0.0672	0.1504	0.3636	0.2449	-0.2736	-0.2938	0.6564	0.3321	-0.4057	-0.1784	-0.3303	-0.1863	-0.1863	-0.1863	-0.1863	-0.1863	-0.1863	-0.1863	-0.1863	-0.1863	-0.1863	-0.1863	-0.1863	-0.1863	-0.1863	-0.1863	-0.1863	-0.1863	
	501	-0.4730	0.3370	0.3161	-0.0174	0.5140	0.4836	0.2847	-0.3837	0.0946	-0.7537	0.1456	-0.3692	-0.2046	-0.1426	-0.5175	-0.4422	-0.5249	-0.6590	-0.7397	-0.7191	-0.7233	-0.4656	-0.2833	0.7448	-0.0113	-0.4232	0.1422	0.4469	-0.2441	0.2823	0.2837	
2021	107	0.0143	-0.1946	-0.7694	-0.1977	-0.5815	0.3308	0.2644	0.2700	0.2242	-0.3714	0.4888	-0.0854	-0.0714	-0.7376	-0.1254	-0.4518	0.8315	-0.5212	-0.1979	-0.1853	-0.0506	0.0737	0.3610	-0.2114	-0.4125	0.1927	0.7398	0.0499	0.1919			
	205	0.2187	0.1503	-0.6995	-0.5942	-0.3881	0.5487	0.3177	0.4132	0.2822	-0.4622	0.3938	0.0819	-0.1310	-0.7011	-0.4095	-0.1283	-0.5752	-0.8254	-0.5176	-0.2677	-0.3464	-0.0464	-0.0268	0.1394	-0.2942	-0.4748	0.4839	0.1664	-0.0911	-0.1715	-0.1339	
	288	0.3871	0.2440	-0.6769	-0.5688	-0.2177	0.6195	0.2386	0.5140	0.2899	-0.4010	0.3478	0.0819	-0.1310	-0.7011	-0.4095	-0.1283	-0.5752	-0.8254	-0.5176	-0.2677	-0.3464	-0.0464	-0.0268	0.1394	-0.2942	-0.4748	0.4839	0.1664	-0.0911	-0.1715	-0.1339	
	385	0.4801	0.1309	-0.6720	-0.3825	-0.1539	0.6196	0.1014	0.6066	0.2755	-0.3646	0.4689	0.1887	-0.1016	-0.9080	-0.5174	-0.2507	-0.5114	-0.7780	-0.5461	-0.2863	-0.0514	-0.0001	0.0758	0.1071	-0.2626	-0.4161	0.8884	-0.1384	-0.1997	-0.0795	-0.1981	
	501	0.3885	0.6840	-0.5054	-0.1262	0.1533	0.5617	0.4493	0.4654	0.5848	0.8910	0.6936	0.6936	0.6936	0.6936	0.6936	0.6936	0.6936	0.6936	0.6936	0.6936	0.6936	0.6936	0.6936	0.6936	0.6936	0.6936	0.6936	0.6936	0.6936	0.6936	0.6936	
2017	107	0.2461	-0.2526	0.4357	-0.3403	-0.6585	0.6883	-0.6213	0.4792	0.9760	-0.6092	-0.5658	0.6458	-0.2334	-0.2875	-0.4981	-0.5895	-0.6404	-0.5895	-0.6404	-0.5895	-0.6404	-0.5895	-0.6404	-0.5895	-0.6404	-0.5895	-0.6404	-0.5895	-0.6404	-0.5895	-0.6404	
	205	0.2993	-0.0638	0.0620	-0.1225	-0.5121	-0.3283	-0.6226	0.5432	-0.5178	-0.7579	-0.9420	0.6966	0.7450	-0.1969	-0.7430	-0.1234	-0.4510	0.1688	-0.6227	-0.2524	-0.3381	-0.3434	-0.3434	-0.3434	-0.3434	-0.3434	-0.3434	-0.3434	-0.3434	-0.3434	-0.3434	
	288	0.3559	0.0703	0.2288	-0.1272	-0.4075	-0.6770	-0.5805	0.6401	-0.4681	-0.5029	-0.7913	-0.5856	0.4554	-0.1437	-0.7045	-0.1194	-0.4449	0.2284	-0.1609	-0.3253	-0.3641	-0.3793	-0.3793	-0.3793	-0.3793	-0.3793	-0.3793	-0.3793	-0.3793	-0.3793	-0.3793	
	385	0.4251	0.1538	0.2769	-0.0348	-0.3825	-0.5832	-0.4580	0.6815	-0.3997	-0.4040	-0.6363	0.3386	0.2322	-0.0229	-0.7048	-0.1048	-0.4851	0.2620	-0.7797	-0.1671	-0.3321	-0.3718	-0.3718	-0.3718	-0.3718	-0.3718	-0.3718	-0.3718	-0.3718	-0.3718	-0.3718	
	501	0.4469	0.1214	0.2522	-0.0421	-0.4462	-0.5339	-0.2232	0.6844	-0.3197	-0.4006	-0.6363	0.3312	0.4625	-0.0229	-0.7048	-0.1048	-0.4851	0.2620	-0.7797	-0.1671	-0.3321	-0.3718	-0.3718	-0.3718	-0.3718	-0.3718	-0.3718	-0.3718	-0.3718	-0.3718	-0.3718	
2020	107	-0.4000	0.6025	-0.5168	-0.3451	-0.1201	0.4453	-0.7438	-0.7208	-0.8391	-0.9760	-0.7071	-0.7376	-0.2420	0.1673	-0.2078																	

Table C.7: Correlation values between Kite and PV Energy in Marseille (monthly-yearly)

	Height (m)	Jan	Feb	Mar	Apr	May	Jun	Jul	Aug	Sep	Oct	Nov	Dec	Winter	Spring	Summer	Fall	1st Half	2nd Half	Year
2017	107	-0,0409	-0,0810	-0,0840	-0,0443	0,0097	-0,0934	-0,0683	0,0045	0,0016	-0,0130	-0,0585	-0,1303	-0,1161	-0,0675	-0,0185	-0,0819	-0,1040	-0,0875	-0,0963
	205	-0,0566	-0,1210	-0,1803	-0,0590	0,0070	-0,1120	-0,0929	0,0085	-0,0004	-0,0172	-0,0317	-0,1753	-0,1714	-0,0690	-0,0278	-0,0963	-0,1356	-0,1051	-0,1206
	288	-0,0213	-0,1049	-0,2041	-0,0695	0,0097	-0,1174	-0,0968	0,0075	-0,0013	-0,0205	-0,0201	-0,1642	-0,1663	-0,0731	-0,0296	-0,0978	-0,1361	-0,1063	-0,1215
	385	0,0038	-0,0787	-0,2100	-0,0815	0,0158	-0,1061	-0,0960	0,0043	0,0052	-0,0155	-0,0123	-0,1364	-0,1515	-0,0710	-0,0277	-0,0908	-0,1277	-0,0996	-0,1141
	501	0,0153	-0,0571	-0,1927	-0,0947	0,0191	-0,0763	-0,1007	-0,0033	0,0172	0,0023	-0,0064	-0,1106	-0,1314	-0,0642	-0,0276	-0,0759	-0,1131	-0,0894	-0,1017
2018	107	-0,0739	0,0243	-0,0330	-0,1820	-0,0762	-0,0461	-0,0825	-0,0747	-0,0437	-0,0829	-0,0611	0,0152	-0,0143	-0,1008	-0,0639	-0,0397	-0,1190	-0,1009	-0,1084
	205	-0,1604	-0,0570	-0,1154	-0,1870	-0,0564	-0,0653	-0,0682	-0,1038	-0,0207	-0,0646	-0,0375	0,0228	-0,1047	-0,1054	-0,0618	-0,0285	-0,1628	-0,1022	-0,1298
	288	-0,1769	-0,0749	-0,1356	-0,1868	-0,0495	-0,0662	-0,0602	-0,1138	-0,0018	-0,0390	-0,0212	0,0551	-0,1276	-0,1044	-0,0566	-0,0098	-0,1724	-0,0971	-0,1316
	385	-0,1793	-0,0756	-0,1338	-0,1856	-0,0571	-0,0624	-0,0485	-0,1218	0,0143	-0,0097	0,0054	0,0734	-0,1309	-0,1059	-0,0503	0,0080	-0,1751	-0,0908	-0,1296
	501	-0,1725	-0,0663	-0,1141	-0,1816	-0,0794	-0,0702	-0,0446	-0,1239	-0,0227	-0,0105	0,0265	0,0844	-0,1213	-0,1152	-0,0466	0,0092	-0,1772	-0,0914	-0,1309
2019	107	-0,0159	-0,1426	-0,1563	-0,1055	-0,0881	-0,1035	-0,0470	-0,1387	0,0539	-0,0892	-0,0876	-0,1539	-0,1543	-0,1127	-0,0582	-0,0974	-0,1425	-0,1008	-0,1162
	205	-0,0484	-0,1794	-0,2361	-0,1187	-0,0999	-0,0750	-0,0411	-0,1302	0,0065	-0,0756	-0,1135	-0,1461	-0,2040	-0,1114	-0,0716	-0,0964	-0,1615	-0,1206	-0,1372
	288	-0,0422	-0,1828	-0,2558	-0,1129	-0,1023	-0,0676	-0,0303	-0,1090	-0,0093	-0,0697	-0,1042	-0,1111	-0,2119	-0,1075	-0,0668	-0,0821	-0,1619	-0,1188	-0,1372
	385	-0,0243	-0,1818	-0,2512	-0,1054	-0,1041	-0,0605	-0,0283	-0,0844	-0,0169	-0,0611	-0,0904	-0,0854	-0,2070	-0,1037	-0,0604	-0,0668	-0,1562	-0,1161	-0,1331
	501	0,0198	-0,1833	-0,2278	-0,1060	-0,1350	-0,0520	-0,0321	-0,0629	-0,0277	-0,0517	-0,0789	-0,0994	-0,0994	-0,1856	-0,1131	-0,0584	-0,1493	-0,1196	-0,1315
2020	107	-0,1116	0,0302	-0,0403	-0,1125	-0,0937	-0,0866	-0,0055	-0,0702	0,0668	-0,0377	-0,1399	-0,0714	-0,0350	-0,0474	0,0055	-0,0694	-0,0638	-0,0604	-0,0630
	205	-0,1189	-0,0682	-0,0806	-0,1160	-0,0981	-0,1178	-0,0317	-0,1163	0,0623	-0,0078	-0,1115	-0,0806	-0,0886	-0,0645	-0,0229	-0,0545	-0,0997	-0,0838	-0,0925
	288	-0,0774	-0,0706	-0,0755	-0,1011	-0,0995	-0,1225	-0,0418	-0,1254	0,0542	0,0220	-0,0865	-0,0736	-0,0810	-0,0652	-0,0331	-0,0336	-0,0989	-0,0850	-0,0927
	385	-0,0269	-0,0324	-0,0626	-0,0814	-0,1041	-0,1217	-0,0503	-0,1185	0,0412	0,0399	-0,0779	-0,0603	-0,0576	-0,0639	-0,0393	-0,0220	-0,0905	-0,0853	-0,0886
	501	-0,0014	0,0001	-0,0482	-0,0466	-0,1154	-0,1211	-0,0559	-0,0953	0,0275	0,0451	-0,0944	-0,0460	-0,0460	-0,0407	-0,0623	-0,0405	-0,0240	-0,0844	-0,0875
2021	107	0,0222	-0,0396	0,0168	-0,0307	-0,0676	-0,1486	-0,0542	-0,0456	-0,1460	-0,1405	0,0417	-0,0763	-0,0345	-0,0801	-0,0370	-0,0504	-0,0710	-0,0804	-0,0748
	205	-0,0676	-0,1306	-0,0535	-0,0748	-0,0692	-0,1505	-0,0582	-0,0489	-0,1682	-0,1312	0,0344	-0,1154	-0,1266	-0,0940	-0,0544	-0,0687	-0,1196	-0,0992	-0,1081
	288	-0,0446	-0,1545	-0,0688	-0,0968	-0,0638	-0,1431	-0,0413	-0,0365	-0,1594	-0,1280	0,0375	-0,0960	-0,1434	-0,0958	-0,0455	-0,0675	-0,1284	-0,0913	-0,1079
	385	0,0085	-0,1508	-0,0767	-0,1126	-0,0529	-0,1369	-0,0270	-0,0200	-0,1439	-0,1311	0,0455	-0,0711	-0,1379	-0,0936	-0,0330	-0,0647	-0,1248	-0,0804	-0,0999
	501	0,0548	-0,1151	-0,0829	-0,1174	-0,0406	-0,1305	-0,0107	-0,0073	-0,1325	-0,1388	0,0494	-0,0604	-0,1187	-0,0868	-0,0221	-0,0676	-0,1135	-0,0730	-0,0894

Table C.8: Correlation values between Kite and PV Energy in Marseille (weekly)

Height (m)	Week 1	Week 2	Week 3	Week 4	Week 5	Week 6	Week 7	Week 8	Week 9	Week 10	Week 11	Week 12	Week 13	Week 14	Week 15	Week 16	Week 17	Week 18	Week 19	Week 20	Week 21	Week 22	Week 23	Week 24	Week 25	Week 26	
2017	107	-0.0039	-0.1453	-0.0782	-0.0955	-0.0474	-0.0876	-0.1082	0.0597	-0.0572	0.0875	-0.1205	-0.1244	-0.1735	-0.0251	-0.0817	-0.1177	-0.0710	-0.2181	0.0210	0.0384	-0.0528	0.0580	-0.1189	-0.0665	-0.0211	-0.0017
	205	-0.0035	-0.2853	-0.0397	-0.0924	-0.0918	-0.1353	-0.1224	-0.0119	-0.1104	0.0389	-0.2046	-0.3027	-0.2609	0.0493	-0.0393	-0.1262	-0.2450	-0.0101	-0.0562	0.0101	0.0295	0.0133	0.0072	-0.1049	-0.2691	-0.1136
	288	0.0195	-0.3105	0.0504	-0.0230	-0.0859	-0.0845	-0.0954	-0.0190	-0.1118	0.0424	-0.2215	-0.3630	-0.2765	0.0530	-0.0456	-0.1218	-0.1737	-0.2648	0.0530	0.0117	-0.0254	0.0133	0.0072	-0.1049	-0.2691	-0.1136
2018	107	-0.0498	-0.2220	0.2057	-0.2743	-0.1085	-0.0135	0.0172	-0.0679	-0.1427	-0.0997	-0.1608	0.1645	0.0652	-0.2586	-0.2557	-0.2058	0.0057	0.0171	-0.1071	-0.2676	0.0870	-0.1042	-0.0386	0.0174	-0.2305	-0.0792
	205	-0.0969	-0.0186	0.0382	-0.4147	-0.2245	-0.1375	-0.0378	-0.2065	-0.2188	-0.1687	-0.2843	0.1336	0.0119	-0.1490	-0.3061	-0.1995	-0.0608	0.0341	-0.1117	-0.2654	0.0901	-0.1791	0.0627	0.0025	-0.2749	-0.1416
	288	-0.1218	0.0153	-0.0464	-0.4032	-0.2558	-0.1884	-0.0427	-0.1885	-0.2042	-0.1909	-0.3058	0.1363	-0.0055	-0.1096	-0.3295	-0.1862	-0.0729	0.0391	0.0017	-0.2456	0.1177	-0.1950	0.0888	0.0033	-0.2764	-0.1583
2019	107	-0.1397	0.0467	-0.1062	-0.3534	-0.2601	-0.2066	-0.0427	-0.1232	-0.2022	-0.2003	-0.2979	0.1485	-0.0003	-0.1122	-0.3639	-0.1560	-0.0686	0.0337	-0.0048	-0.2426	0.1236	-0.1935	0.1027	-0.0028	-0.2694	-0.1569
	205	-0.1566	0.0575	-0.1679	-0.2328	-0.2347	-0.1972	-0.0442	-0.0641	-0.1378	-0.1848	-0.2656	0.1646	0.0081	-0.1332	-0.3750	-0.1224	-0.0606	0.0274	-0.0474	-0.2505	0.0657	-0.1901	0.1043	-0.0439	-0.2759	-0.1535
	288	-0.3134	0.0574	-0.1566	0.0310	-0.1618	-0.2175	-0.1244	-0.1065	-0.1690	-0.2123	-0.2069	-0.2428	-0.1489	-0.3751	-0.0239	-0.2806	-0.0375	0.1375	-0.2579	-0.0907	-0.2069	-0.2378	0.2515	-0.1699	-0.2070	-0.0462
2020	107	-0.0518	-0.1672	-0.1617	0.0220	-0.1489	-0.2028	-0.1414	-0.1024	-0.1791	-0.2571	-0.2119	-0.2712	-0.1595	-0.3336	-0.0046	-0.2746	-0.0459	0.1451	-0.2649	-0.1010	-0.1987	-0.2388	0.2942	-0.1926	-0.1756	-0.0685
	205	-0.0468	0.1728	-0.1265	0.0282	-0.1322	-0.1808	-0.1447	-0.0658	-0.2010	-0.2680	-0.2022	-0.2498	-0.1666	-0.2926	0.0000	-0.2529	-0.0494	0.1346	-0.2479	-0.1252	-0.1945	-0.2272	0.3079	-0.2278	-0.0991	-0.1022
	288	0.0772	0.1627	-0.0749	0.0697	-0.1547	-0.1742	-0.1282	-0.0680	-0.2285	-0.2683	-0.1812	-0.1807	-0.1636	-0.2711	-0.0181	-0.2082	-0.0619	-0.0119	-0.1817	-0.1974	-0.1987	-0.2031	0.3100	-0.2851	-0.0148	-0.1223
2021	107	-0.1940	-0.1252	0.0031	0.0672	0.0547	0.0379	0.0820	-0.1508	-0.1032	0.0411	0.1707	-0.1202	-0.0087	-0.1036	0.0241	-0.1511	-0.1610	-0.1138	-0.1848	0.2586	-0.0213	-0.3593	-0.2006	-0.2648	-0.1965	-0.1283
	205	-0.2340	-0.0971	-0.0845	-0.0252	-0.0922	-0.0553	0.0076	-0.2294	-0.1377	-0.0040	-0.0610	-0.0423	-0.0755	-0.1153	-0.0423	-0.1671	-0.2428	-0.0721	-0.1132	0.2291	-0.0934	-0.3648	-0.0863	-0.2328	-0.2546	0.0344
	288	-0.1843	-0.0106	-0.1090	0.0066	-0.1033	-0.0953	-0.0028	-0.2385	-0.1293	-0.0181	-0.1073	-0.2680	-0.0859	-0.1292	-0.0934	-0.1591	-0.2814	-0.0574	-0.0879	0.2280	-0.1028	-0.3329	-0.0496	-0.2232	-0.2637	0.0076
2017	107	-0.1054	0.0897	-0.1096	0.0674	-0.0764	-0.1046	0.0146	-0.2276	-0.1106	-0.0436	-0.0876	-0.3007	-0.0873	-0.1389	-0.1466	-0.1404	-0.3019	-0.0274	-0.0696	0.2337	-0.1079	-0.2733	-0.0309	-0.2146	-0.2695	-0.0171
	205	-0.0452	0.1542	-0.0927	0.0987	-0.0281	-0.0941	0.0877	-0.1896	-0.1111	-0.0557	-0.0388	-0.2895	-0.0786	-0.1606	-0.1847	-0.1236	-0.2758	0.0198	-0.0422	0.2316	-0.1161	-0.2219	-0.0232	-0.2135	-0.2584	-0.0234
	288	-0.1868	-0.0336	-0.0632	-0.1479	0.0231	0.1737	-0.0635	0.0406	0.0231	0.0872	-0.1388	-0.0604	-0.1785	0.0651	-0.0391	-0.0635	0.0538	-0.0410	-0.2016	-0.0933	-0.1045	-0.0748	0.0332	-0.1583	-0.2755	-0.1941
2018	107	-0.1690	-0.0602	-0.0983	-0.2409	0.1084	0.2174	-0.0690	0.0056	-0.0329	0.0844	-0.0476	-0.1197	-0.2582	0.1106	-0.0282	-0.1130	0.0089	-0.0683	0.0280	-0.0773	-0.0064	-0.0538	0.0223	-0.2937	-0.4197	-0.1842
	205	-0.1889	-0.0428	-0.0768	-0.2439	0.0932	0.2166	-0.0475	-0.0175	-0.0559	0.1032	-0.0312	-0.1100	-0.2645	0.1040	-0.0343	-0.0984	0.0106	-0.0797	0.0362	-0.0657	-0.0380	-0.0333	0.0345	-0.2975	-0.3715	-0.1511
	288	-0.0763	0.0273	0.0048	-0.1790	-0.0339	-0.0956	-0.1078	-0.1180	-0.0938	0.1330	-0.0903	-0.1095	-0.0921	0.0567	0.0155	-0.1309	-0.0470	-0.0008	-0.0267	0.0243	-0.1733	0.1566	-0.0601	0.1575	0.0510	-0.0652
2019	107	-0.0528	0.0672	0.0165	-0.2020	-0.0309	-0.0920	-0.1319	-0.1261	-0.1132	0.1377	-0.0906	-0.0859	0.0285	0.1559	-0.1559	-0.1206	0.0662	0.0035	-0.0523	0.0608	-0.1466	0.2312	-0.0698	0.1938	0.0906	-0.0547
	205	-0.0984	-0.0188	-0.0020	-0.1397	-0.0451	-0.0858	-0.0941	-0.1109	-0.0714	0.1004	-0.1163	-0.1207	-0.0904	0.1372	-0.0868	-0.1353	-0.0993	-0.0016	0.0001	-0.0115	-0.1947	0.0942	-0.0758	0.1199	0.0166	-0.1019
	288	0.0700	0.0224	-0.1268	0.0656	-0.0516	-0.2391	-0.0558	-0.2558	-0.1685	0.1323	-0.0830	-0.1323	-0.0591	-0.0399	-0.0794	-0.2517	-0.0854	-0.1794	0.0664	0.0362	-0.0756	-0.4465	-0.2075	-0.0248	-0.0823	-0.0981
2020	107	0.0620	0.0218	-0.0975	0.0413	-0.0094	-0.2403	-0.0404	-0.2499	-0.1580	0.1084	-0.0881	-0.0892	-0.0733	-0.0214	-0.0782	-0.2778	-0.0727	-0.1304	0.0760	0.0508	-0.0521	-0.4302	-0.2311	0.0320	-0.0470	-0.0385
	205	-0.0620	0.0213	-0.0726	-0.2207	-0.0240	-0.2330	-0.0474	-0.0893	-0.1129	-0.0693	-0.0752	-0.0632	-0.0632	-0.0021	0.2402	-0.1052	-0.0107	0.0003	0.0003	0.0326	-0.1466	0.2312	-0.0698	0.1938	0.0906	-0.0547
	288	0.0319	-0.1149	-0.1104	0.0042	0.0520	-0.4833	-0.1436	-0.0019	0.0966	0.1249	-0.1749	0.0382	0.0076	-0.1672	0.0140	-0.1688	0.0693	-0.1149	-0.1443	0.0628	-0.1500	-0.3350	-0.1096	0.0525	-0.1341	-0.0665
2021	107	0.0375	-0.1156	-0.1410	0.0615	0.0462	-0.4610	-0.1751	-0.0537	0.0714	0.1612	-0.1100	-0.0217	-0.0621	-0.1189	0.1118	-0.1856	0.1155	-0.1270	-0.0639	0.0976	-0.1053	-0.4251	-0.1422	0.0577	-0.1466	-0.1603
	205	0.0436	-0.1018	-0.1530	0.0010	0.0426	-0.4331	-0.1511	-0.0895	0.0617	0.1645	-0.0745	-0.0423	-0.0809	-0.0682	-0.1402	-0.1288	-0.0844	-0.2051	0.0464	0.0064	-0.0939	-0.3851	-0.2166	-0.0861	-0.1289	-0.1687
	288	0.0545	-0.0992	-0.1548	0.0410	0.0402	-0.4403	-0.1089	-0.0607	0.0696	0.1639	-0.0701	-0.0707	-0.0821	-0.0463	0.1542	-0.0901	0.1727	-0.1081	-0.0462	0.0830	-0.0801	-0.2705	-0.1631	0.1619	-0.1089	-0.1477
2022	107	0.0552	-0.1015	-0.1397	-0.0622	0.0307	-0.4601	-0.0451	-0.0515	0.1147	0.1519	-0.0552	-0.1016	-0.0817	-0.0505	0.1519	-0.0803	0.1813	-0.0783	-0.0870	0.0427	-0.0985	-0.2098	-0.1781	0.1688	-0.0760	-0.0688
	205	-0.0861	-0.1516	-0.1318	0.0259	0.1033	-0.1311	-0.0272	-0.1623	-0.0227	-0.2427	-0.2181	-0.0618	-0.1047	-0.1162	-0.1345	-0.3120	-0.1345	-0.3120	-0.1345	-0.3120	-0.1345	-0.3120	-0.1345	-0.3120	-0.1345	-0.3120
	288	0.0050	-0.0604	-0.1815	-0.0486	0.1533	-0.0606	-0.0362	-0.2220	-0.0741	-0.1855	-0.2438	-0.1135	-0.1639	-0.1012	-0.0781	-0.2987	-0.0250	-0.1627	0.1506	0.0206	-0.1532	0.1072	0.0051	-0.2345	-0.2652	-0.0410
2023	107	-0.0030	-0.0149	-0.1727	-0.0237	0.1663	0.0273	-0.0404	-0.1921	-0.0764	-0.0974	-0.2536	-0.0488	-0.1677	-0.1067	-0.0950	-0.3158	0.0141	-0.0691	0.1642	0.0401	-0.1571	0.0640	-0.0133	-0.0349	-0.1659	0.0040
	205	-0.0188	0.0230	-0.1426	0.0079	0.1825	0.0479	-0.0625	-0.1480	-0.0495	-0.0658	-0.2650	-0.0358	-0.1742	-0.0737	-0.1404	-0.3163	0.0244	-0.0459	0.1470	0.0584	-0.1489	0.0384	-0.0440	-0.0007	-0.1040	0.0104
	288	-0.0030	-0.0149	-0.1727	-0.0237	0.1663	0.0273	-0.0404	-0.1921	-0.0764	-0.0974	-0.2536	-0.0488	-0.1677	-0.1067	-0.0950	-0.3158	0.0141	-0.0691	0.1642	0.0401	-0.1571	0.0640	-0.0133	-0.0349	-0.1659	0.0040

Table C.10: Correlation values between Kite and PV Energy in Marseille Q2 (daily)

Year	Day 91	Day 92	Day 93	Day 94	Day 95	Day 96	Day 97	Day 98	Day 99	Day 100	Day 101	Day 102	Day 103	Day 104	Day 105	Day 106	Day 107	Day 108	Day 109	Day 110	Day 111	Day 112	Day 113	Day 114	Day 115	Day 116	Day 117	Day 118	Day 119	Day 120		
2017	107	-0.129	0.187	0.076	0.203	0.166	0.357	-0.154	-0.420	-0.496	0.424	-0.453	0.475	-0.318	-0.647	-0.316	-0.509	-0.265	0.607	-0.398	-0.602	0.077	0.490	0.039	0.210	-0.769	0.163	-0.979	-0.243	0.545		
	205	0.135	0.008	0.372	0.286	0.159	0.259	0.150	-0.521	-0.430	0.390	-0.326	0.543	-0.700	-0.830	0.178	-0.330	0.992	-0.164	-0.133	0.992	-0.716	-0.075	0.266	-0.096	0.730	-0.846	-0.893	-0.992	-0.454	0.327	
	285	0.284	0.038	0.438	0.286	0.230	0.147	0.217	-0.603	-0.529	0.386	-0.293	0.576	-0.710	-0.939	0.226	-0.469	-0.083	-0.185	-0.199	0.881	-0.718	-0.195	0.138	-0.086	0.848	-0.388	-0.388	-0.937	0.321		
	385	0.424	0.462	0.407	0.164	0.068	0.223	-0.318	0.532	-0.526	0.399	-0.284	0.646	0.119	-0.284	0.188	0.620	0.124	0.169	0.169	0.681	-0.534	-0.218	0.139	-0.144	-0.630	-0.852	-0.767	-0.673	0.374	0.263	
	507	0.074	-0.403	-0.262	0.107	0.088	-0.273	-0.055	-0.013	-0.186	-0.161	0.389	0.616	-0.547	-0.523	0.886	-0.244	-0.547	-0.246	-0.100	-0.327	0.262	-0.130	0.282	-0.576	0.265	-0.247	0.681	0.360	0.378		
2018	205	0.217	-0.470	-0.142	-0.186	0.575	-0.304	-0.327	0.318	-0.037	0.766	0.476	-0.776	-0.520	-0.268	-0.796	-0.184	-0.960	-0.302	-0.192	-0.132	-0.363	-0.540	-0.026	-0.491	0.534	-0.244	0.303	0.230			
	285	0.232	-0.472	-0.409	-0.726	0.634	-0.332	-0.194	0.349	-0.921	-0.016	0.204	0.330	-0.490	-0.274	-0.606	-0.126	-0.428	-0.307	-0.143	-0.383	-0.175	-0.459	-0.349	-0.249	0.463	0.226	0.187				
	385	0.613	-0.478	-0.357	-0.819	-0.777	-0.081	-0.084	-0.214	0.345	-0.419	-0.639	-0.115	-0.286	-0.378	-0.478	-0.276	-0.175	-0.348	0.057	-0.607	0.530	-0.262	0.446	0.442	0.218	0.197					
	507	-0.438	-0.464	0.086	-0.267	-0.724	0.461	-0.218	-0.065	-0.441	-0.029	-0.094	0.270	-0.762	-0.078	-0.359	-0.364	-0.383	-0.540	-0.582	-0.303	-0.349	0.023	-0.107	-0.486	0.490	-0.587	-0.753				
	205	-0.284	-0.471	0.086	-0.031	-0.711	0.332	-0.489	-0.379	0.260	0.223	-0.702	-0.289	0.115	-0.800	-0.026	-0.384	-0.299	-0.320	-0.512	-0.990	-0.277	-0.866	-0.081	-0.232	-0.836						
2019	205	-0.260	-0.445	0.083	-0.052	-0.436	0.441	-0.386	0.265	0.223	-0.702	-0.289	0.115	-0.800	-0.026	-0.384	-0.299	-0.320	-0.512	-0.990	-0.277	-0.866	-0.081	-0.232	-0.836							
	285	-0.260	-0.445	0.083	-0.052	-0.436	0.441	-0.386	0.265	0.223	-0.702	-0.289	0.115	-0.800	-0.026	-0.384	-0.299	-0.320	-0.512	-0.990	-0.277	-0.866	-0.081	-0.232	-0.836							
	385	-0.260	-0.445	0.083	-0.052	-0.436	0.441	-0.386	0.265	0.223	-0.702	-0.289	0.115	-0.800	-0.026	-0.384	-0.299	-0.320	-0.512	-0.990	-0.277	-0.866	-0.081	-0.232	-0.836							
	507	-0.260	-0.445	0.083	-0.052	-0.436	0.441	-0.386	0.265	0.223	-0.702	-0.289	0.115	-0.800	-0.026	-0.384	-0.299	-0.320	-0.512	-0.990	-0.277	-0.866	-0.081	-0.232	-0.836							
	205	-0.260	-0.445	0.083	-0.052	-0.436	0.441	-0.386	0.265	0.223	-0.702	-0.289	0.115	-0.800	-0.026	-0.384	-0.299	-0.320	-0.512	-0.990	-0.277	-0.866	-0.081	-0.232	-0.836							
2020	205	0.009	-0.858	0.473	-0.088	-0.442	-0.855	-0.250	-0.194	-0.117	-0.597	-0.544	0.492	0.100	-0.581	-0.317	-0.351	-0.258	0.781	0.052	0.132	0.932	-0.496	-0.303	0.778	-0.152	0.270	0.432	-0.083	-0.1945		
	285	0.247	-0.439	0.543	-0.754	-0.434	-0.639	-0.449	-0.870	-0.194	-0.418	-0.482	-0.545	-0.346	-0.421	-0.167	-0.167	-0.268	0.188	0.281	0.310	-0.300	-0.325	-0.231	0.109	-0.423	-0.347	0.081				
	385	0.643	-0.451	0.188	-0.046	-0.313	0.715	-0.452	-0.708	-0.160	-0.443	-0.514	-0.316	-0.423	-0.270	-0.036	-0.473	-0.200	0.736	0.312	0.076	0.243	-0.322	-0.393	-0.348	-0.165	-0.561	-0.434	0.051			
	507	0.754	-0.462	0.684	-0.411	-0.647	-0.039	-0.207	-0.777	-0.179	-0.081	-0.084	-0.214	0.345	-0.419	-0.639	-0.115	-0.286	-0.378	0.057	-0.607	0.530	-0.262	0.446	0.442	0.218	0.197					
	205	-0.438	-0.464	0.086	-0.267	-0.724	0.461	-0.218	-0.065	-0.441	-0.029	-0.094	0.270	-0.762	-0.078	-0.359	-0.364	-0.383	-0.540	-0.582	-0.303	-0.349	0.023	-0.107	-0.486	0.490	-0.587	-0.753				
2021	205	-0.442	-0.358	0.493	0.263	0.395	0.434	-0.415	0.958	0.441	-0.694	0.241	0.145	-0.750	-0.791	-0.330	-0.193	0.478	0.704	0.575	0.385	0.125	-0.185	-0.389	-0.391	0.224	0.167	0.278				
	285	-0.461	-0.387	0.300	0.366	-0.116	0.284	0.284	0.720	0.150	0.723	0.116	0.102	0.024	-0.261	-0.292	-0.277	-0.021	-0.244	0.632	0.700	0.187	-0.312	-0.444	-0.206	-0.182	-0.308	-0.349	0.105	0.430		
	385	-0.429	-0.367	0.243	0.354	-0.044	0.208	0.194	-0.749	0.672	0.165	-0.810	0.183	-0.060	-0.432	-0.746	-0.325	0.151	-0.182	-0.199	-0.558	0.210	-0.245	-0.200	-0.276	-0.149	-0.257	-0.181	0.304	-0.059		
	507	-0.430	-0.369	0.243	0.354	-0.044	0.208	0.194	-0.749	0.672	0.165	-0.810	0.183	-0.060	-0.432	-0.746	-0.325	0.151	-0.182	-0.199	-0.558	0.210	-0.245	-0.200	-0.276	-0.149	-0.257	-0.181	0.304	-0.059		
	205	-0.430	-0.369	0.243	0.354	-0.044	0.208	0.194	-0.749	0.672	0.165	-0.810	0.183	-0.060	-0.432	-0.746	-0.325	0.151	-0.182	-0.199	-0.558	0.210	-0.245	-0.200	-0.276	-0.149	-0.257	-0.181	0.304	-0.059		
2018	107	-0.543	-0.830	-0.231	-0.307	-0.175	-0.203	0.692	-0.125	0.735	-0.649	-0.283	0.013	-0.601	-0.601	0.190	-0.673	-0.249	-0.068	0.837	0.179	-0.425	-0.292	0.1072	-0.911	-0.287	0.132	0.1754	0.5106	0.626	0.2050	
	205	-0.516	-0.862	-0.196	-0.254	-0.147	-0.190	0.770	-0.672	0.484	-0.675	0.125	0.142	-0.289	-0.456	0.261	-0.710	-0.342	-0.185	0.728	0.243	-0.372	-0.321	0.253	-0.803	-0.262	0.142	0.1052	0.519	0.481	0.1157	
	285	-0.570	-0.405	-0.745	-0.164	0.023	-0.574	0.456	0.696	0.890	-0.280	-0.420	0.149	-0.555	-0.416	0.272	-0.769	-0.231	0.071	0.746	0.1703	-0.3403	-0.1975	-0.3089	-0.1460	0.085	0.099	0.5168	0.494	0.084	0.1258	
	385	-0.498	-0.425	-0.142	0.091	0.004	-0.486	0.429	0.724	0.692	-0.191	0.680	0.372	-0.489	-0.389	0.267	-0.620	-0.287	0.620	0.605	-0.345	-0.1001	0.433	-0.726	-0.1460	0.085	0.099	0.5168	0.494	0.084	0.1258	
	507	-0.524	-0.453	-0.222	0.226	0.144	-0.688	0.300	-0.789	0.530	0.495	-0.198	-0.345	-0.382	-0.229	-0.237	0.397	0.394	0.948	0.548	-0.328	-0.053	0.490	-0.720	-0.0239	0.088	0.241	0.819	0.4430	0.1805	0.3217	
2019	205	-0.123	0.468	-0.438	0.216	-0.234	-0.023	0.365	0.705	0.676	0.493	-0.262	0.169	-0.642	-0.535	-0.219	-0.707	-0.188	-0.108	0.322	0.042	0.026	-0.455	-0.1789	0.0316	0.1277	0.2769	-0.937	-0.2634	0.3783		
	285	-0.123	0.468	-0.438	0.216	-0.234	-0.023	0.365	0.705	0.676	0.493	-0.262	0.169	-0.642	-0.535	-0.219	-0.707	-0.188	-0.108	0.322	0.042	0.026	-0.455	-0.1789	0.0316	0.1277	0.2769	-0.937	-0.2634	0.3783		
	385	-0.123	0.468	-0.438	0.216	-0.234	-0.023	0.365	0.705	0.676	0.493	-0.262	0.169	-0.642	-0.535	-0.219	-0.707	-0.188	-0.108	0.322	0.042	0.026	-0.455	-0.1789	0.0316	0.1277	0.2769	-0.937	-0.2634	0.3783		
	507	-0.123	0.468	-0.438	0.216	-0.234	-0.023	0.365	0.705	0.676	0.493	-0.262	0.169	-0.642	-0.535	-0.219	-0.707	-0.188	-0.108	0.322	0.042	0.026	-0.455	-0.1789	0.0316	0.1277	0.2769	-0.937	-0.2634	0.3783		
	205	-0.123	0.468	-0.438	0.216	-0.234	-0.023	0.365	0.705	0.676	0.493	-0.262	0.169	-0.642	-0.535	-0.219	-0.707	-0.188	-0.108	0.322	0.042	0.026	-0.455	-0.1789	0.0316	0.1277	0.2769	-0.937	-0.2634	0.3783		
2020	205	-0.126	0.586	-0.803	0.314	-0.418	0.696	-0.428	-0.673	0.772	0.485	-0.212	-0.284	-0.520	-0.494	-0.536	-0.235	-0.601	-0.179	-0.504	0.342	-0.186	0.240	-0.342	-0.104	-0.254	0.548	0.262	0.3678	0.1900	-0.2925	-0.3692
	285	-0.126	0.586	-0.803	0.314	-0.418	0.696	-0.428	-0.673	0																						

Table C.12: Correlation values between Kite and PV Energy in Marseille Q4 (daily)

Height (m)	Day 274	Day 275	Day 276	Day 277	Day 278	Day 279	Day 280	Day 281	Day 282	Day 283	Day 284	Day 285	Day 286	Day 287	Day 288	Day 289	Day 290	Day 291	Day 292	Day 293	Day 294	Day 295	Day 296	Day 297	Day 298	Day 299	Day 300	Day 301	Day 302	Day 303	Day 304	
107	0.4649	-0.3571	-0.3836	-0.1665	-0.2751	0.2829	0.1032	0.2531	-0.1526	-0.7366	-0.5777	-0.4666	-0.4488	-0.3937	-0.3382	-0.3983	0.1670	0.1488	-0.4480	-0.4347	0.0211	-0.0288	0.3537	-0.4472	-0.2440	-0.4791	0.5233	-0.4689	0.6566	-0.7450		
205	0.5900	-0.3672	-0.4033	0.1005	-0.3099	0.2201	0.4467	0.4079	0.0448	0.6544	-0.7507	-0.4633	-0.4474	-0.3579	-0.4053	-0.1162	0.3767	0.3854	-0.4589	-0.4005	-0.1166	0.2882	0.3854	-0.3649	-0.2804	-0.3731	0.6694	-0.4069	0.4315	-0.7121		
285	0.9871	-0.3786	-0.4417	0.1317	-0.8192	0.1470	0.4853	0.3808	0.1288	0.8240	-0.7610	-0.5244	-0.6276	-0.4803	-0.3991	-0.3587	0.3620	0.3113	-0.4675	-0.4003	-0.1072	0.2682	0.3767	-0.3869	-0.2804	-0.3113	0.6673	0.3152	0.4815	-0.9803		
385	0.4448	-0.4040	-0.3303	-0.2461	0.1646	0.2537	0.5290	0.1835	0.0456	0.6766	-0.6976	-0.4954	-0.4837	-0.3433	-0.1478	0.2944	0.2944	0.2944	-0.4637	-0.3772	0.2944	0.3535	-0.3327	0.3746	-0.1890	-0.6964	0.3582	0.4432	-0.4380			
107	0.3018	-0.1024	-0.6428	0.1609	-0.3834	-0.6887	-0.0984	0.2970	0.3647	-0.1440	-0.4375	-0.4191	-0.1847	-0.4520	-0.3858	-0.3235	0.1947	0.1840	-0.4044	-0.4044	-0.3858	-0.3235	0.1947	-0.6761	0.1840	-0.4044	-0.3858	-0.3235	0.1947	-0.1637	-0.4321	
205	0.3134	-0.2248	0.4146	0.3816	-0.5131	-0.2751	0.5004	0.0904	0.6885	-0.2419	-0.4662	0.0277	-0.6592	0.0277	-0.7563	0.0927	0.1011	-0.8327	-0.5261	-0.6776	-0.4824	-0.5868	-0.2497	-0.3248	-0.6321	-0.4013	-0.4023	-0.3801	-0.1633	-0.5271		
285	0.3045	-0.2559	-0.0012	0.3726	-0.3160	-0.5827	-0.3277	-0.3169	0.3569	0.1835	-0.1046	-0.1466	-0.4310	-0.5903	-0.0036	-0.0443	-0.2276	-0.1858	-0.1858	-0.1858	-0.1858	-0.1858	-0.1858	-0.1858	-0.1858	-0.1858	-0.1858	-0.1858	-0.1858	-0.1858	-0.1858	
385	0.3118	-0.3355	-0.1450	0.1906	0.4873	-0.6164	-0.3850	-0.3132	0.8172	0.4248	0.1044	-0.7113	-0.4826	-0.1788	-0.0959	-0.0042	-0.3300	0.1910	0.1910	0.1910	0.1910	0.1910	0.1910	0.1910	0.1910	0.1910	0.1910	0.1910	0.1910	0.1910	0.1910	
507	0.3234	-0.3623	-0.2828	-0.1181	0.8380	0.8986	-0.0322	0.0851	-0.1516	-0.2885	-0.0690	-0.7940	0.6977	-0.1010	-0.3588	-0.3162	-0.3439	0.2746	0.1424	0.2485	-0.0749	0.3216	0.4681	-0.6973	-0.4040	0.4482	-0.2411	-0.2089	0.2823	-0.3271	-0.4112	
205	0.4833	-0.3235	-0.5830	-0.2740	0.3391	0.3038	0.0915	-0.3316	-0.0775	-0.2885	-0.0979	-0.8979	0.7891	-0.1000	-0.2958	-0.3162	-0.3439	0.2746	0.1424	0.2485	-0.0749	0.3216	0.4681	-0.6973	-0.4040	0.4482	-0.2411	-0.2089	0.2823	-0.3271	-0.4112	
285	0.4833	-0.3235	-0.5830	-0.2740	0.3391	0.3038	0.0915	-0.3316	-0.0775	-0.2885	-0.0979	-0.8979	0.7891	-0.1000	-0.2958	-0.3162	-0.3439	0.2746	0.1424	0.2485	-0.0749	0.3216	0.4681	-0.6973	-0.4040	0.4482	-0.2411	-0.2089	0.2823	-0.3271	-0.4112	
385	0.3238	-0.1920	-0.5523	-0.1853	0.1748	0.3181	0.1748	0.3181	0.1748	0.3181	0.1748	0.3181	0.1748	0.3181	0.1748	0.3181	0.1748	0.3181	0.1748	0.3181	0.1748	0.3181	0.1748	0.3181	0.1748	0.3181	0.1748	0.3181	0.1748	0.3181	0.1748	0.3181
507	0.2921	0.1687	0.1538	0.0831	0.2845	0.0812	0.1687	0.1538	0.0831	0.2845	0.0812	0.1687	0.1538	0.0831	0.2845	0.0812	0.1687	0.1538	0.0831	0.2845	0.0812	0.1687	0.1538	0.0831	0.2845	0.0812	0.1687	0.1538	0.0831	0.2845	0.0812	0.1687
107	0.2092	0.4654	-0.3430	-0.6800	-0.2841	-0.0938	0.1154	-0.1680	-0.1150	-0.2017	-0.0559	0.0032	-0.4790	0.4892	0.5001	-0.0963	0.4264	0.0945	-0.1870	-0.0963	0.4264	0.0945	-0.1870	-0.0963	0.4264	0.0945	-0.1870	-0.0963	0.4264	0.0945	-0.1870	-0.0963
205	0.2577	0.4868	-0.3485	-0.6852	-0.1403	-0.4589	-0.2420	0.3640	-0.3378	0.1554	-0.4471	-0.2744	0.2446	-0.4126	0.3805	0.1741	-0.1866	0.1866	0.1741	-0.1866	0.1866	0.1741	-0.1866	0.1866	0.1741	-0.1866	0.1866	0.1741	-0.1866	0.1866	0.1741	-0.1866
285	0.2823	0.4886	-0.2272	-0.3846	0.3824	-0.4800	-0.3811	0.4262	-0.3145	0.2471	-0.8569	-0.2936	0.3289	-0.4067	-0.0426	-0.0011	-0.4093	-0.3444	-0.2036	0.2175	-0.1381	0.0317	0.3224	0.8171	0.4229	0.2022	0.2003	-0.2277	-0.3316	-0.4149	-0.0686	
385	0.3196	0.4711	-0.0438	-0.3676	0.3864	-0.6626	-0.3814	0.4483	-0.1106	0.2871	-0.7114	-0.3186	0.3965	-0.3070	-0.1535	-0.0624	-0.5088	-0.2848	-0.1542	-0.3000	0.0540	0.3477	-0.2451	0.1789	-0.1035	-0.3491	0.7525	0.2586	0.6081	-0.1556	0.2707	
507	0.3231	0.4743	0.1271	-0.7071	0.1729	0.2796	-0.1629	0.4421	-0.0558	0.3036	0.8256	-0.3583	0.4372	-0.4279	-0.2127	0.0166	-0.4627	0.2714	-0.0911	0.0230	-0.1975	0.0592	-0.3102	0.6210	0.4343	0.2845	0.2390	-0.3042	-0.1926	-0.2652	-0.0710	
107	0.4059	-0.7688	0.8422	-0.2552	-0.1425	0.4669	-0.3761	-0.2487	-0.3887	-0.1847	-0.6878	-0.2203	0.7317	-0.1722	-0.1165	-0.2429	-0.4614	-0.2335	-0.4125	-0.1250	-0.6703	0.2045	-0.3102	-0.1852	-0.3789	-0.2221	-0.3789	-0.2221	-0.3789	-0.2221	-0.3789	
205	0.4891	-0.5200	0.6852	-0.1005	-0.1000	-0.2821	-0.0585	-0.1007	0.1394	0.8190	0.0056	-0.1460	-0.1460	-0.1460	-0.1460	-0.1460	-0.1460	-0.1460	-0.1460	-0.1460	-0.1460	-0.1460	-0.1460	-0.1460	-0.1460	-0.1460	-0.1460	-0.1460	-0.1460	-0.1460	-0.1460	
285	0.4891	-0.5200	0.6852	-0.1005	-0.1000	-0.2821	-0.0585	-0.1007	0.1394	0.8190	0.0056	-0.1460	-0.1460	-0.1460	-0.1460	-0.1460	-0.1460	-0.1460	-0.1460	-0.1460	-0.1460	-0.1460	-0.1460	-0.1460	-0.1460	-0.1460	-0.1460	-0.1460	-0.1460	-0.1460	-0.1460	
385	0.3033	-0.2826	-0.6809	-0.7929	0.3870	0.4874	-0.7622	-0.0112	-0.3018	-0.0728	0.2628	0.1437	0.4546	-0.2184	-0.3142	-0.3630	-0.1507	-0.3794	0.2686	-0.6024	0.2000	0.0237	0.1380	0.1341	0.3145	-0.3084	-0.0488	0.9675	-0.0654	0.3262		
507	0.2904	-0.2977	-0.3891	-0.6222	0.3714	0.4576	-0.7238	-0.6830	-0.2317	-0.6000	-0.0159	0.3824	-0.3954	-0.3430	-0.1435	-0.3289	-0.1507	-0.3514	0.3289	-0.6024	0.2000	0.0237	0.1380	0.1341	0.3145	-0.3084	-0.0488	0.9675	-0.0654	0.3262		
Height (m)	Day 305	Day 306	Day 307	Day 308	Day 309	Day 310	Day 311	Day 312	Day 313	Day 314	Day 315	Day 316	Day 317	Day 318	Day 319	Day 320	Day 321	Day 322	Day 323	Day 324	Day 325	Day 326	Day 327	Day 328	Day 329	Day 330	Day 331	Day 332	Day 333	Day 334		
107	0.3688	0.9238	-0.1742	0.4376	-0.3132	-0.3692	-0.4467	-0.6217	-0.4718	-0.6740	0.2004	0.1439	0.2099	0.4465	-0.1603	-0.4672	-0.7387	-0.7492	-0.1886	-0.1886	-0.1886	-0.1886	-0.1886	-0.1886	-0.1886	-0.1886	-0.1886	-0.1886	-0.1886	-0.1886		
205	0.3633	0.8292	-0.1545	0.4592	-0.3732	-0.4933	-0.4278	-0.2968	-0.3274	-0.2041	0.2488	0.2675	0.0240	0.4384	-0.2022	-0.4721	-0.5520	-0.5173	0.0415	-0.2832	-0.3262	-0.3655	0.1018	-0.2266	-0.4485	0.7250	0.2071	0.5197	-0.1971	0.3210		
285	0.2920	0.7629	-0.1597	0.4296	-0.2543	-0.4428	0.0335	0.1291	0.1770	0.1957	0.2995	0.0594	0.3972	0.0053	-0.5088	-0.2848	-0.4091	-0.4188	0.5325	-0.1628	0.0032	0.3170	-0.0722	0.1772	-0.1035	-0.2299	0.6040	0.3029	0.4682	-0.1192	0.2339	
385	0.3675	0.7895	-0.1689	0.2980	0.0645	-0.2796	0.3233	0.3915	0.1436	0.4443	-0.1431	0.2195	0.1099	0.3385	0.0284	-0.4971	0.1498	0.5325	-0.1628	0.0032	0.3170	-0.0722	0.1772	-0.1035	-0.2299	0.6040	0.3029	0.4682	-0.1192	0.2339		
507	0.4073	0.8292	-0.1948	0.2821	-0.1043	-0.5930	0.2283	0.4685	0.2263	0.1814	-0.2454	0.1483	0.1627	0.2930	0.0516	-0.3873	0.1937	-0.3211	0.0416	0.2287	-0.1086	-0.2837	-0.1259	-0.0485	0.9223	0.3465	0.3197	-0.1411	0.2284			
107	0.3657	0.8292	-0.1948	0.2821	-0.1043	-0.5930	0.2283	0.4685	0.2263	0.1814	-0.2454	0.1483	0.1627	0.2930	0.0516	-0.3873	0.1937	-0.3211	0.0416	0.2287	-0.1086	-0.2837	-0.1259	-0.0485	0.9223	0.3465	0.3197	-0.1411	0.2284			
205	0.3657	0.8292	-0.1948	0.2821	-0.1043	-0.5930	0.2283	0.4685	0.2263	0.1814	-0.2454	0.1483	0.1627	0.2930	0.0516	-0.3873	0.1937	-0.3211	0.0416	0.2287	-0.1086	-0.2837	-0.1259	-0.0485	0.9223	0.3465	0.3197	-0.1411	0.2284			
285	0.3160	-0.1538	0.4245	0.4																												

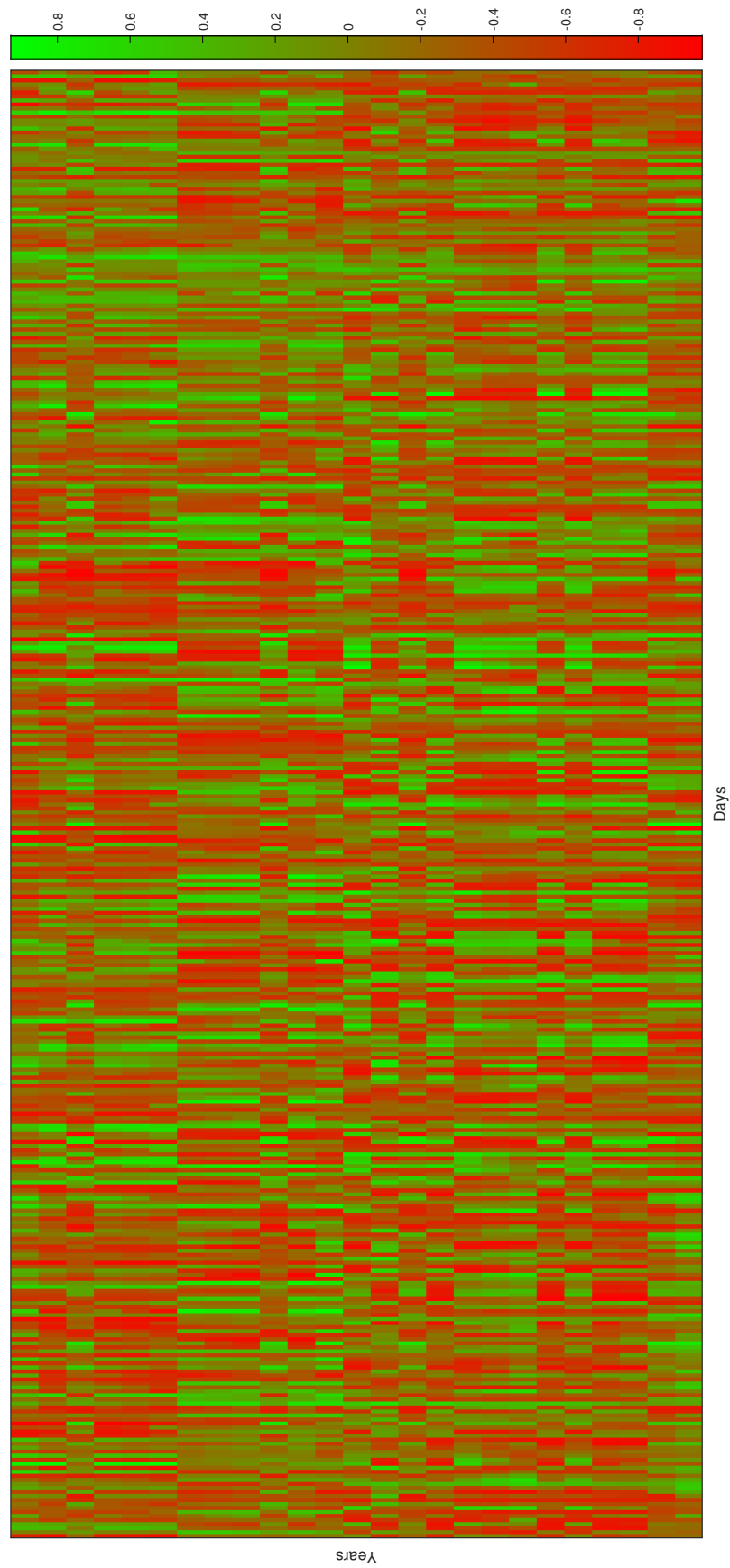
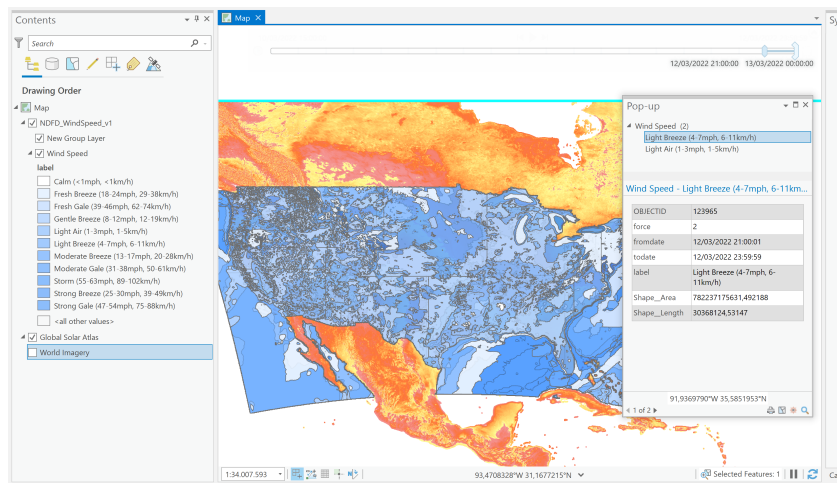


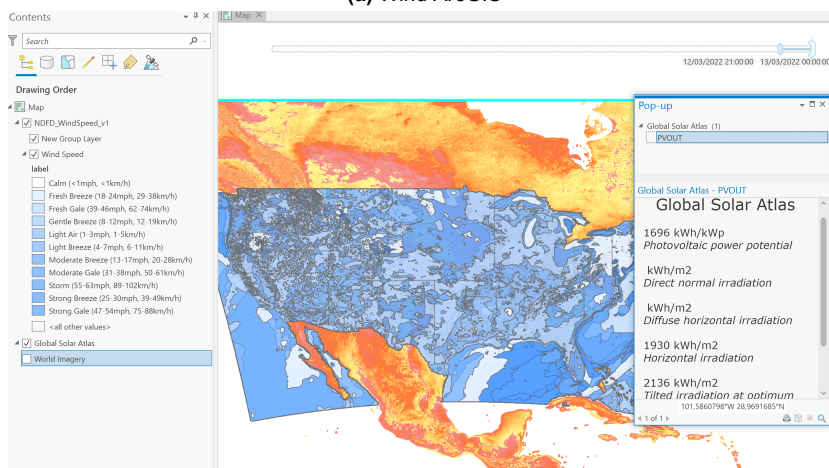
Figure C.1: Visual of annual correlation of resources over five heights from 2017-2021 Marseille

D

Appendix D



(a) Wind ArcGIS



(b) Solar ArcGIS

Figure D.1: ArcGIS